A Modeling Approach to Analyze Performance of a Minimal Aeration Biological Nutrient Removal (BNR) Pilot-Scale Plant

Prepared By:

Nick Bayer

A thesis submitted in partial fulfillment of the requirements for the degree of

Master of Science (Environmental Engineering)

UNIVERSITY OF WISCONSIN- MADISON
2018

TABLE OF CONTENTS

LIST OF FREQUENTLY USED ABBREVIATIONS

AOB	Ammonia Oxidizing Bacteria
BOD	Biological Oxygen Demand
BOD_5	5-Day Biological Oxygen Demand
$CBOD_5$	5-Day Carbonaceous Biological Oxygen Demand
COD	Chemical Oxygen Demand
CBOD	Carbonaceous BOD
DO	Dissolved Oxygen
EBPR	Enhanced Biological Phosphorus Removal
HRT	Hydraulic Retention Time
NOB	Nitrite Oxidizing Bacteria
NO_x	Nitrogen Oxides (NO_2^--N + NO_3^--N)
MLSS	Mixed Liquor Suspended Solids
OUR	Oxygen Uptake Rate
PAO	Polyphosphate Accumulating Organisms
rbCOD	Readily Biodegradable COD
SRT	Solids Retention Time
TAN	Total Ammoniacal Nitrogen (NH_4^+-N plus NH_3-N)
tCOD	Total COD
TKN	Total Kjeldahl Nitrogen (TAN + Organic-N)
TN	Total Nitrogen (TKN + NO_2^--N + NO_3^--N)
TP	Total Phosphorus (PO_4^{3-}P + Organic-P)
TSS	Total Suspended Solids
UCT	University of Cape Town Configuration
VFA	Volatile Fatty Acids
VSS	Volatile Suspended Solids
WWTP	Wastewater Treatment Plant

LIST OF FIGURES

LIST OF TABLES

ACKNOWLEDGEMENTS

I thank Dr. Dan Noguera for this great opportunity and for his advisement throughout this research. Without his expertise and continued support, this thesis would not be possible. I am grateful to have worked with such talented individuals and it is no wonder why they gravitate to the Noguera lab. This project was funded by the Madison Metropolitan Sewerage District (MMSD) and I would like to thank the individuals at the Nine Springs Wastewater Treatment Plant that were indispensable to this research, particularly the lab staff who have been a great part of this project over the years. I would like to especially thank Dr. Mathew Seib, research engineer at MMSD, for his dedication to and collaboration on this project. I thank the members of my committee Dr. Trina McMahon and Dr. Greg Harrington. The insights I learned from their instruction and their commentary were invaluable to this research. I want to thank the members of the Noguera and McMahon labs for sharing their advice and ideas throughout this project. This includes Pamela Camejo, Natalie Cook, Abel Ingle, Chris Lawson, Franciso Moya, Zach Oshlag, Brian Owen, Miguel Perez, and Matthew Scarborough. A special thanks goes to Natalie Keene. This research was an extension of her hard work and the knowledge gained from her research was a great contribution to the success of this project. I would like to thank Evan Chambers. We completed our graduate programs and operated the pilot plant together, neither would have been possible without his collaboration. A great thank you goes to Jackie Bastyr-Cooper, lab manager, for her advice and assistance. I thank Cam Potter and Tara Meyers, undergraduate researchers, for their hard work in the laboratory and at the pilot plant. It was an honor to work on this project and I will be forever grateful for this experience.

ABSTRACT

The aeration of wastewater in the activated sludge process for biological nutrient removal is energy intensive. For the average wastewater treatment plant (WWTP), aeration contributes 60% of the electrical energy costs required for plant operation. Conventional wastewater treatment operates the aeration basins at dissolved oxygen (DO) concentrations greater than 2 mg-DO/L, where stable nutrient removal is achieved. However, a 5-month study conducted at the Nine Springs WWTP in Madison, WI, demonstrated that operating a large portion of the aeration zone at less than 0.5 mg-DO/L achieved reliable phosphorus and nitrogen removal. Research conducted by the University of Wisconsin-Madison, in collaboration with the Madison Metropolitan Sewerage District, demonstrated that sequentially reducing the DO concentration within the aeration zone from conventional high aeration to low-DO operation of a University of Cape Town (UCT) pilot-scale plant throughout one year was effective at providing stable nitrogen and phosphorus removal; this research is an extension of that project. This pilot plant, continuously fed settled wastewater, was operated for an additional 19 month period at an average DO concentration throughout the aeration zone of 0.39 mg-DO/L. This long-term operation revealed challenges in performance that need to be understood before full-scale implementation of low-DO operation can be recommended. With seasonal water temperatures reaching below 14°C, the pilot experienced reduced nitrogen removal performance. A BioWin™ 5.2 dynamic model, utilizing experimentally determined nitrogen removal kinetic parameters, was used to simulate the performance of the pilot plant, elucidate the causes of poor performance, and propose corrective actions. Low DO operation affords a significant operational energy cost reduction; by understanding the factors that drive performance and simulating conditions that lead to effective low-DO operation, this research contributes to proving the efficacy of a stable and sustainable approach to wastewater treatment.

CHAPTER 1 INTRODUCTION

Wastewater treatment is critical to the protection of societal health and natural resources. With populations rising, global weather patterns changing, and source water quality degrading, the challenges faced by the environmental engineering profession are becoming increasingly complex. The substantial energy demands of wastewater treatment facilities place sustainable treatment as an important factor in re-envisioning the water energy nexus [Bauer, 2014]. Since the inception of the Clean Water Act in 1972, there have been significant advances in understanding the scientific principles behind wastewater treatment. This knowledge has resulted in technological advancements that contribute to a reduction in energy demands. Moreover, the embodied energy in wastewater and produced biosolids has been estimated to be greater than 10-times the operational energy of these facilities [WERF, 2011]; therefore, there is interest in tapping into this embodied energy for self-sufficient operation of wastewater treatment plants. The goal of energy neutral wastewater treatment has driven the reconceptualization of these facilities as resource recovery centers [ASCE, 2011]. Reducing the operational energy of these facilities by optimizing aeration demands for the activated sludge process is an important step towards achieving this goal.

1.1 Activated Sludge Wastewater Treatment

Aeration of the activated sludge process is generally the largest consumer of energy in wastewater treatment. The activated sludge process utilizes bacterial communities to remove nutrients from wastewater. These bacteria are cultivated in engineered systems to consume

nitrogen, phosphorus, and organic carbon under selected environmental conditions. The combination of the microbial culture and the wastewater is called the mixed liquor, and the concentration of microorganisms in this culture is referred to as the mixed liquor suspended solids (MLSS). The structure of the bacterial communities within the MLSS is complex and diverse [Nielsen and McMahon, 2014]. Understanding the dynamics of these bacterial communities is essential to the design of wastewater treatment systems.

For plants achieving nitrogen removal, the MLSS is alternatingly exposed to aerobic and anoxic environments. Nitrogen is primarily removed from wastewater by aerobic bacteria that oxidize total ammoniacal nitrogen, TAN (NH_3 + NH_4^+), to nitrogen oxides, NO_x (NO_2^-+NO_3^-), in the presence of oxygen, then removing nitrogen from the water by bacterial denitrification of NO_x to nitrogen gas in the absence of oxygen. Treatment plants achieving biological nitrogen removal are designed with separate aerobic and anoxic tanks, where ammonia oxidation occurs in aerated tanks and denitrification occurs in anoxic tanks.

In the aerated tanks, ammonia oxidizing bacteria (AOB) oxidize ammonia to nitrite (NO_2^-), then nitrite oxidizing bacteria (NOB) oxidize nitrite to nitrate (NO_3^-). In the anoxic tanks, heterotrophic organisms consume carbon while utilizing nitrite and nitrate as terminal electron acceptors, denitrifying NO_x to nitrogen gas.

For plants achieving enhanced biological phosphorus removal (EBPR), the MLSS is alternatingly exposed to aerobic and anaerobic environments. In the anaerobic tanks, poly-phosphate accumulating organisms (PAOs) have a selective advantage over ordinary heterotrophic organisms (OHOs) by consuming carbon while releasing stored polyphosphate

compounds in the absence of oxygen and NOx. Phosphorus is subsequently removed from wastewater by phosphate uptake by PAOs in the aerobic tanks [Tchobanoglous, 2003].

The bacteria consuming these nutrients represent a fraction of the diverse communities within the MLSS. For plants performing EBPR and nitrogen removal, the fraction of PAOs is estimated to be approximately 15–20% of the entire bacterial population [Mielczarek, 2013], while for nitrifying plants, the fraction of AOBs is estimated to be approximately 1-3% [Harms, 2003].

The microbial communities in the MLSS form flocs that create mass transport limitations for oxygen. Therefore, with conventional treatment, aerobic zones are typically operated with DO concentrations greater than 2 mg-DO/L [US-EPA, 2013]. At these DO concentrations, a safety factor is provided to ensure that all organisms in the MLSS are exposed to adequate amounts of oxygen. This aeration is an energy intensive process, consuming up to 60% of the energy use for wastewater treatment [WERF, 2011]. For the Nine Springs WWTP in Madison, WI, 42% of the operational electrical energy is consumed to aerate the activated sludge process [Brown and Caldwell, 2014]. Recent research has demonstrated that this energy demand can be reduced, while still providing high levels of nutrient removal, by reducing the DO concentrations within the aerobic zone. However, this mode of operation reduces the safety factor associated with high aeration and can lead to process instability. In particular, efficient nitrification with low DO requires careful design considerations to ensure efficient operation.

1.2 Low-DO Operation

Nitrification in activated sludge is a sensitive process. The instability of these systems is due to the susceptibility of nitrifying organisms to a variety of factors including oxygen concentration, inhibitory elements in the wastewater, and carbon dioxide limitations [Denecke, 2003]. Process failures occur when the nitrifiers are growing slower than the rate at which they are being removed from the system, therefore diminishing nitrifier population. When process failures occur, the slow growth rate of nitrifiers prolongs the recovery of these systems to stable process performance. To minimize nitrification failures, these systems are designed with a biological safety factor [Rittmann, 2001].

In a study conducted at the Nine Springs WWTP, one UCT configured treatment train of the full-scale plant was converted to low-DO operation [Park, 2006]. DO concentrations were maintained below 0.5 mg-DO/L for a large portion of the aerated tank and below 1 mg-DO/L for the entirety for the aeration zone. This operational strategy effectively removed ammonia but experienced spikes in ammonia effluent. One reason for these upsets is the increase in flow rate to the treatment train that was necessary to suppress oxygen concentrations, reducing HRT, thereby reducing the safety factor of the system. This reduction in safety factor was evident by tracking ammonia concentrations in the aeration zone. During normal high-DO operation all ammonia was removed by the middle of the aerated tank, whereas for low-DO operation complete ammonia removal did not occur until nearly the end of the aerated tank [Park, 2006].

Additional research on low-DO nitrification suggests that DO exerts a selective pressure on AOB communities. Lab-scale nitrifying enrichment cultures, seeded from the Nine Springs plant and maintained at low and high-DO conditions, showed low-DO enriched communities had

higher growth rates than high-DO enriched communities. In addition, the low-DO enriched communities exhibited inhibition by high levels of oxygen (K_I=5.11 ± 0.79 mg-DO/L), thus predicting limited growth at DO greater than 2 mg-DO/L [Park and Noguera, 2004]. The growth yield of low-DO enriched AOBs has been demonstrated to be greater than typical values [Bellucci, 2011]. The decay rates of low-DO enriched AOBs are also an important consideration. Low-DO enriched AOB communities have been shown to exhibit significantly lower decay rates than typically used in nitrification modelling [Park and Noguera, 2007].

NOBs subject to a reduction in DO have been shown to have higher affinity for oxygen [Liu, 2013]. In this study, SRT and DO affected the composition of the NOB community. Nitrite concentration in response to SRT was likely the driving factor in NOB community shift at different SRTs. Additionally, low-DO enriched NOBs exhibited a higher affinity for oxygen than AOBs. Both AOB and NOB populations increased in response to low-DO conditions. It was suggested that the reduced endogenous decay of AOBs and NOBs led to greater populations at low-DO conditions.

The kinetic factors of low-DO operation in connection with operational factors, HRT and SRT, need to be considered comprehensively for the design of viable low-DO nitrification processes. These considerations should be utilized with appropriate design principles to afford a sufficiently high biological safety factor that guarantees process stability.

1.3 Nitrification Modeling

The rates of bacterial growth and substrate removal are typically modelled using Monod kinetics [Monod, 1949]. This mathematical model (Equation 1.1) uses two empirical kinetic parameters; the half saturation constant, K_S, and the maximum specific growth rate, u_{max}. The half saturation constant is the concentration of the limiting substrate at which the specific growth rate of the microorganism is ½ of the maximum growth rate. The maximum specific growth rate of the microorganisms is the growth rate where the limiting substrate is in excess.

$$u = u_{max} * \frac{S}{K_S + S} \quad 1.1$$

Where:

u = Specific growth rate of the microorganism $\left(\frac{1}{d}\right)$

u_{max} = Maximum specific growth rate of the microorganism $\left(\frac{1}{d}\right)$

K_S = Half saturation constant $\left(\frac{\text{mg}-\text{S}}{L}\right)$

S = Limiting substrate concentration $\left(\frac{\text{mg}-\text{S}}{L}\right)$

The governing equations used to model nitrogen oxidation in the Activated Sludge Model (ASM) are described below (Equations 1.2 to 1.5) [Henze, 1999]. These equations assume continuously stirred tank reactor (CSTR) conditions and ideal clarifier performance where no biomass leaves the system in the effluent and is only removed by decay and wasting.

The concentration of organisms within the MLSS is simulated using a mass balance and Monod kinetics according to Equation 1.2 (example for aerobic growth of AOB):

$$\frac{d\,(X)}{dt} = u_{max} * \frac{NH_3}{K_{NH_3} + NH_3} * \frac{DO}{K_{DO} + DO} * X - b * X - \frac{1}{\theta_x} * X \qquad 1.2$$

Where:

X = AOB concentration $\left(\frac{mg-VSS}{L}\right)$

K_{NH3} = Ammonia half saturation constant $\left(\frac{\text{mg}-\text{NH3}-\text{N}}{L}\right)$

K_{DO} = Oxygen half saturation constant $\left(\frac{\text{mg}-\text{DO}}{L}\right)$

NH_3 = Ammonia concentration within reactor $\left(\frac{\text{mg}-\text{N}}{L}\right)$

DO = Oxygen concentration within reactor $\left(\frac{\text{mg}-\text{DO}}{L}\right)$

b = decay coefficient $\left(\frac{1}{d}\right)$

θ_x = Solids retention time (d)

The Arrhenius temperature consideration is applied to the maximum specific growth rate, u_{max}, according to Equation 1.3 [Tchobanoglous, 2003]:

$$u_{max,T} = u_{max,20} * \theta_T^{(T-T_{20})} \qquad 1.3$$

Where:

$u_{max,T}$ = Maximum specific growth rate at temperature, T $\left(\frac{1}{d}\right)$

$u_{max,20}$ = Maximum specific growth rate at 20°C $\left(\frac{1}{d}\right)$

θ_T = Arrhenius temperature coefficient (dimensionless)

T = Temperature (°C, T_{20} = 20°C)

The maximum specific growth rate is related to the maximum substrate utilization rate according to Equation 1.4:

$$u_{max} = Y * q_{max} \quad 1.4$$

Where:

Y = Growth yield coefficient $\left(\frac{mg-VSS}{mg-N}\right)$

q_{max} = Maximum specific substrate utilization rate $\left(\frac{\text{mg}-\text{N}}{\text{mg}-\text{VSS}-\text{d}}\right)$

The substrate concentration is simulated using a mass balance and Monod kinetics according to Equation 1.5 (example for ammonia):

$$\frac{d\,(NH_3)}{dt} = \frac{NH_{3,i} - NH_3}{\text{HRT}} - q_{max} * \frac{NH_3}{K_{NH_3} + NH_3} * \frac{DO}{K_{DO} + DO} * X \quad 1.5$$

Where:

$NH_{3,i}$ = Influent ammonia concentration $\left(\frac{\text{mg}-\text{N}}{L}\right)$

NH_3 = Ammonia concentration within reactor $\left(\frac{\text{mg}-\text{N}}{L}\right)$

DO = Oxygen concentration within reactor $\left(\frac{\text{mg}-\text{DO}}{L}\right)$

HRT = Hydraulic retention time (d)

There are two important operational factors in these governing equations; the hydraulic retention time (HRT) and the solids retention time (SRT). The HRT is the average amount of time that a drop of water spends in the reactor and is calculated according to Equation 1.6:

$$\mathrm{HRT} = \frac{V}{Q} \tag{1.6}$$

Where:

V = Volume of reactor $(gal.)$

Q = Flow rate $\left(\frac{gal.}{d}\right)$

The SRT is the average amount of time that a bacterial cell spends in the reactor and is calculated from a solids mass balance considering biomass wasting according to Equation 1.7:

$$\theta_x = \frac{V * MLSS}{Q_w * MLSS_w} \tag{1.7}$$

Where:

MLSS = Mixed liquor suspended solids concentration within reactor $\left(\frac{mg-TSS}{L}\right)$

Q_w = Flow rate at which biomass is wasted $\left(\frac{gal.}{d}\right)$

$MLSS_w$ = Mixed liquor suspended solids concentration in waste stream $\left(\frac{mg-TSS}{L}\right)$

The steady-state solutions to these governing equations help describe some important concepts regarding reactor operation that control performance [Tchobanoglous, 2003]. The steady-state solution for biomass concentration (Equation 1.8) shows that the biomass concentration is inversely proportional to HRT.

$$(X)_{SS} = \frac{\theta_x}{\mathrm{HRT}} * \frac{Y * [NH_{3,i} - (NH_3)_{SS}]}{(1 + b * \theta_x)} \quad 1.8$$

Where:

$(X)_{SS}$ = Steady-state AOB concentration $\left(\frac{mg-VSS}{L}\right)$

$(NH_3)_{SS}$ = Steady-state ammonia concentration $\left(\frac{\mathrm{mg-N}}{L}\right)$

The steady-state solution for ammonia concentration (Equation 1.9) shows that ammonia concentration within the reactor is dependent on SRT.

$$(NH_3)_{SS} = K_{NH_3} * \frac{1 + b * \theta_x}{Y * q_{max} * \theta_x - (1 + b * \theta_x)} \quad 1.9$$

Regarding reactor conditions, a crucial concept is the minimum SRT. An organism needs to be growing faster than it is being removed for net growth to occur within the reactor. Therefore, there is a minimum SRT where, below which, the organism's population is being diminished by biomass wasting. This occurrence is called washout. Considering water temperatures by Equation 1.3, the minimum SRT will increase with colder conditions according to Equation 1.10.

$$\theta_c = [u_{max,20} * \theta_T^{(T-T_{20})} * \frac{NH_3}{K_{NH_3} + NH_3} * \frac{DO}{K_{DO} + DO} - b]^{-1} \quad 1.10$$

Where:

θ_c = Minimum SRT (d)

1.4 Thesis Objectives

This research aims to use simulations of the wastewater treatment process to explain the poor ammonia removal performance experienced by a low-DO pilot plant during cold water temperatures. Taking into consideration the varying nutrient loading throughout the operation of the system, the water temperature, experimentally determined kinetic parameters of the low DO nitrifying communities, DO concentrations within the aerobic tanks, and operational factors (HRT and SRT), a dynamic simulation was used to elucidate the factors contributing to the seasonal decline in pilot performance. The model was then utilized to propose corrective actions to achieve stable performance.

CHAPTER 2 : CONTINUOUS FLOW PILOT PLANT

The continuous flow pilot plant has been operating since June 2014. The original research with the pilot plant system was to determine if sequentially reducing the DO within the aerobic tanks could stably provide high levels of nutrient removal performance and to investigate the response of the nutrient removing bacterial communities to low DO conditions [Keene, 2016]. Initially, the pilot plant was configured as a University of Cape Town (UCT) process, emulating the West treatment trains of the full-scale Nine Springs WWTP. The pilot plant received primary effluent (PE) from the full-scale plant. The pilot plant was then operated for a period of time (October 2015 to June 2016) in a Johannesburg configuration. This configuration eliminated the anaerobic return flow and returned the biomass from the clarifier to a pre-anoxic tank before proceeding to the anaerobic tanks. The plant was returned to a UCT configuration on June 10th, 2016.

This research focuses on the sustained phase of UCT operation from June 10th, 2016 to December 31st, 2017. During this time, the average DO across the aeration tanks was maintained at 0.39 ± 0.16 mg-DO/L. This operational strategy showed seasonal variation in nutrient removal performance. During times of warmer water temperatures, the pilot was able to effectively remove phosphorus and nitrogen whereas during times of colder water temperatures, the pilot experienced poor nitrogen removal.

2.1 Configuration and Operation

The configuration of the pilot plant is a UCT process without nitrate recycle to achieve EBPR and ammonia oxidation (Figure 2.1). The wastewater enters the anaerobic tanks where phosphorus release occurs and easily degradable organic substrates, such as acetate and propionate are taken up. In the anoxic stage, NOx returned with mixed liquor from the clarifier is denitrified, removing nitrogen from the water. The wastewater then enters the aerobic tanks where ammonia oxidation to NO_x and phosphorus uptake occurs. The biomass is separated from the water in the clarifier and returned to the anoxic tank via the return activated sludge (RAS) flow. Mixed liquor, absent of NO_x, is returned from the anoxic tank to the anaerobic tanks via the anaerobic return flow.

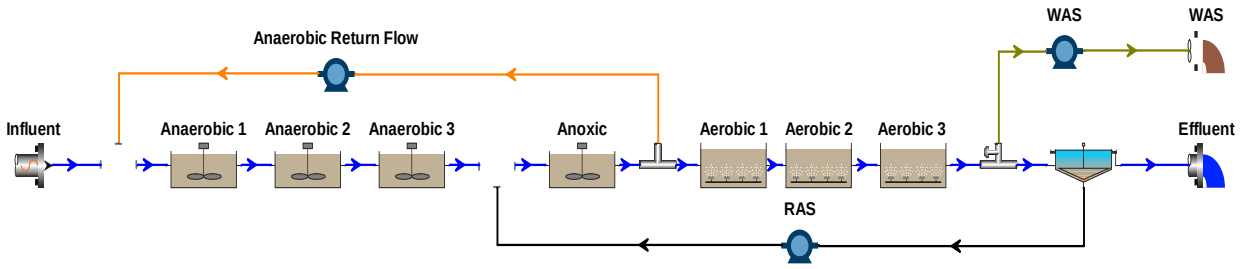

Figure 2.1 Configuration of the pilot plant as a UCT process without nitrate recycle

The pilot plant influent flow was kept constant at 3.2 ± 0.4 liters per minute (lpm) throughout the operation by a constant head tank being continuously fed PE from the full-scale plant. The flow rates for the influent and return flows are listed in Table 2.1. The anaerobic return flow was about equal to the influent flow and the return activated sludge (RAS) flow was about two times the influent flow. The full-scale plant operates the RAS flow at about ½ the influent flow [Brown and Caldwell, 2017]; the pilot plant required a higher RAS flow to ameliorate solids

loading rate limitations of the pilot plant clarifier. This increased RAS flow allowed for greater total nitrogen, TN (NO_x + TAN + organic nitrogen), removal than the full-scale plant experiences because of the increased NO_x return rate to the anoxic tank.

Biomass was removed from the pilot plant, from the third aerobic tank, by a peristaltic pump. To maintain an SRT of 10-12 days, the pump operated for a certain number of hours per day according to a mass balance SRT calculation. The Nine Springs plant operates the activated sludge system at an SRT of approximately 9.5 – 10.4 days [Reusser, 2002]. The waste activated sludge (WAS) flow rate in liters per minute (lpm) and liters per day (lpd) are shown in Table 2.1.

Table 2.1 Pilot plant flow rates

Flow	*Flow Rate (lpm)*
Influent	3.2 ± 0.4
Anaerobic Return	3.0 ± 0.4
RAS	6.4 ± 0.4
WAS	0.089 ± 0.01

The volumes and corresponding HRTs of the anaerobic, anoxic, and aerobic sections of the pilot plant and the clarifier are listed in Table 2.2. All tanks were continuously mixed with paddle mixers. The HRTs were calculated from the influent flow according to Equation 1.6.

Table 2.2 Pilot plant tank volumes and HRTs

Tank	*Volume (L)*	*HRT (hr)*
Anaerobic	295	1.5
Anoxic	397	2.1
Aerobic	1192	6.2
Total Treatment Train	1884	9.8
Clarifier	1011	5.3
Total w/ Clarifier	2895	15.1

The pilot plant volumes and HRTs do not replicate the Nine Springs plant. The volumes (million gallons, MG) and HRTs for the anaerobic, anoxic, and aerobic zones of one West plant UCT configured treatment train are listed in Table 2.3. The HRTs were calculated considering an influent flow of 4.38 million gallons per day (MGD) [Brown and Caldwell, 2017].

Table 2.3 Full-scale volumes and HRTs

Zone	*Volume (MG)*	*HRT (hr)*
Anaerobic	0.50	2.72
Anoxic	0.17	0.91
Aerobic	2.36	12.91
Total Tankage	3.02	16.55

The pilot plant aerobic tanks were aerated using one membrane fine bubble diffuser (Sanitaire Silver Series II, Brown Deer, WI) installed at the bottom of each tank, approximately 4 ft. deep. Air was provided from a connection to the full-scale plant air header and the air flow rate to the individual tanks was controlled by rotameters.

DO concentrations were continuously monitored by an optical DO probe (YSI IQ SensorNet FDO Optical DO sensor) installed in the second aerobic tank and connected to a DO meter (YSI IQ SensorNet 182 meter). The aeration to the three aerobic tanks was controlled by an on/off solenoid actuated valve in response to a maximum DO concentration set point of 0.5 mg-DO/L. The valve turned off if DO exceeded 0.5 mg-DO/L in the second aerobic tank and on if DO dropped below this threshold. Oxygen concentrations were recorded every 20 minutes using LABVIEW (National Instruments, Austin, TX) data acquisition software.

During daily maintenance, DO within the individual aerobic tanks was measured using a portable DO probe (WTW Multi 3410 Multiparameter Meter with FDO 925-6 DO probe). These

spot checks were compared to the optical probe reading in aerobic tank 2 to verify probe accuracy.

2.2 Sampling

To evaluate pilot performance, grab samples were collected from the plant three times per week. Approximately 15 mL of influent and effluent grab samples were filtered through 0.45-µm mixed cellulose esters membrane filters (MF-Millipore, Cork, Ireland) and stored for analysis in the environmental engineering laboratory at the University of Wisconsin-Madison. These filtered samples were analyzed for TAN, reactive phosphorus (orthophosphate, PO_4^{3-}), NO_2^-, NO_3^-, acetate, and soluble chemical oxygen demand (sCOD). To characterize the carbon fractionation of the primary settled wastewater, unfiltered influent grab samples were taken three times per week to measure total chemical oxygen demand (tCOD) at the UW laboratory.

To determine nutrient removal through the treatment train, grab samples were taken weekly or bi-weekly from each tank of the pilot plant. Approximately 25 mL of sample was filtered through 0.45-µm membrane filters for analysis at the MMSD laboratory. These samples were analyzed for total Kjeldahl nitrogen (TKN, organic-N + TAN) and total phosphorus (TP, PO_4^{3-} + organic-P). These samples were also analyzed for TAN, PO_4^{3-}, NO_2^-, NO_3^-, acetate, and sCOD at the UW laboratory. To characterize the nitrogen and phosphorus fractionation of the primary settled wastewater, unfiltered influent grab samples were also used to measure soluble and insoluble TKN and TP at the MMSD laboratory.

To determine MLSS concentrations, 10 mL of mixed liquor samples were taken three times per week from the 2nd anaerobic tank, 2nd aerobic tank, RAS flow, and WAS flow. To assess

clarifier performance, 40 mL of unfiltered effluent were collected. These samples were tested for total suspended solids (TSS) and volatile suspended solids (VSS) at the UW laboratory.

2.3 Sample Analysis

Analytical testing for TAN, PO_4^{3-}, COD, TSS, and VSS were conducted according to Standard Methods for the Examination of Water and Wastewater [American Public Health Association, 2005].

High-pressure liquid chromatography (HPLC) with a Restek Ultra Aqueous C18 column (Restek Corporation, Bellefonte, PA) and a Shimadzu HPLC system (Shimadzu Scientific Instruments, Columbia, MD) was used to analyze for NO_2^-, NO_3^-, and acetate. Sample detection was performed at two wavelengths; 214 nm for NO_2^- and NO_3^- and 210 nm for acetate.

2.4 Primary Effluent Wastewater

The concentration and flow data for the full-scale plant were provided by MMSD. The PE concentration data are from 24-hour time composite sampling of the primary settler effluent from the west primary settlers. The seasonal variability in concentrations to the plant is in concert with seasonal flow variation (Figures 2.2 and 2.3). The TKN and ammonia concentration in the PE are plotted from June 10th, 2016 to December 31st, 2017 (Figure 2.2).

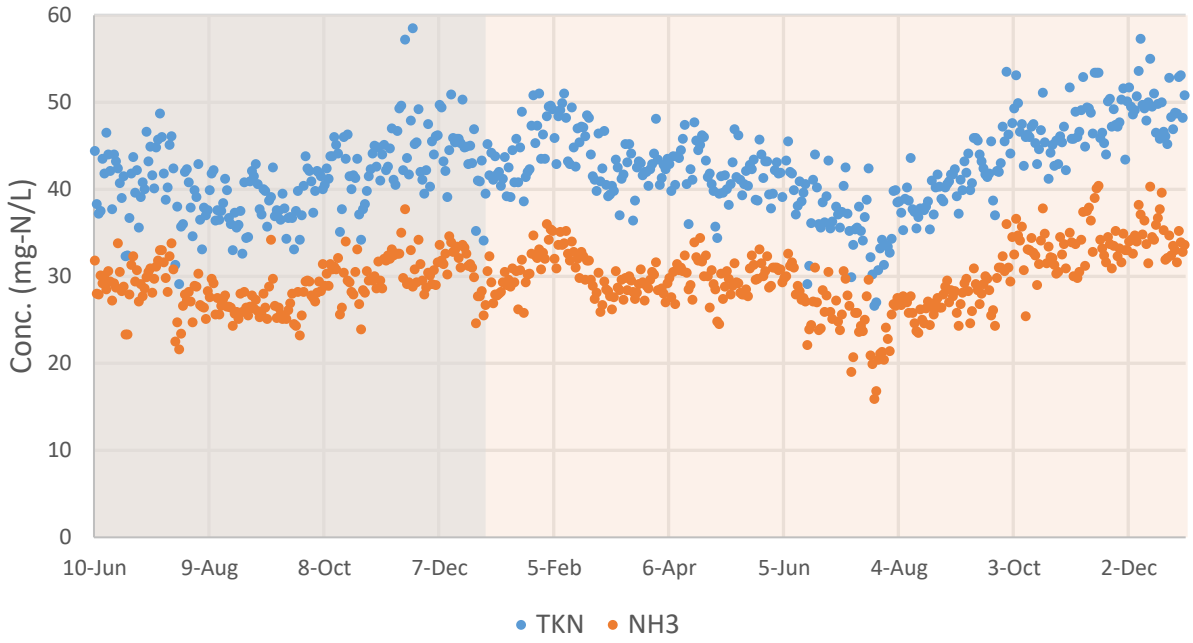

Figure 2.2 Primary effluent seasonal nitrogen concentrations (06/10/2016 to 12/31/2017; shaded regions delineate year)

The flow rate that the full-scale plant receives varies seasonally. With late summer rain storms, inflow and infiltration into the sewers increases the flow rate and dilutes the influent nutrient concentration to the plant, while during the winter, the flow rates decrease and concentrations increase. This is illustrated in Figure 2.3 where July 2017 rain storms dilute the PE TKN concentrations, whereas decreased flow rates in subsequent months are accompanied by an increase in concentrations.

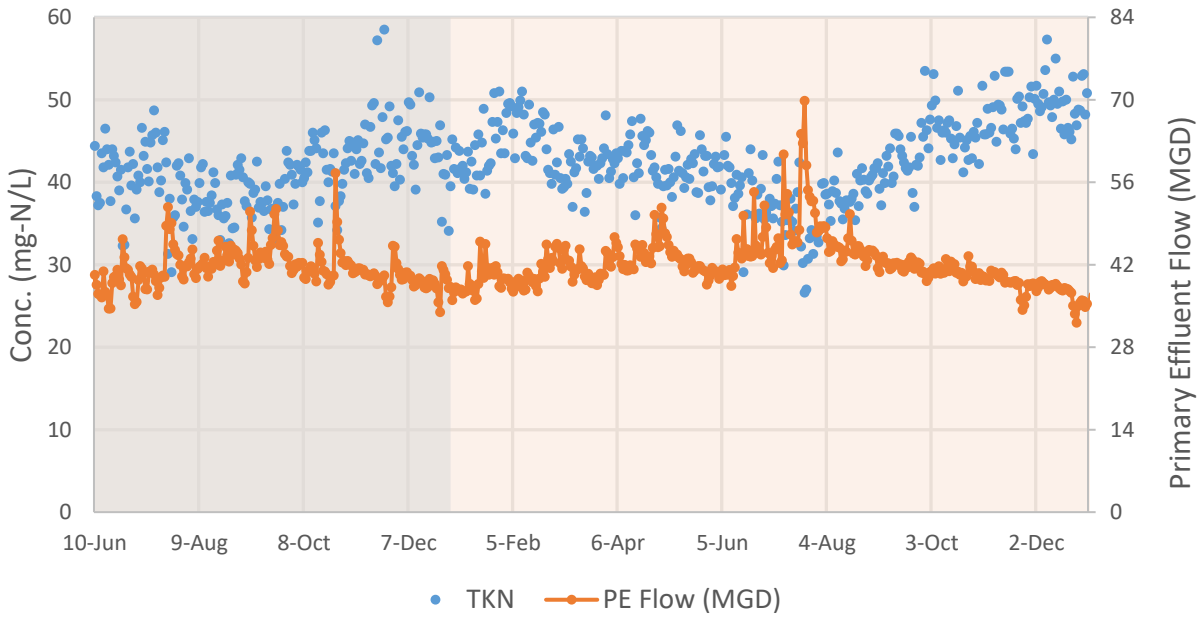

Figure 2.3 Primary effluent flow rates and seasonal nitrogen concentrations (06/10/2016 to 12/31/2017; shaded regions delineate year)

The TP concentration in the PE are plotted (Figure 2.4). Operational changes to the sidestream struvite ($NH_4MgPO_4 \cdot 6H_2O$) harvester have reduced TP concentrations in the PE from June 2016. Seasonal trends are experienced, e.g. July 2017 dilution.

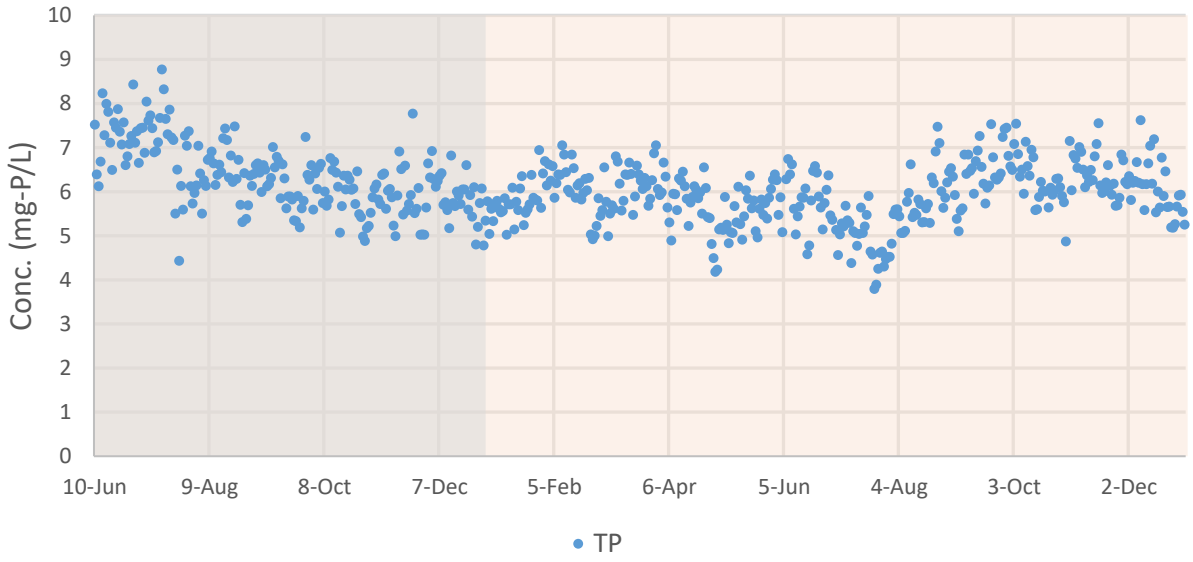

Figure 2.4 Primary effluent seasonal phosphorus concentrations (06/10/2016 to 12/31/2017; shaded regions delineate year)

The five-day biological oxygen demand (BOD_5) and five-day carbonaceous oxygen demand ($CBOD_5$) concentration in the PE are plotted (Figure 2.5). Strong seasonal variation is experienced.

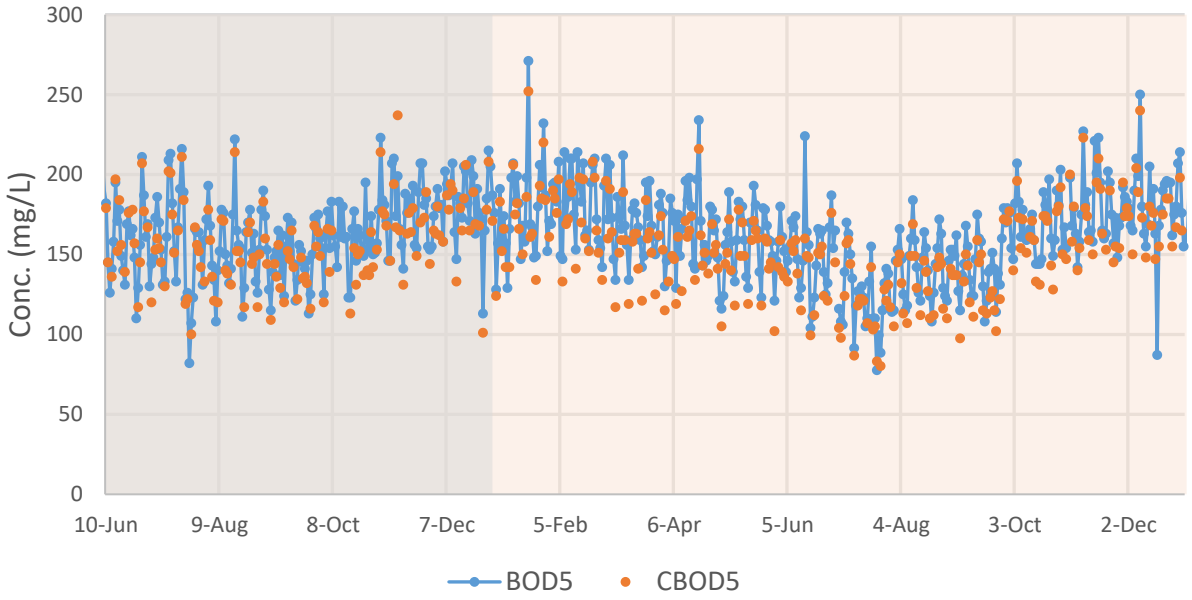

Figure 2.5 Primary effluent seasonal BOD_5 and $CBOD_5$ concentrations (06/10/2016 to 12/31/2017; shaded regions delineate year)

2.5 Pilot Plant Influent

The pilot plant is continuously fed PE from the full-scale west primary settlers. The seasonal variation in PE concentrations has a greater effect on pilot plant influent nutrient loading than on the full-scale plant. The mass loading to the full-scale plant during times of high concentrations are buffered by the lower flow rates. The pilot plant is fed by a constant flow rate; therefore, the nutrient loading to the pilot has a stronger seasonal variation than observed for the full-scale plant (Figure 2.6). Similar seasonal variation is experienced with ammonia, TP, BOD_5, and $CBOD_5$ loadings.

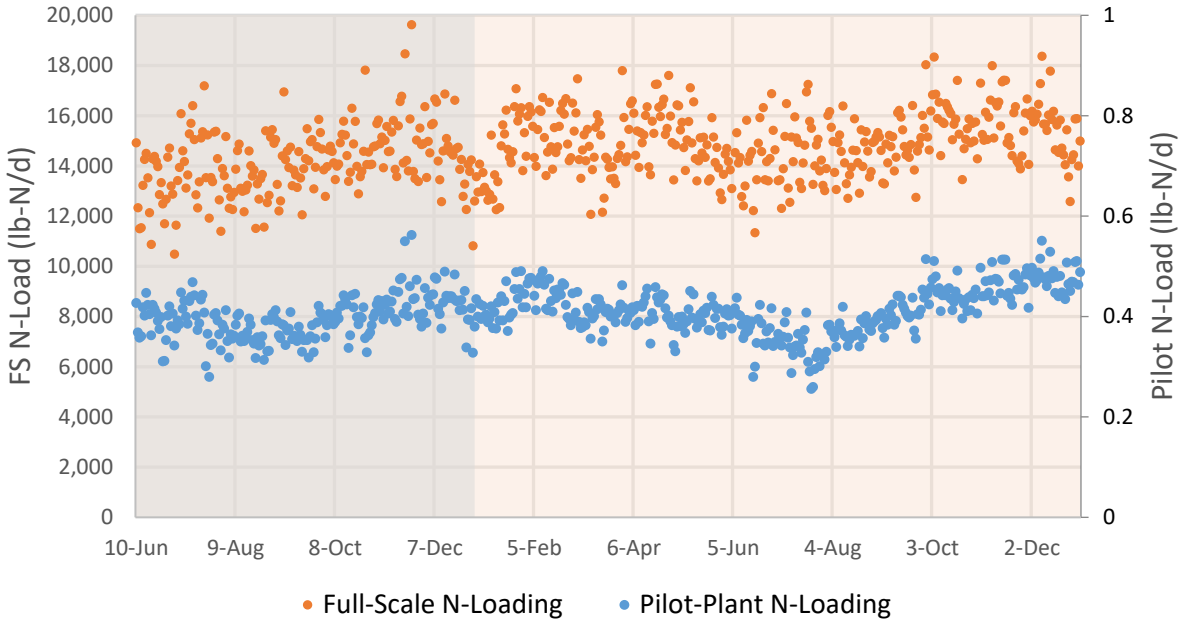

Figure 2.6 Pilot-plant and full-scale seasonal TKN loading (06/10/2016 to 12/31/2017; shaded regions delineate year)

The average and standard deviation for the pilot plant influent concentrations are listed in Table 2.4. These data are from the PE concentration data and the influent sampling COD and acetate measurements. These data are used to characterize pilot plant influent to develop the dynamic model (Section 4.3).

Table 2.4 Pilot plant influent concentrations and WW characteristics

Concentrations	
NH_3 (mg-N/L)	30.7 ± 3.6
TKN (mg-N/L)	43.4 ± 4.8
PO_4^{3-} (mg-P/L)	3.5 ± 0.6
TP (mg-P/L)	6.8 ± 1.0
$CBOD_5$ (mg-O_2/L)	152 ± 26.8
BOD_5 (mg-O_2/L)	165 ± 26.5
Influent Filtered (mg-O_2/L)	226 ± 60.4
Influent Unfiltered (mg-O_2/L)	302 ± 77.8
Influent Acetate (mg/L)	44.4 ± 19.2
WW Characteristics	
NH_3/TKN (-)	0.71 ± 0.05
PO_4^{3-}/TP (-)	0.56 ± 0.08
$CBOD_5$/BOD_5 (-)	0.91 ± 0.06
Filtered/Unfiltered COD (-)	0.75 ± 0.11

2.6 Pilot Plant Performance

The pilot plant performance and nutrient plots presented below (Figures 2.8 – 2.17) span the UCT operation from June 10th, 2016 to December 31st, 2017. The water temperature in the pilot plant during this operational period is presented in Figure 2.7.

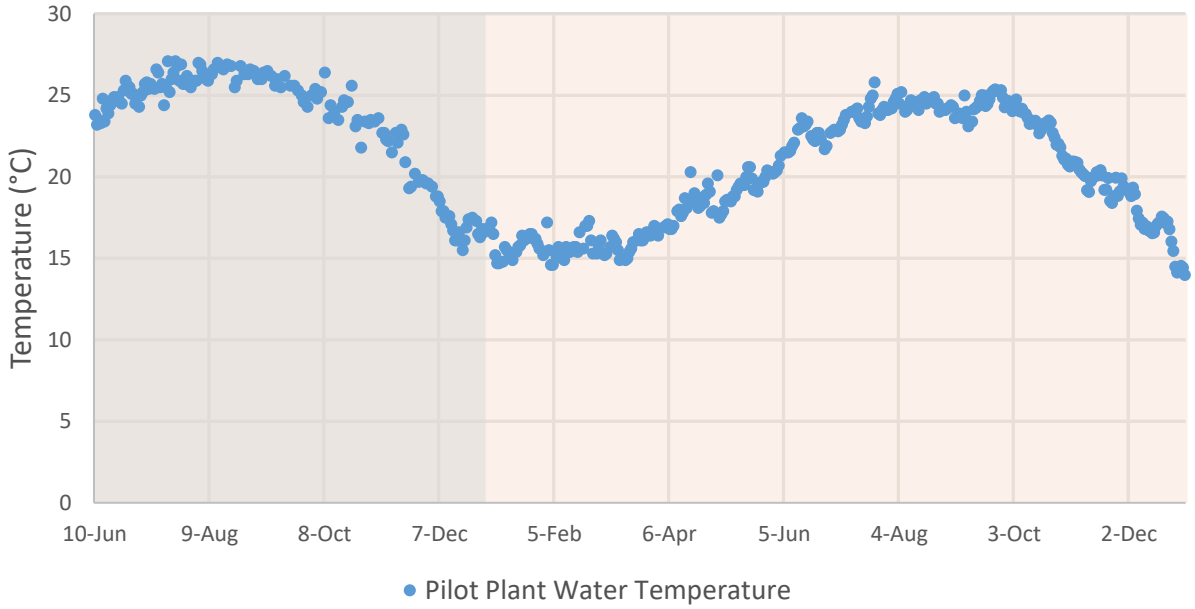

Figure 2.7 Pilot plant seasonal water temperatures (06/10/2016 to 12/31/2017; shaded regions delineate year)

The MLSS sampling measurements of the pilot plant are shown in Figure 2.8. The VSS measurements are indicative of the amount of active biomass in the pilot plant. The anaerobic MLSS concentration is diluted by the mixing of the influent feed with the anaerobic return flow at approximately a 1:1 ratio (Figure 2.1), and therefore it is about ½ the aerobic MLSS concentration.

The trend in MLSS concentration, with OHOs and PAOs comprising a majority of the biomass, is determined by the SRT and the carbon loading to the pilot. The SRT was kept relatively constant while the carbon loading followed seasonal trends (Figure 2.5). There is a lag between

the peak carbon loading to the pilot plant and the peak MLSS concentration as the biomass growth reaches equilibrium. The peak carbon loadings occur by the middle of January, 2017 and the peak MLSS concentration in the pilot occurs by March, 2017. With consistently increasing carbon loading to the pilot plant, a greater MLSS concentration is reached during the winter.

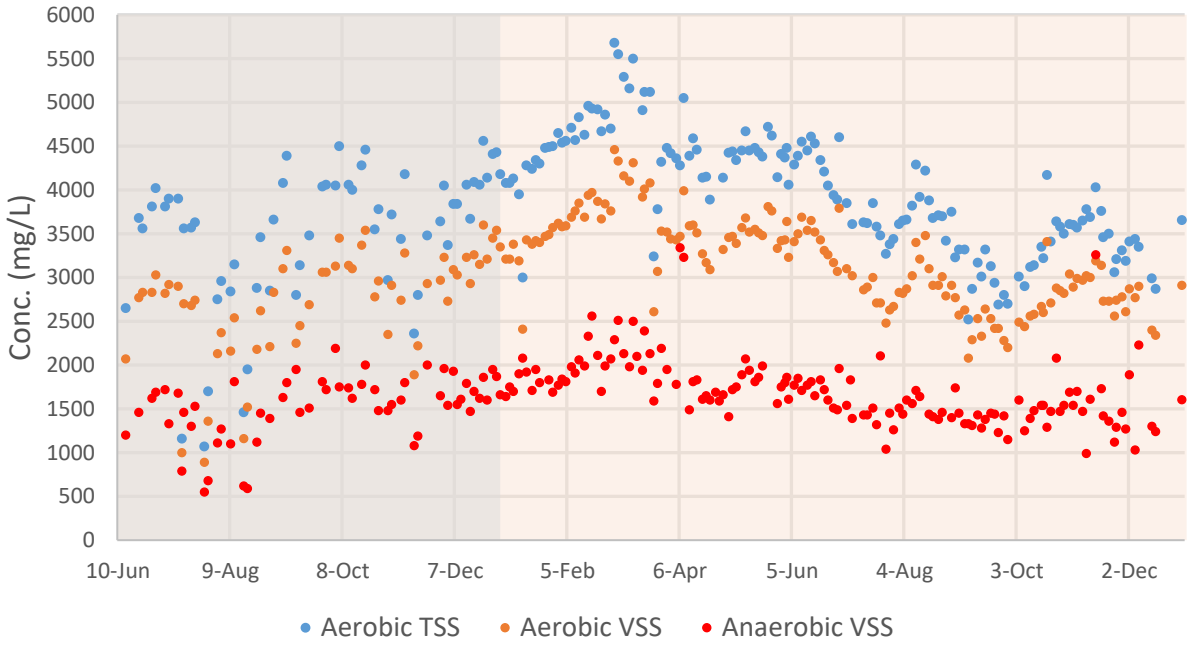

Figure 2.8 Pilot plant MLSS concentrations (06/10/2016 to 12/31/2017; shaded regions delineate year)

The amount of time that the wasting pump was operated per day was adjusted according to Equation 2.1 to maintain an SRT of 10-12 days. Wasting was also adjusted after operational upsets to allow for faster biomass accumulation. Operational upsets occurred on March 22nd and September 28th, 2017, where wasting was reduced or turned off to recover biomass. The wasting pump operation (hours per day, hr/d) and the volume of mixed liquor wasted (liters per day, lpd) are plotted in Figure 2.9. The average wasting rate for the operational period was 127.6 ± 16.4 lpd.

On March 4th, 2017, the wasting time was increased from 1.33 hr/d to a consistent operation of 1.5 hr/d, excepting operational upsets. For 1.5 hr/d of wasting, the wasting rate is 133.7 lpd.

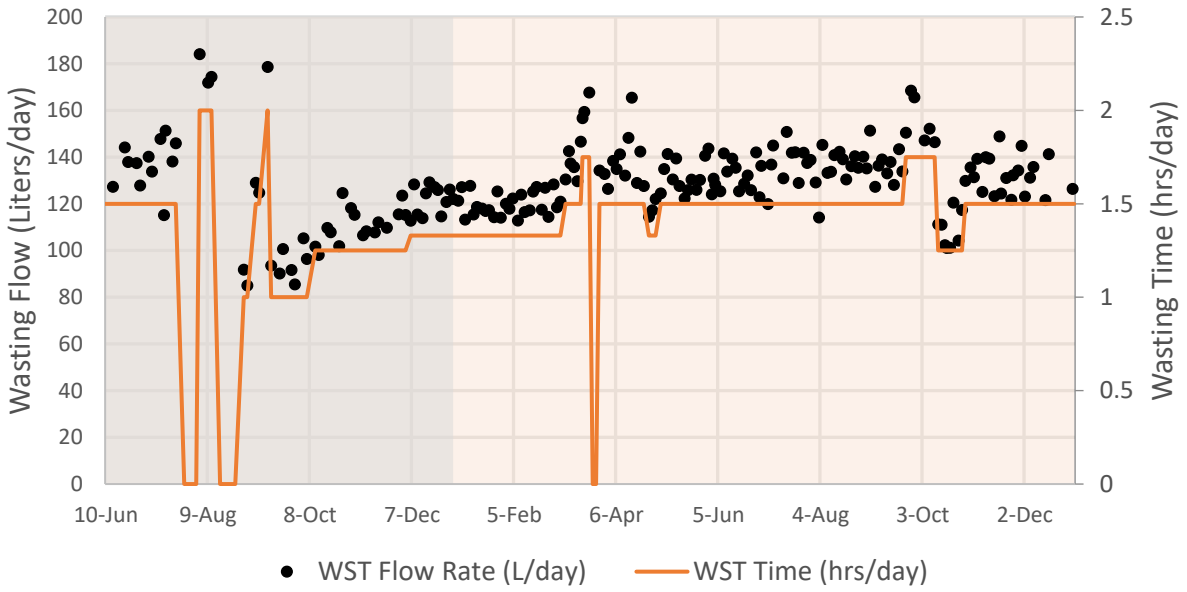

Figure 2.9 Pilot plant wasting flow rates and durations (06/10/2016 to 12/31/2017; shaded regions delineate year)

The MLSS sampling measurements were used to calculate SRT according to Equation 2.1:

$$SRT\ (days) = \frac{V_{anaerobic} * MLSS_{anaerobic} + (V_{anoxic} + V_{aerobic}) * MLSS_{aerobic}}{Q_w * MLSS_{wasting} + (Q_{effluent} - Q_w) * MLSS_{effluent}} \quad 2.1$$

Where:

V_x = Volume of specified tankage (L)

$MLSS_x$ = MLSS concentration of specified sample $\left(\frac{mg-TSS}{L}\right)$

Q_w = Wasting flow rate $\left(\frac{L}{d}\right)$

$Q_{effluent}$ = Effluent flow rate = influent flow rate $\left(\frac{L}{d}\right)$

The calculated SRTs for the UCT operation are shown in Figure 2.10. The initial stabilization period after UCT reconfiguration showed sporadic upsets in SRT due to poor clarifier performance leading to biomass in the effluent. After which, the SRT remained fairly constant, excepting operational upsets. For the operational period studied, the SRT was 12.0 ± 2.1 days.

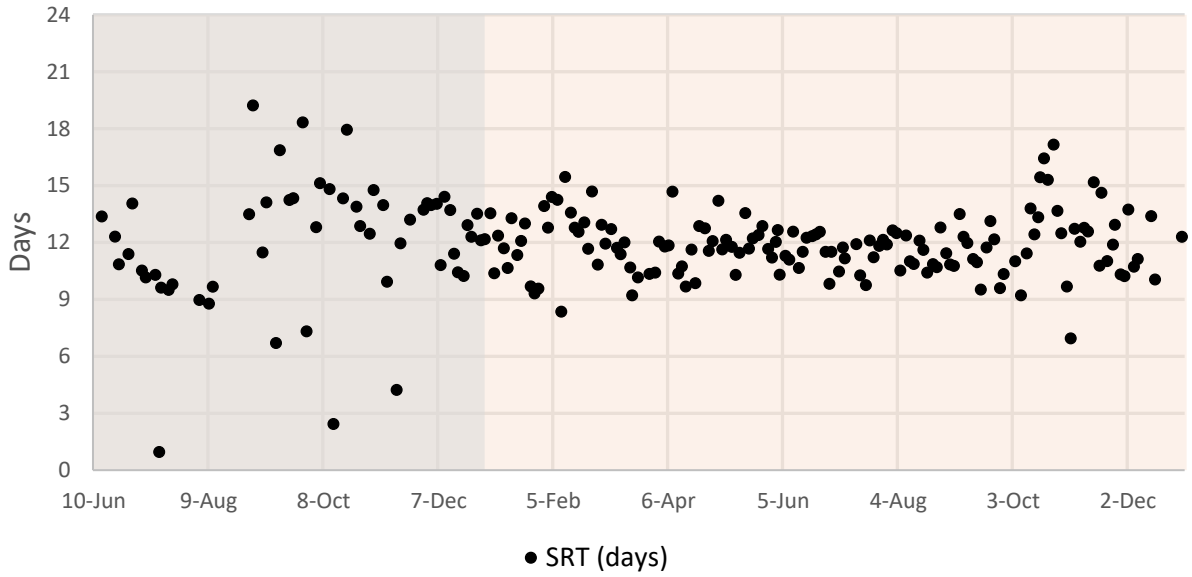

Figure 2.10 Pilot plant SRT (06/10/2016 to 12/31/2017; shaded regions delineate year)
*For SRTs considering biomass wasting from clarifier scum removal, see Appendix.

The air flow rates to each aerobic tank were tapered in response to decreasing oxygen demand as wastewater is treated through the aeration zone (Figures 2.11 – 2.13). The average DO concentration over the operation within the aerobic tanks are listed in Table 2.5. The DO concentrations within aerobic tank 3 (AER3) were more variable in response to fluctuating oxygen demand loading to the pilot plant. The average DO across all three tanks was 0.39 ± 0.16 mg-DO/L.

Table 2.5 Aerobic tank average DO concentrations

Aeration Tank	*DO Conc. (mg/L)*
AER1	0.38 ± 0.16
AER2	0.38 ± 0.11
AER3	0.42 ± 0.38
Across All Tanks	0.39 ± 0.16

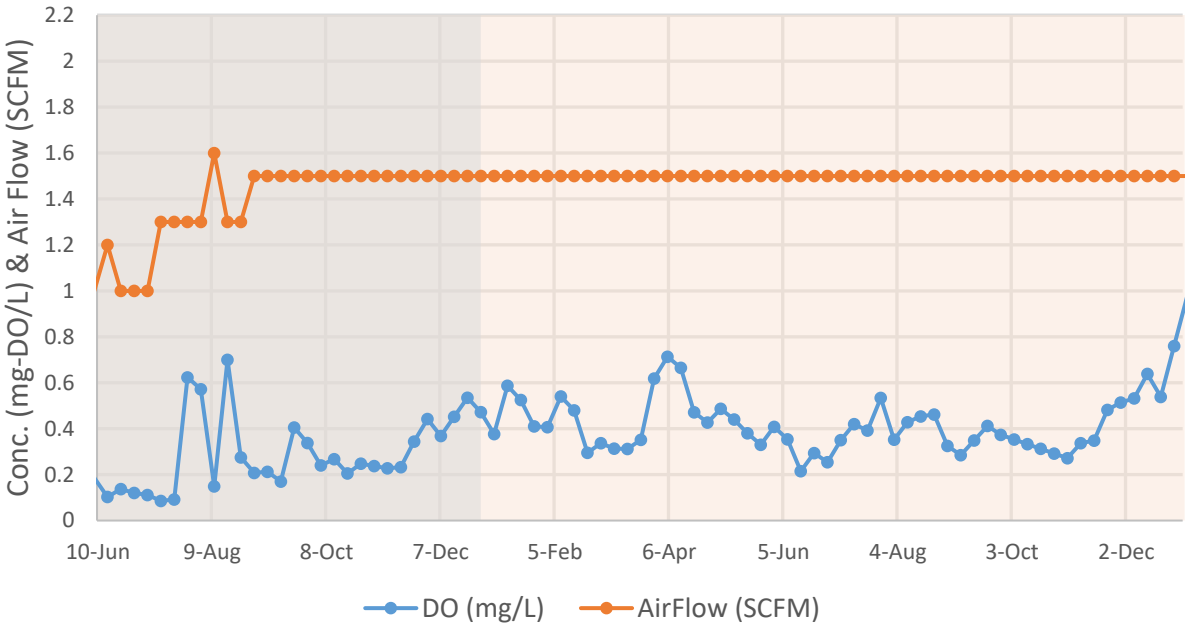

Figure 2.11 Aer 1 weekly average DO concentrations; data from daily spot checks (06/10/2016 to 12/31/2017; shaded regions delineate year)

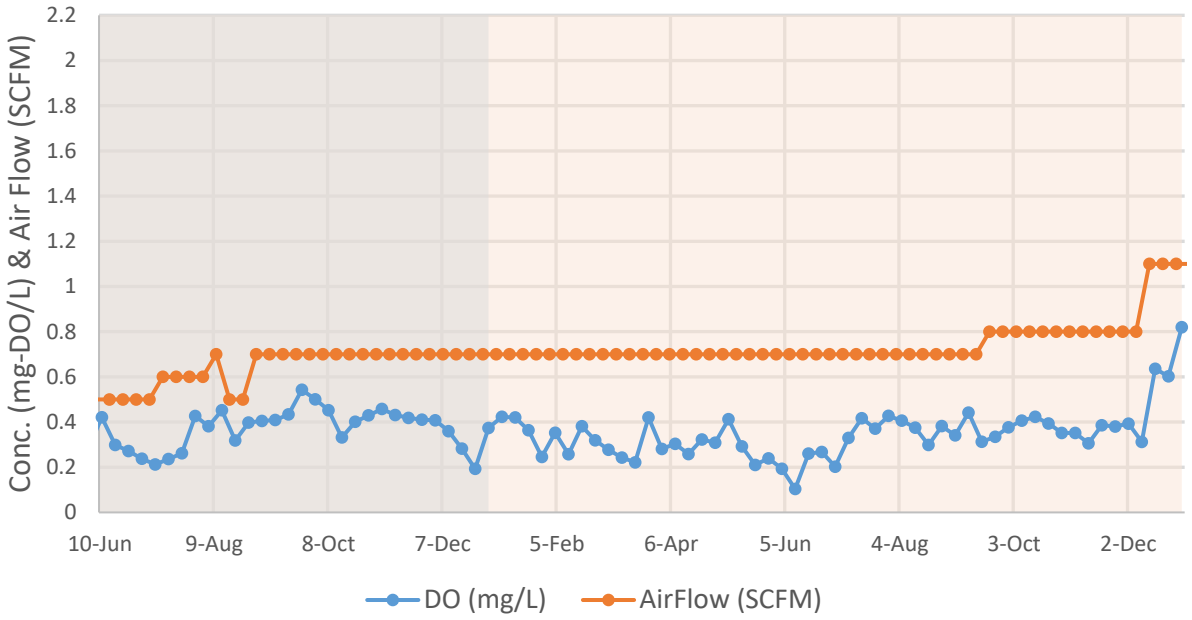

Figure 2.12 Aer 2 weekly average DO concentrations; data from continuously monitoring optical probe (06/10/2016 to 12/31/2017; shaded regions delineate year)

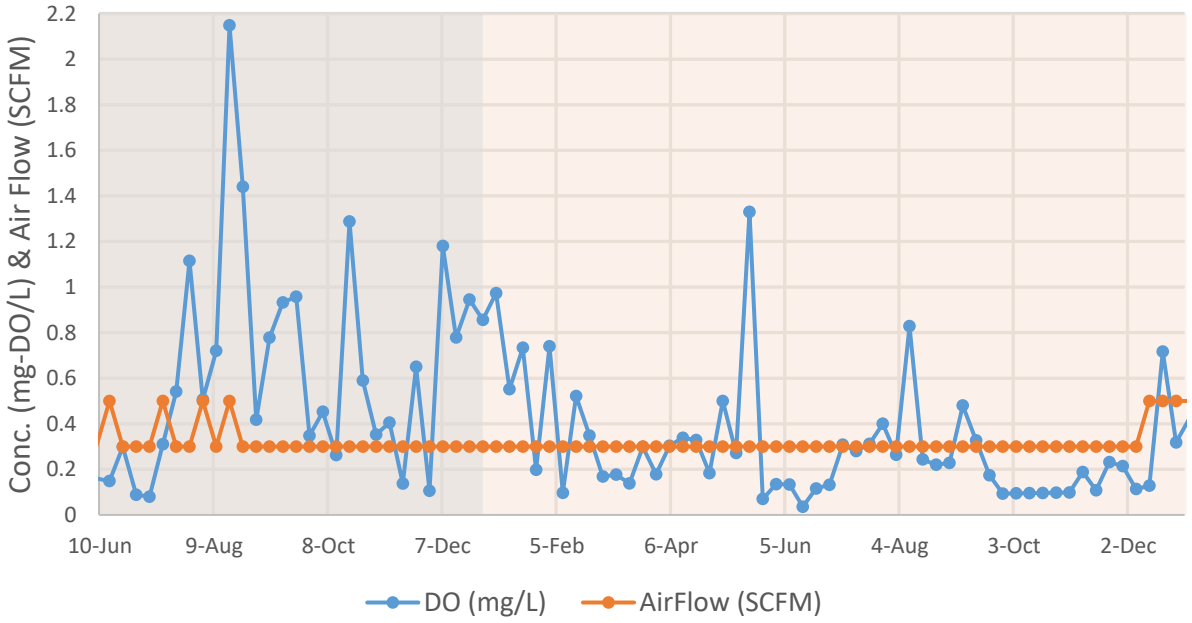

Figure 2.13 Aer 3 weekly average DO concentrations; data from daily spot checks (06/10/2016 to 12/31/2017; shaded regions delineate year)

The total air flow rate to the aeration train is shown in Figure 2.14, along with the average DO across the aeration train. The figure shows two periods where increased oxygen demand loading may have caused suppressed oxygen concentrations. The higher loading throughout the winter may explain the reduced DO experienced from February 15th, 2016 to March 15th, 2017. The spike in BOD loading experienced on June 14th, 2017 (Figure 2.5) may explain the drop in observed DO.

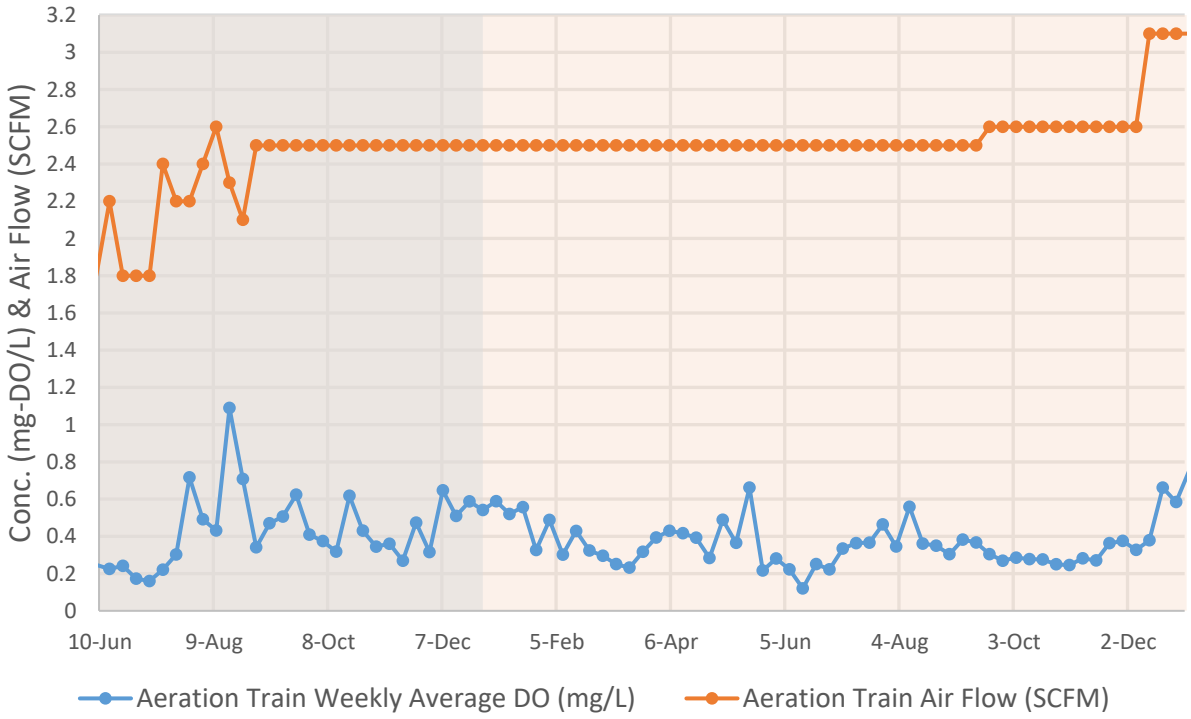

Figure 2.14 Weekly average DO concentrations and total air flow across aeration train (06/10/2016 to 12/31/2017; shaded regions delineate year)

TKN concentrations are plotted in Figure 2.15. After stabilization by August 4th, 2016, TKN removal was consistent throughout the summer and into the winter. The first occurrence of poor TKN removal was measured on January 26th, 2017. Consistent removal did not return until July 20th, 2017. The upset measured on September 28th was due to an operational failure where removal recovered by October 26th, 2017. Deteriorating TKN removal performance was observed again by December 12th, 2017.

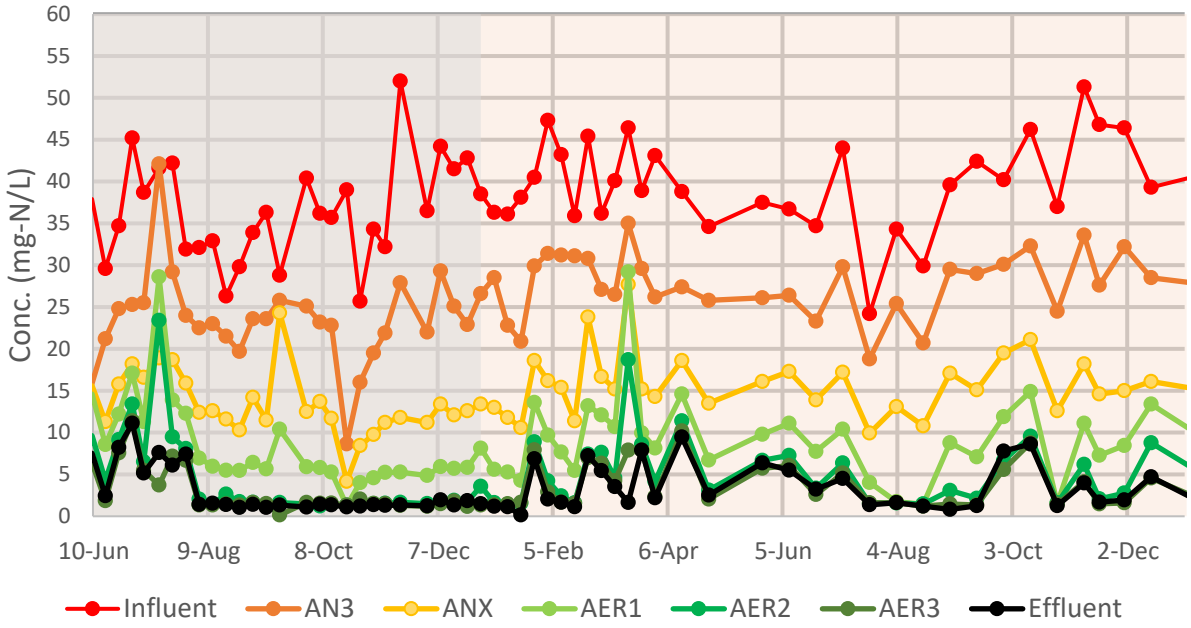

Figure 2.15 Pilot plant TKN concentration profile data (06/10/2016 to 12/31/2017; shaded regions delineate year)

The NO_x concentration data at the end of the aerobic zone (Figure 2.16) shows that the pilot plant did not experience significant accumulation of NO_2^- throughout the operation; therefore, throughout the entire operation, AOB and NOB responded similarly to changes in operational and environmental conditions. No accumulation of NO_x within the anoxic tank was observed where all NO_x returned via the RAS flow was denitrified.

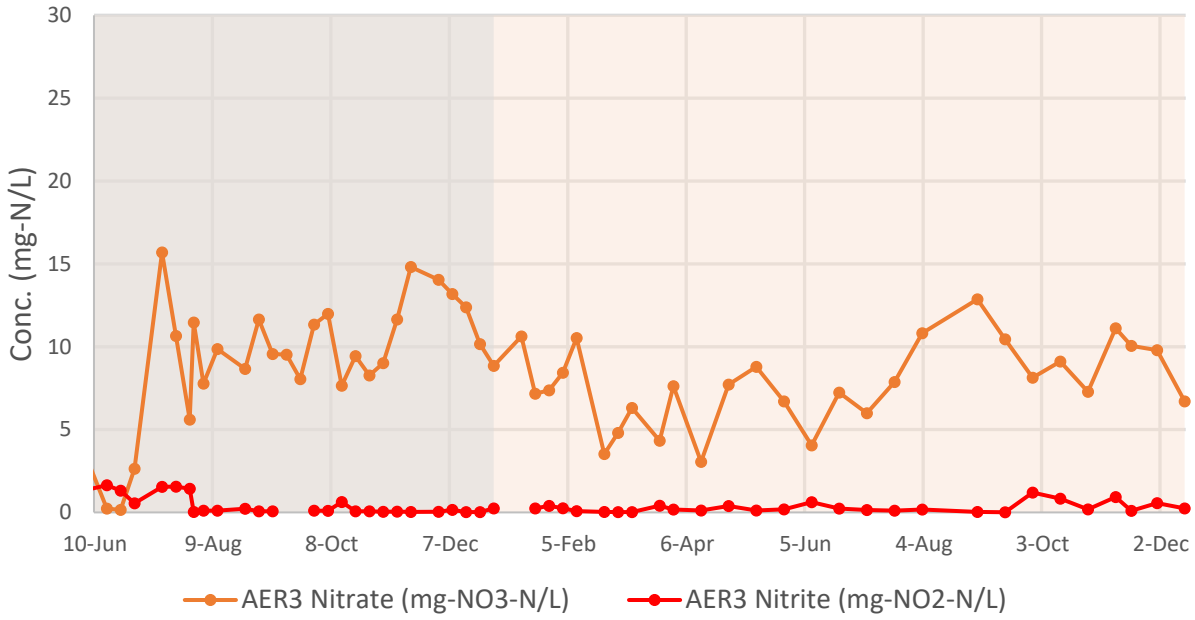

Figure 2.16 Pilot plant NOx performance (06/10/2016 to 12/14/2017; shaded regions delineate year)

The ammonia concentration is diluted from the anaerobic train to the anoxic tank by the RAS flow. The reduced NO_3^- concentration at the end of the aerobic zone, especially during the winter, may be partially explained by low DO conditions contributing to simultaneous nitrification denitrification (SND) in the aerobic zone or by the on/off nature of the aeration control system.

The TP concentration data are plotted in Figure 2.17. Phosphorus release occurs in the anaerobic zone where the concentration is diluted in the anoxic tank by the RAS flow. Phosphorus uptake in the aerobic zone is rapid with an average TP concentration for the UCT operation in aerobic tank 1 of 4.5 ± 4.1 mg-P/L and in aerobic tank 2 of 0.70 ± 1.3 mg-P/L.

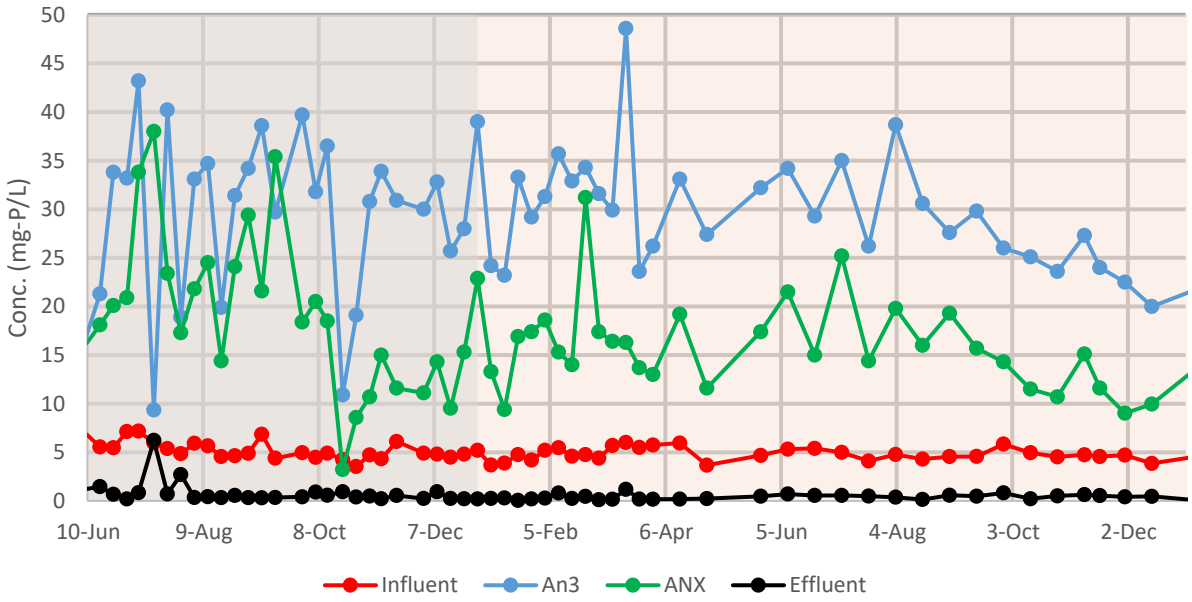

Figure 2.17 Pilot plant TP performance (06/10/2016 to 12/14/2017; shaded regions delineate year)

The sampling procedure captures one data point in time for pilot plant performance. These samples do not reflect the diurnal variations that occur with pilot plant nutrient loading. A sampling event, performed by Nine Springs plant in October 2014, illustrates the diurnal loading pattern experienced by the full-scale plant (Figure 2.18) [Brown and Caldwell, 2017]. The pilot plant sampling was performed during daily maintenance, typically in the earlier part of the morning. It is unknown if any particular sample captured the peak daily loading conditions. Furthermore, these loading patterns will be affected by seasonal and weather related conditions

(Section 2.5). The profile grab sampling procedure is limited in capturing real pilot plant performance.

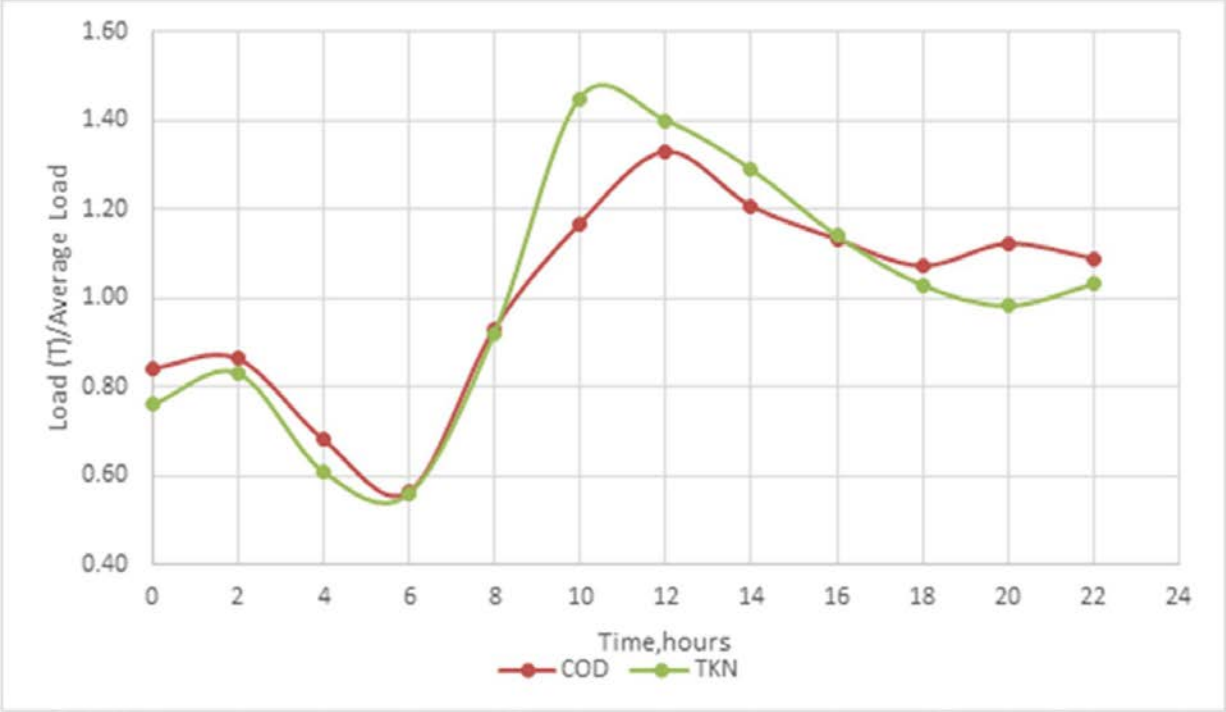

Figure 2.18 Pilot plant diurnal load profile from October 2014 sampling event performed by Brown and Caldwell consultants [Brown and Caldwell, 2017]

CHAPTER 3 : BATCH KINETIC TESTING

To characterize the performance of the AOB and NOB communities growing in low DO conditions, batch kinetic experiments were performed. These experiments were conducted to estimate the Monod kinetic parameters of the organisms growing in the pilot plant. Since this research concerns the performance of AOB and NOB at low DO conditions, DO was the substrate of interest regarding Monod kinetics (Equation 1.1).

To evaluate the seasonal variation of kinetic parameters for the low-DO AOB and NOB communities within the pilot plant, experiments were performed at different times throughout the year.

In addition, batch kinetic experiments were performed on full-scale activated sludge to compare the performance of low-DO communities to those growing in high DO conditions. This data is presented in the Appendix.

3.1 Methods

Activated sludge samples were collected and transported to the UW laboratory. Experiments were performed in a 3.2 L batch reactor placed on top of a hotplate with a continuously mixing magnetic stir bar. For winter experiments, sludge was heated to approximately 20°C. Upon reaching this temperature, aeration was turned on to initiate the experiments.

Air was supplied using an aquarium air pump and a ceramic diffuser stone. The air pump was turned on or off by a digital switch according to a maximum DO concentration set point. The

DO was measured by a portable DO probe and meter (WTW Multi 3410 Multiparameter Meter with FDO 925-6 dissolved oxygen probe) interfacing with a data logging and supervisory control module (LABVIEW, National Instruments, Austin, TX). DO concentration data was recorded at one second intervals.

Before the start of aeration, 10 mL of sample were filtered through 0.45-µm mixed cellulose esters membrane filters (MF-Millipore, Cork, Ireland) to measure initial substrate concentrations. To measure MLSS, 10 mL of unfiltered sample were taken. Upon start of aeration, samples were collected and filtered at regular intervals for at least one hour to measure substrate consumption rates.

For AOB kinetic experiments, 3 L of activated sludge were collected from the end of the anaerobic zone, where residual ammonia concentration is high. For NOB kinetic experiments, 3 L of activated sludge were taken from the end of the aerobic zone where BOD and ammonia concentrations are low. A solution of sodium nitrite ($NaNO_2$) was used to spike nitrite into the batch reactor before the start of aeration. To prevent oxidation of residual ammonia within the mixed liquor, allylthiourea (ATU) was added to the batch reactor to a concentration of 5 mg/L [Camejo, 2016].

These experiments were also performed on full-scale activated sludge from the West, UCT configured plant. Similar to experiments with pilot plant samples, activated sludge was collected from the end of the anaerobic and end of aerobic zones for AOB and NOB experiments, respectively (see Appendix).

3.2 Data Analysis

The ammonia and nitrite removal rates were determined from ANOVA linear regression of concentrations over time for experiments conducted at different DO concentrations. Specific removal rates were calculated, dividing the rates by the measured VSS concentration for each batch experiment.

The specific ammonia and nitrite utilization rates at each DO were used to determine the Monod kinetic parameters q_{max} and K_{DO} (Equation 3.1). Utilizing the non-linear regression Solver function in Excel, the sum of squared errors (SSE) between observed and modeled specific utilization rates was minimized as a function of the q_{max} and K_{DO} parameters. The significance, p-value, and standard error (SE) of these model fitted parameters were analyzed with a dose response model for a two-parameter fit using R statistical computing software [Ritz, 2015].

$$q = q_{max} \times \frac{DO}{K_{DO} + DO} \qquad 3.1$$

Where:

q = Specific rate of substrate utilization at specific DO concentration $\left(\frac{\text{mg}-\text{N}}{\text{mg}-\text{VSS}-\text{d}}\right)$

DO = Dissolved oxygen concentration $\left(\frac{\text{mg}-\text{DO}}{\text{L}}\right)$

q_{max} = Maximum specific rate of substrate utilization $\left(\frac{\text{mg}-\text{N}}{\text{mg}-\text{VSS}-\text{d}}\right)$

K_{DO} = Oxygen half saturation constant $\left(\frac{\text{mg}-\text{DO}}{L}\right)$

The maximum ammonia removal rates for specific DO experiments were determined from ANOVA linear regression of the concentration over time data. The significance of the difference in slopes between the March and September data was analyzed by a t-test comparison of the standard error of the regression model slopes for two independent samples using an unequal and pooled error variance assumption [Andrade, 2014].

3.3 Results

3.3.1 Best-fit Kinetic Parameters for AOB

The best-fit kinetic parameters for AOB and the average pilot water temperature for the month the experiments were conducted are listed in Table 3.1. The estimated q_{max} for September 2017 was significantly higher than the estimated value for March 2017 (Figure 3.1).

Table 3.1 AOB batch test results

Experiment	Mar-2017		Sep-2017	
Monthly Average Pilot Water Temperatures (°C)	15.9 ± 0.6		24.5 ± 0.6	
Parameter	$q_{max}\left(\frac{mg-N}{mg-VSS-d}\right)$	$K_{DO}\left(\frac{mg-DO}{L}\right)$	$q_{max}\left(\frac{mg-N}{mg-VSS-d}\right)$	$K_{DO}\left(\frac{mg-DO}{L}\right)$
Model Fit ± SE	0.097 ± 0.0040	0.42 ± 0.070	0.17 ± 0.018	0.36 ± 0.16
*p-value**	<0.00001	0.00055	0.0023	0.10

*p-value of significance from dose response model statistical analysis in R

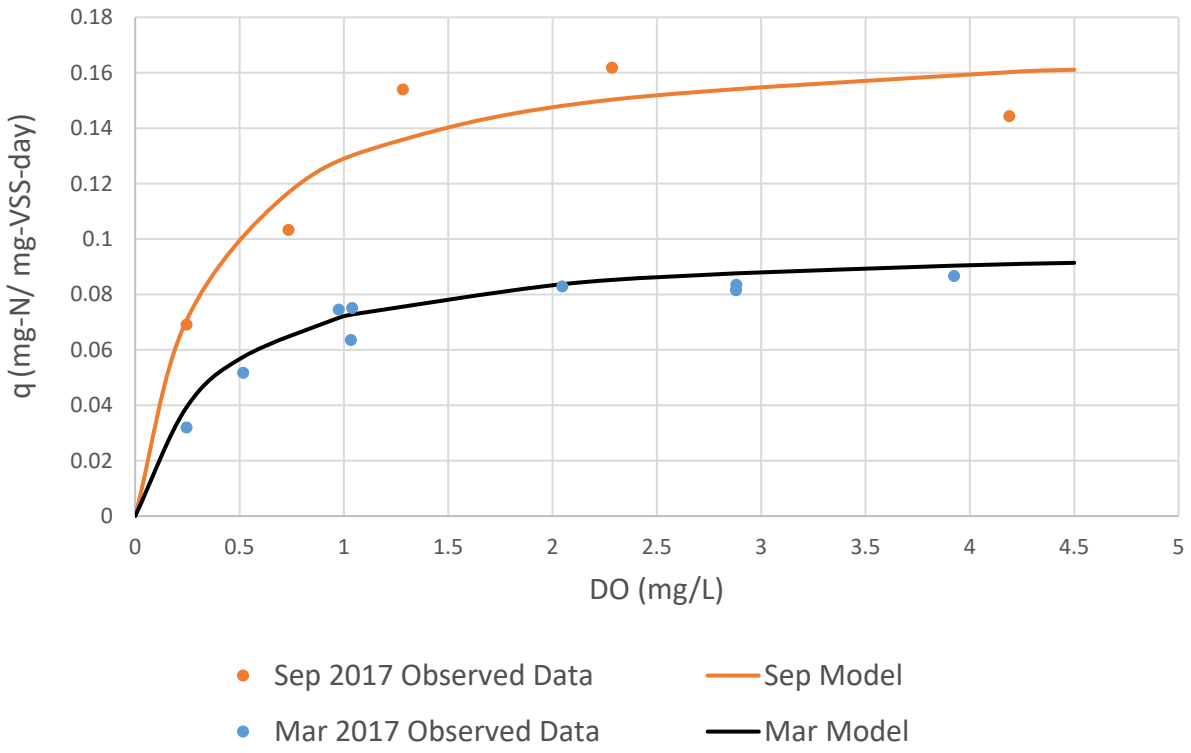

Figure 3.1 AOB batch test data and Monod curves

The best fit estimates for K_{DO} were not significantly different. Given the larger variability of the September 2017 estimate, the K_{DO} estimate for March 2017, 0.42 mg-DO/L, was selected for any further analyses.

The best-fit K_{DO} estimates for the full-scale plant were higher than those for the pilot (Table A.1 - A.2 in Appendix), confirming a prior observation of higher affinity for oxygen of the low-DO enriched AOB communities [Keene, 2016].

3.3.2 AOB Population: Maximum Ammonia Removal Rates

Activated sludge samples with greater populations of AOBs will have higher rates of ammonia removal (Equation 1.5). To compare the populations of AOBs at different times throughout the year, the maximum ammonia removal rates for high DO experiments conducted on March 20th, 2017 and September 2nd, 2017 are calculated.

The conditions of these experiments are listed in Table 3.2. The March 20th, 2017 batch test was heated to 22.5°C. The DO concentrations were in excess, therefore the maximum ammonia removal rates are measured.

Table 3.2 High DO AOB batch test conditions

Experiment	*Monthly AVG Water Temps (°C)*	*AVG Batch Test Water Temps (°C)*	*AVG DO of Experiments (mg-DO/L)*
20-Mar-17	15.9 ± 0.6	22.5 ± 0.9	3.9 ± 0.4
2-Sep-17	24.5 ± 0.6	24.3 ± 0.1	4.2 ± 0.7

The maximum ammonia removal rate for the September 2nd, 2017 experiment is greater than the March 20th, 2017 experiment (Figure 3.2). The ammonia concentrations were in excess and the linear trend in the concentration data reflects no ammonia substrate limitations. These slopes are significantly different ($p < 0.00001$) according to a t-test comparison. The measured maximum ammonia removal rates were 6.40 and 9.04 mg-N/L-hr for the March 20th and September 2nd, 2017 experiments (equations inset in Figure 3.2).

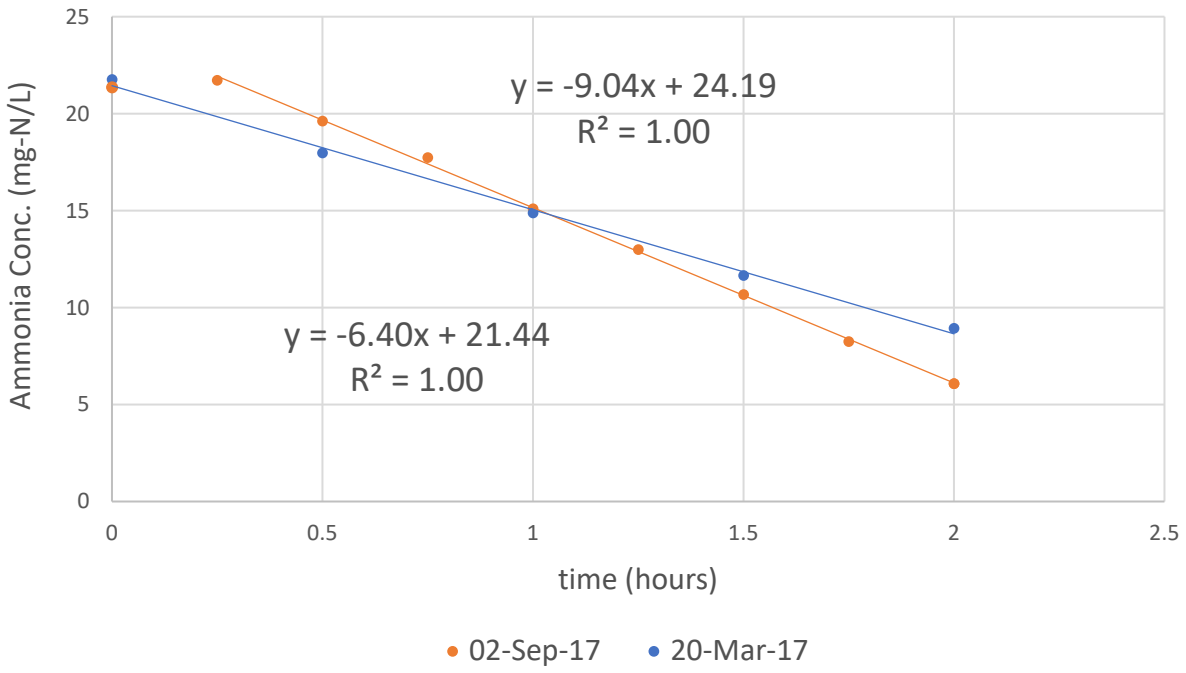

Figure 3.2 Individual high DO batch test data for max AOB N-removal rates

3.3.3 Best-fit Kinetic Parameters for NOB

The best-fit kinetic parameters for NOB are listed in Table 3.3. The estimated q_{max} is greater for the September 2017 experiments than for experiments conducted during times of pilot plant low water temperatures (Figure 3.3).

Table 3.3 NOB batch test results

Experiment	Mar-17		Sep-17		Jan-18	
Parameter	$q_{max}\left(\frac{mg-N}{mg-VSS-d}\right)$	$K_{DO}\left(\frac{mg-DO}{L}\right)$	$q_{max}\left(\frac{mg-N}{mg-VSS-d}\right)$	$K_{DO}\left(\frac{mg-DO}{L}\right)$	$q_{max}\left(\frac{mg-N}{mg-VSS-d}\right)$	$K_{DO}\left(\frac{mg-DO}{L}\right)$
Model Fit ± SE	0.074 ± 0.0095	0.076 ± 0.055	0.13 ± 0.017	0.13 ± 0.11	0.052 ± 0.0039	0.092 ± 0.055
*p-value**	0.0015	0.24	0.087	0.46	0.00091	0.19

*p-value of significance from dose response model statistical analysis in R

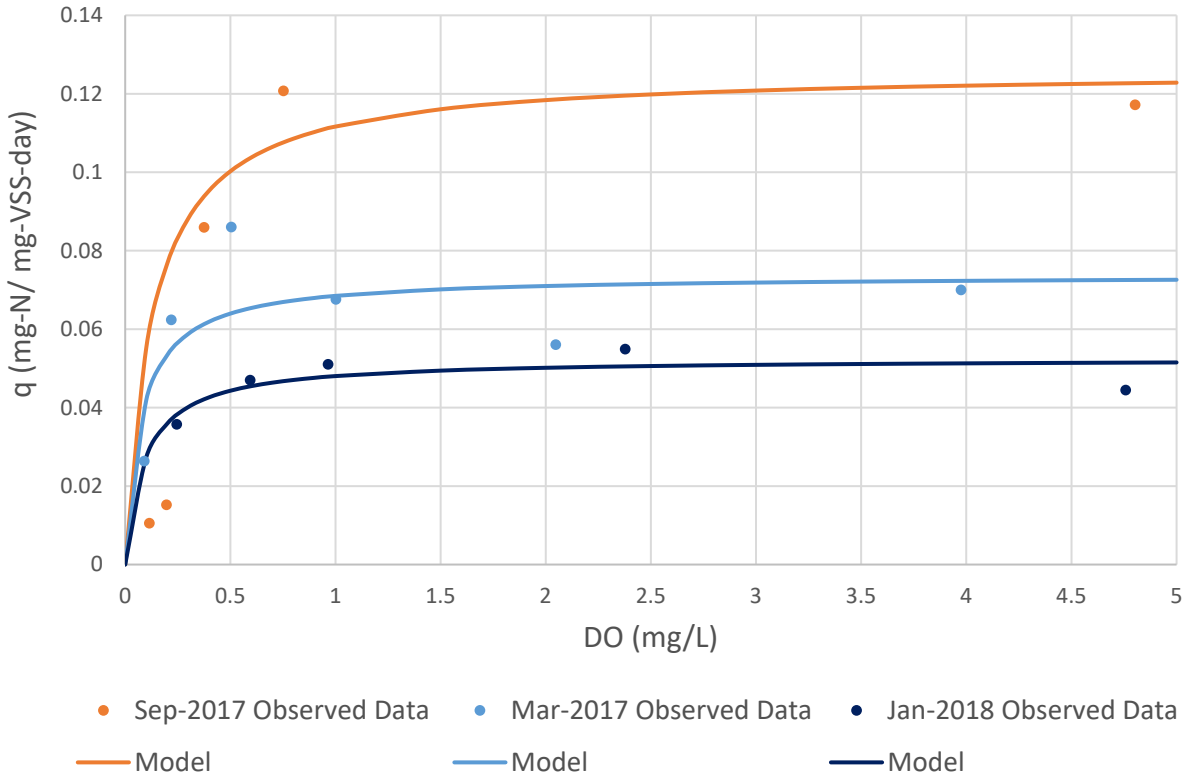

Figure 3.3 NOB batch test data and Monod curves

The average of the K_{DO} estimates for these experiments is 0.099 mg-DO/L. Though the model fits are not significantly different ($p>0.05$), considering the SE they do approximate each other. The NOB K_{DO} of 0.10 mg-DO/L was selected for any further analysis.

The best-fit K_{DO} estimates for the full-scale plant were higher than those for the pilot (Table A.3 - A.4 in Appendix). These data demonstrate that the low-DO enriched NOB communities exhibit a higher affinity for oxygen than the high-DO NOB communities.

CHAPTER 4 : DYNAMIC MODEL

A BioWin™ 5.2 dynamic model was constructed to simulate the nutrient removal performance of the pilot plant. The model was developed in a sequential manner to evaluate the contributing factors to pilot nutrient removal performance.

The model was used to simulate reactor performance from August 9th, 2016, to December 31st, 2017. The following variables were incorporated into the model:

- Pilot plant conditions: Water temperatures, DO concentrations
- Variable nutrient loading
- Operational factors: SRT, HRT
- Kinetic parameters

4.1 Influent Characteristics

The influent inputs to the model varied daily according to the 24-hour time composite PE data (Section 2.4). Direct inputs were TKN and TP concentrations, whereas tCOD concentrations were calculated from BOD_5 PE data by applying a 2.1-times factor [Brown and Caldwell, 2017]. COD, TKN, and TP fractionation were calculated according to default and customized wastewater characterization values. The influent flow rate was set to be constant at 3.15 lpm (4,536 lpd).

The influent alkalinity was constant at 4.54 mmol/L (454 mg /L as $CaCO_3$). The influent Ca^{2+} and M_g^{2+} concentrations were constant at 70 and 40 mg/L [Grande, 2015]. The inorganic fixed suspended solids (ISS) concentration was constant at 3 mg/L. The influent pH varied daily according to PE data.

4.2 Control Simulation

As a control, the model was run using default wastewater characterization and default kinetic parameters. The configuration of the model mirrors the pilot plant UCT configuration (Figure 4.1). The volumes and flow rates were those presented in Section 2.1. Each unit tank was assumed to be completely mixed. The clarifier for these simulations was considered ideal; therefore, no biomass left the system through the effluent and the SRT was completely controlled by the WAS flow rate.

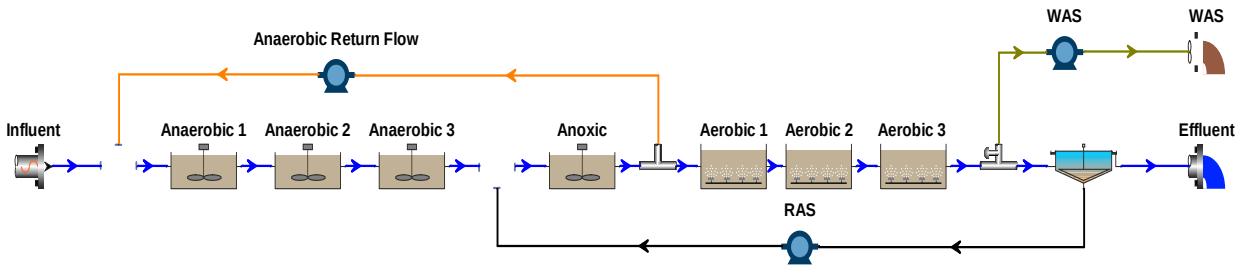

Figure 4.1 Model configuration for Biowin simulations

The simulated water temperatures varied seasonally and the DO concentrations within the aerobic tanks were assumed constant (Figure 4.2). The DO concentrations in the aerobic tanks were the averages for the operational period, Table 2.7.

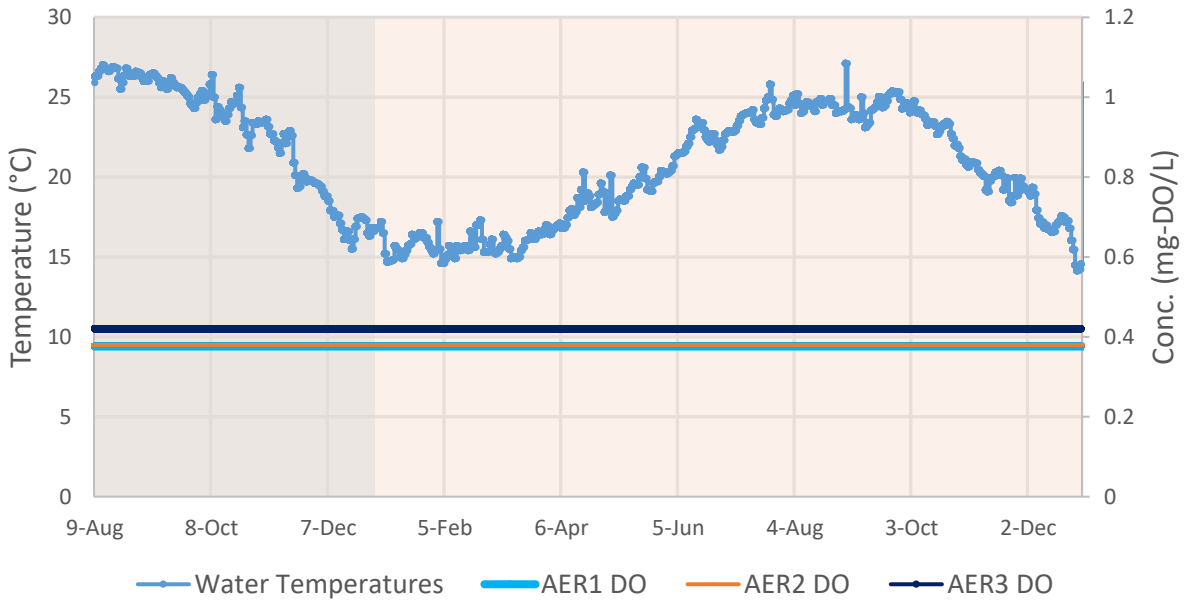

Figure 4.2 Control model simulation water temperatures and constant DOs (08/09/2016 to 12/31/2017; shaded regions delineate year)

The simulated WAS flow rate was determined by specifying an actively controlled SRT. The simulator then calculated a steady state WAS flow rate solution to achieve that SRT. To match the observed pilot plant WAS flow rate of 133.7 lpd for 1.5 hr/d of wasting, the SRT was set to 12.93 days and a wasting flow rate of 133.45 lpd was calculated.

The simulated MLSS concentrations were mostly dependent on tCOD loading and SRT (Figure 4.3). The MLSS concentrations followed the seasonal tCOD loading. The simulated concentrations were about 1,000 mg/L less than the measured concentrations (Figure 2.8).

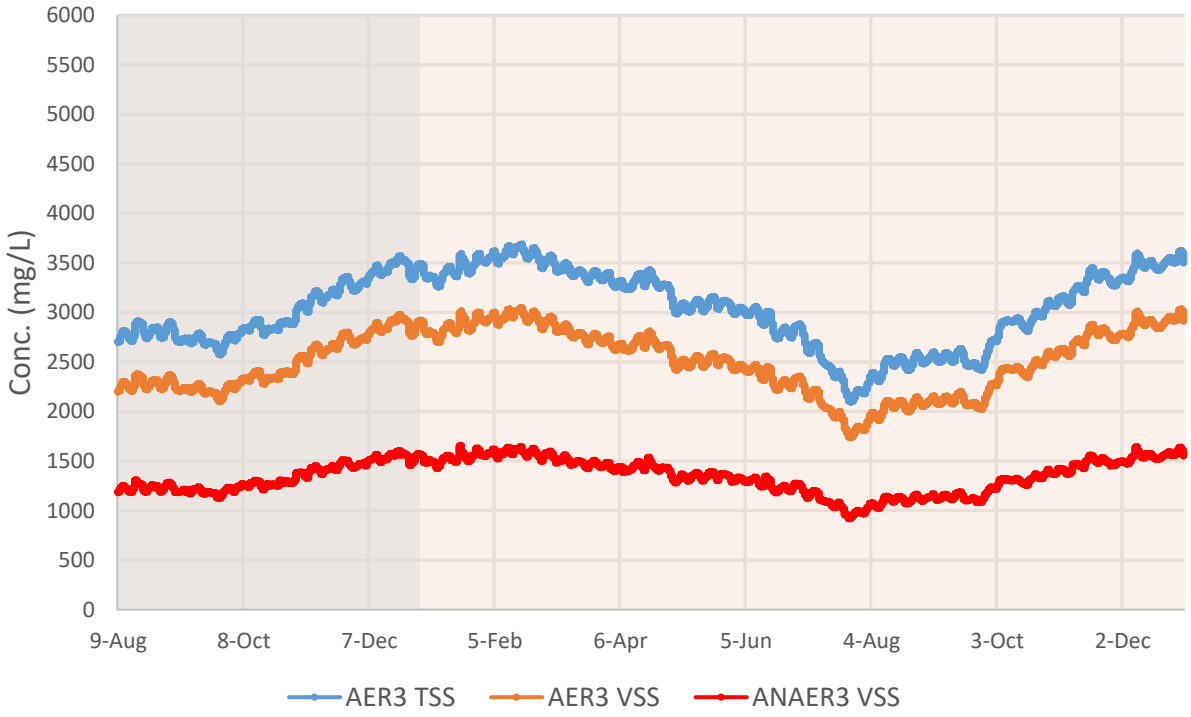

Figure 4.3 Control model simulation MLSS (08/09/2016 to 12/31/2017; shaded regions delineate year)

In the model, the default value for the OHO aerobic decay coefficient was 0.62 (1/d), which is high compared to literature values. Therefore, the model was run again with a typical decay coefficient value of 0.12 (1/d) [Tchobanoglous, 2003]. This simulation resulted in MLSS concentrations that were about 500 mg/L greater (Figure 4.4), which is closer to measured values.

Decay coefficients are temperature dependent, similar to Equation 1.3 [Metcalf & Eddy, 2003]. The temperature dependence may be less sensitive than for conventional activated sludge systems or the aerobic endogenous decay may be reduced for low-DO organisms. These questions should be investigated further to clarify the causes of the high discrepancy in predicted and observed MLSS concentrations.

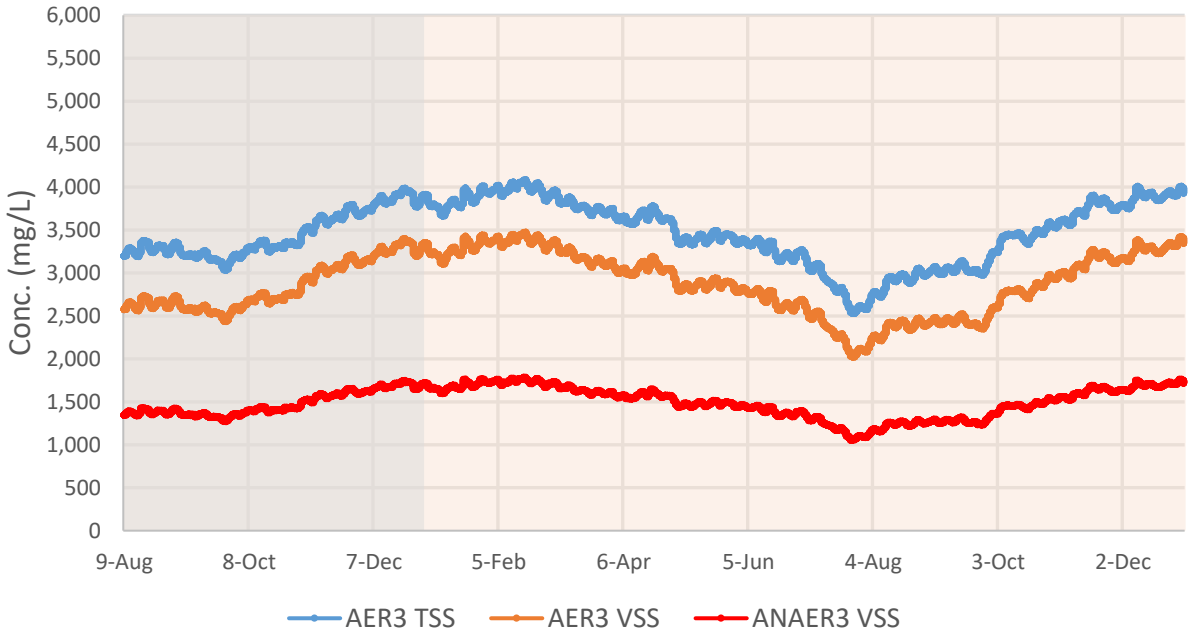

Figure 4.4 Control model simulation MLSS considering 0.12 (1/d) heterotrophic aerobic decay rate (08/09/2016 to 12/31/2017; shaded regions delineate year)

With default NOB kinetic parameters, the simulations show that the NOB population is diminished at colder water temperatures and low DO conditions, whereas the AOB population does not significantly decrease (Figure 4.5). This leads to a prediction of only a minor reduction in ammonia removal efficiency (Figure 4.6), but a significant accumulation of nitrite at low temperatures (Figure 4.7), which does not agree with experimental observation of no nitrite accumulation (Figure 2.15 and 2.16).

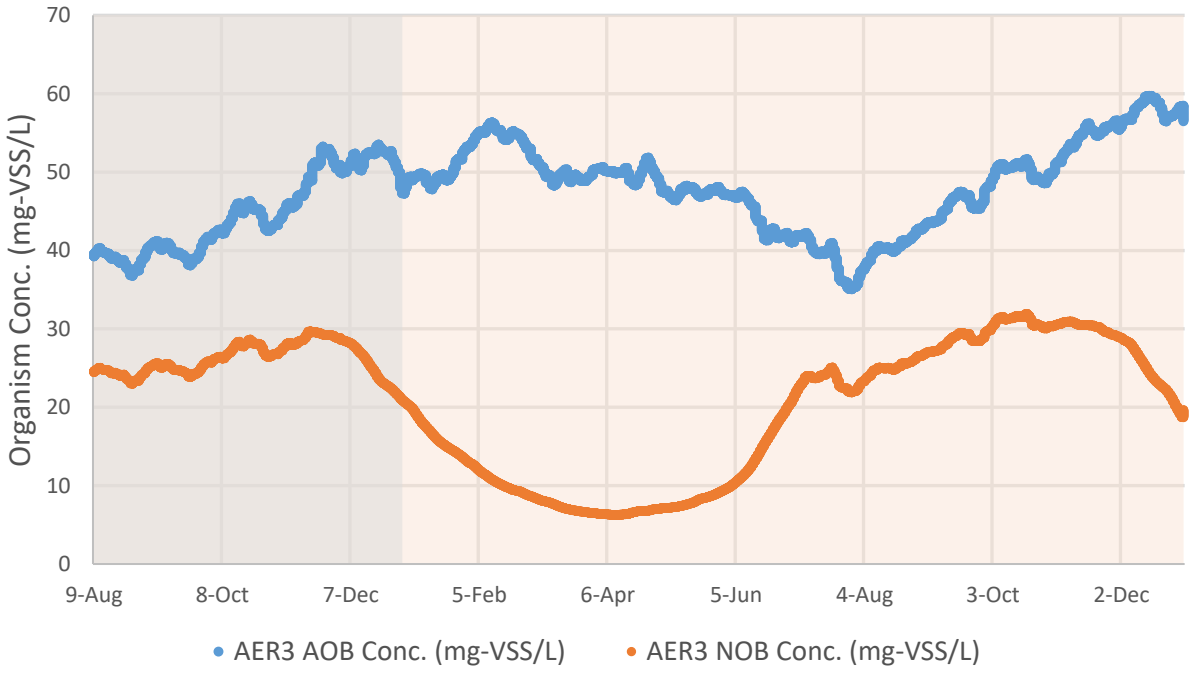

Figure 4.5 Control model simulation AOB and NOB population (08/09/2016 to 12/31/2017; shaded regions delineate year)

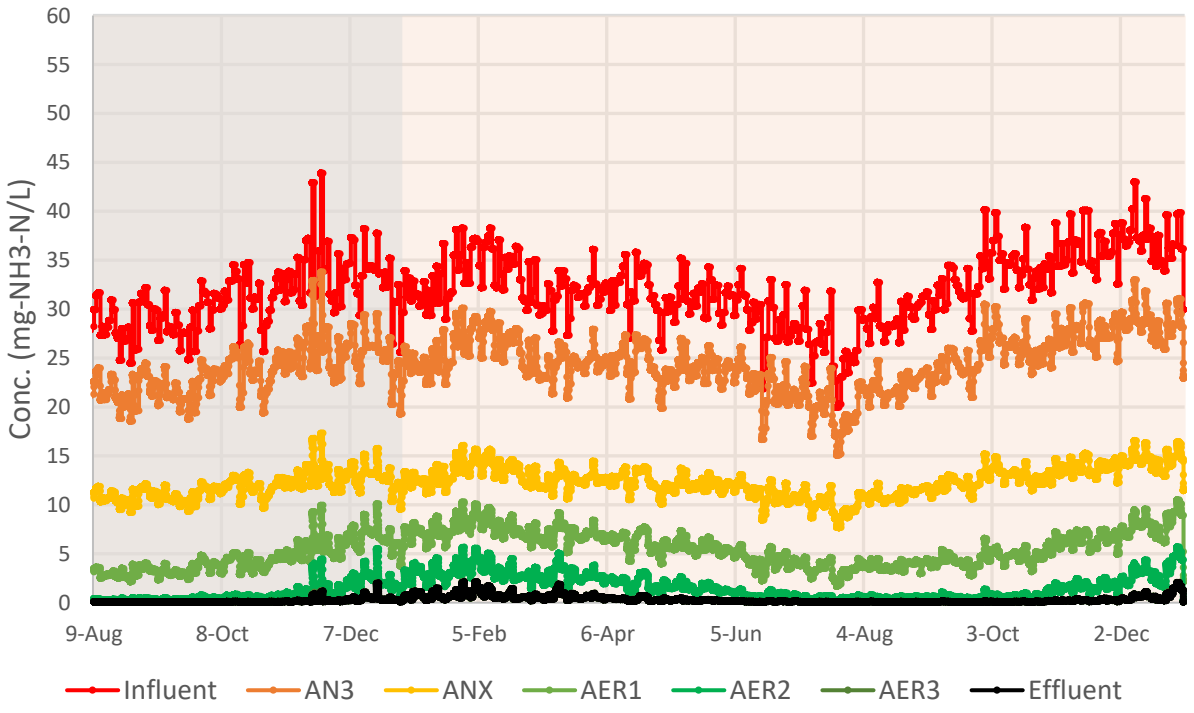

Figure 4.6 Control model simulation ammonia (mg-N/L) concentrations (08/09/2016 to 12/31/2017; shaded regions delineate year)

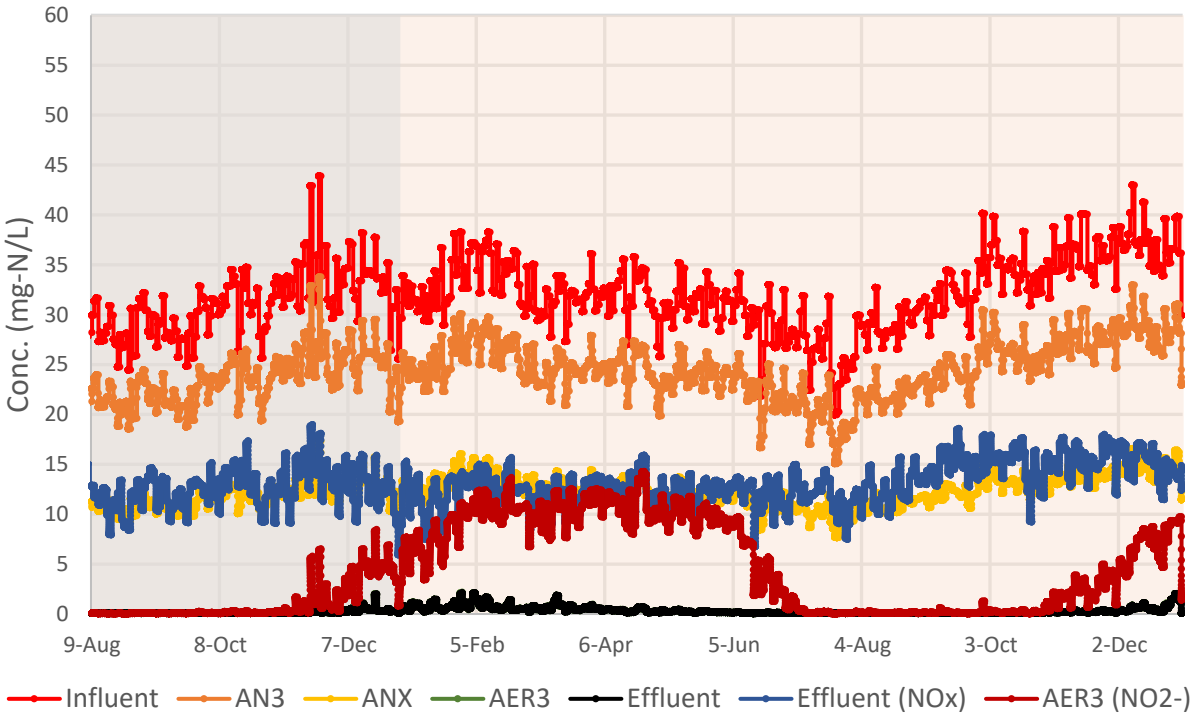

Figure 4.7 Control model simulation ammonia (Influent, AN3, ANX, AER3, Effluent), Effluent NO_x = NO_2^- + NO_3^- (mg-N/L), and AER3 nitrite (mg-NO_2^--N/L) concentrations (08/09/2016 to 12/31/2017; shaded regions delineate year)

With the COD fractionation from default wastewater characterization, the simulated PAOs released less phosphorus by the end of the anaerobic train than observed in the pilot plant (Figure 4.8). This leads to a reduction in phosphorus uptake in the aerobic train and a degradation in phosphorus removal performance during times of low tCOD loading, which was not consistent with the efficient phosphorous removal experimentally observed throughout pilot plant operation (Figure 2.17).

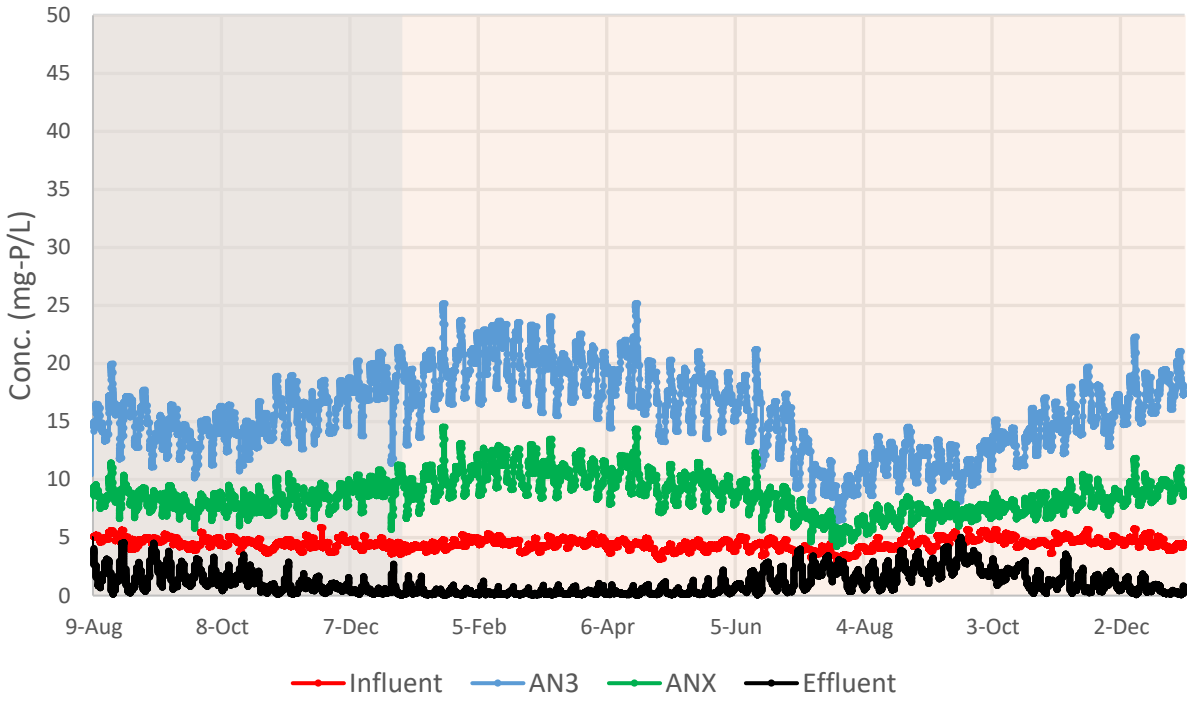

Figure 4.8 Control model simulation phosphorus (mg-PO_4^{3-}-P/L) concentrations (08/09/2016 to 12/31/2017; shaded regions delineate year)

The control simulation with default model parameters and adjustments in the OHO endogenous decay coefficient showed that the operational factors of the pilot plant, HRT and SRT, are adequate to consistently remove seasonal ammonia loadings. This was not observed experimentally; therefore, additional factors are considered to explain pilot plant performance, as discussed below.

4.3 Low-DO Kinetic Parameters and Custom Wastewater Characterization Simulation

The experimentally determined kinetic parameters discussed in Chapter 3 were incorporated into the model. Similar to the control simulation, the temperatures were varied and the DO concentrations in the aerobic tanks were kept constant (Figure 4.2).

The default values and model values for AOB and NOB are listed in Table 4.1. The AOB K_{DO} was increased from the default value of 0.25 to 0.42 mg-DO/L and the NOB K_{DO} was decreased from 0.50 to 0.10 mg-DO/L. The model parameters K_{NH3}, K_{NO2}, u_{max}, θ_T, Y, and b were left at their default values. All other organisms were simulated with default kinetic parameters.

Table 4.1 Model kinetic parameters (highlighted values different from default)

Parameter	*Default*	*Model*	*Arrhenius Theta,* θ_T
AOB DO half sat., K_{DO} [mgO2/L]	0.25	0.42	-
AOB substrate half sat., K_{NH3} [mg-NH3-N/L]	0.70	0.70	-
AOB max specific growth rate, u [1/d]	0.90	0.90	1.072
AOB yield, Y [mg-COD/mg-N]	0.15	0.15	-
AOB aerobic decay rate, b [1/d]	0.17	0.17	1.029
NOB DO half sat., K_{DO} [mgO2/L]	0.50	0.10	-
NOB substrate half sat., K_{NO2} [mg-NO2-N/L]	0.10	0.10	-
NOB max specific growth rate, u [1/d]	0.70	0.70	1.060
NOB yield, Y [mg-COD/mg-N]	0.09	0.09	-
NOB aerobic decay rate, b [1/d]	0.17	0.17	1.029

The model default values for settled wastewater do not represent the PE wastewater influent to the pilot plant. These values were changed from their default values according to measurements from the pilot samples and the 24-hour time composite PE data listed in Table 4.2. A more comprehensive COD characterization of the primary effluent wastewater is suggested, however the following analysis is suited the purposes of this model. These measurements were used with the assumptions described below to characterize the PE wastewater elements in Table 4.3.

Table 4.2 Measurements for wastewater characterization

Measurement	*Value*
Fac - Influent Acetate/ Influent Filtered COD	0.27 ± 0.11
Effluent Filtered COD (mg/L)	21.4 ± 10.6
Fus - Effluent Filtered COD/ Influent Unfiltered COD	0.076
Effluent Filtered TKN (mg-N/L)	1.35 ± 0.23
Fnus - Effluent Filtered TKN/ Influent Unfiltered TKN	0.032
Influent Filtered TKN/ Influent Unfiltered TKN	0.85 ± 0.12

The unbiodegradable soluble portion of the influent tCOD was assumed to be the filtered (0.45-µm) COD left after secondary treatment, i.e. effluent filtered COD. Therefore, the Fus was calculated by:

Fus (unbiodegradable soluble: g-COD/g-tCOD) = effluent filtered COD/ unfiltered COD = 0.076

The readily biodegradable COD is often estimated from the physiochemical flocculated filtered COD method. The flocculated filtered COD method may overestimate the rbCOD fraction [Gillot, 2010]. Standard physiochemical methods were not used, but the primary settled wastewater was considered to be flocculated and the influent filtered (0.45-µm) COD was measured, Table 2.6. Therefore, the readily biodegradable COD including acetate, Fbs, was calculated by:

Fbs (readily biodegradable: g-rbCOD/g-tCOD) = filtered/ unfiltered COD – Fus = 0.75 – 0.076 = 0.674

The stoichiometric oxygen demand of acetate is 1.07 g-O_2/g-acetate. A conservative 1:1 ratio for COD: acetate was assumed to calculate the acetate fraction of the rbCOD, Fac. The Fac was determined by comparing the measured acetate to the filtered COD and to the BOD_5 data by:

Fac (g-acetate COD/g-rbCOD) = acetate/ filtered COD = 0.27 (acetate/BOD_5 = 0.26)

The slowly biodegradable particulate COD (non-colloidal), Fxsp (g-COD/g-slowly degradable COD), was assumed to be 0.85 [Brown and Caldwell, 2017].

The ammonia fraction of TKN, Fna, was from the PE data, Table 2.4, and was calculated by:

Fna (g-NH_3/g-TKN) = PE NH_3/ PE TKN = 0.71

The particulate organic nitrogen fraction of the organic nitrogen, Fnox, was determined by comparing the pilot influent filtered and unfiltered TKN data from the pilot profile sampling. The Fnox was calculated by:

Fnox (particulate organic-N: g-N/g-Organic N) = [1 – (filtered/ unfiltered TKN)]/ (1 – Fna)
= (1 – 0.85)/ (1 – 0.71) = 0.52

The soluble unbiodegradable fraction of TKN, Fnus, was assumed to be the filtered TKN left after secondary treatment, i.e. effluent filtered TKN. Therefore, the Fnus was calculated by:

Fnus (soluble unbiodegradable TKN: g-N/g-TKN) = effluent filtered /influent unfiltered TKN = 0.032

The orthophosphate-P fraction of TP, Fpo4, was from the PE data, Table 2.4, and was calculated by:

Fpo4 (g-PO4-P/ g-TP) = 0.56

The model calculates the tCOD, TKN, and TP fractionation according to the wastewater characterization elements listed in Table 4.3. The tCOD fractionation is important for the simulation of OHO and PAO performance as well as the denitrification capacity of the system.

Table 4.3 Custom and default wastewater fractionation

Element name	*Default for Settled WW*	*Model*
Fbs - Readily biodegradable (including Acetate) [gCOD/g of total COD]	0.27	0.674
Fac - Acetate [gCOD/g of readily biodegradable COD]	0.15	0.27
Fxsp - Non-colloidal slowly biodegradable [gCOD/g of slowly degradable COD]	0.50	0.85
Fus - Unbiodegradable soluble [gCOD/g of total COD]	0.08	0.076
Fna - Ammonia [gNH3-N/gTKN]	0.75	0.71
Fnox - Particulate organic nitrogen [gN/g Organic N]	0.25	0.52
Fnus - Soluble unbiodegradable TKN [gN/gTKN]	0.020	0.032
Fpo4 - Phosphate [gPO4-P/gTP]	0.75	0.56

The results of the simulation with low-DO kinetic parameters and custom wastewater characterization better represent the experimentally observed pilot plant performance than the control simulation. The simulated AOB population trends (Figure 4.9) did not change from the control simulation. Unlike the control simulation, the NOB simulated with the lower K_{DO} did not experience washout during colder water temperatures at an SRT of 12.93 days.

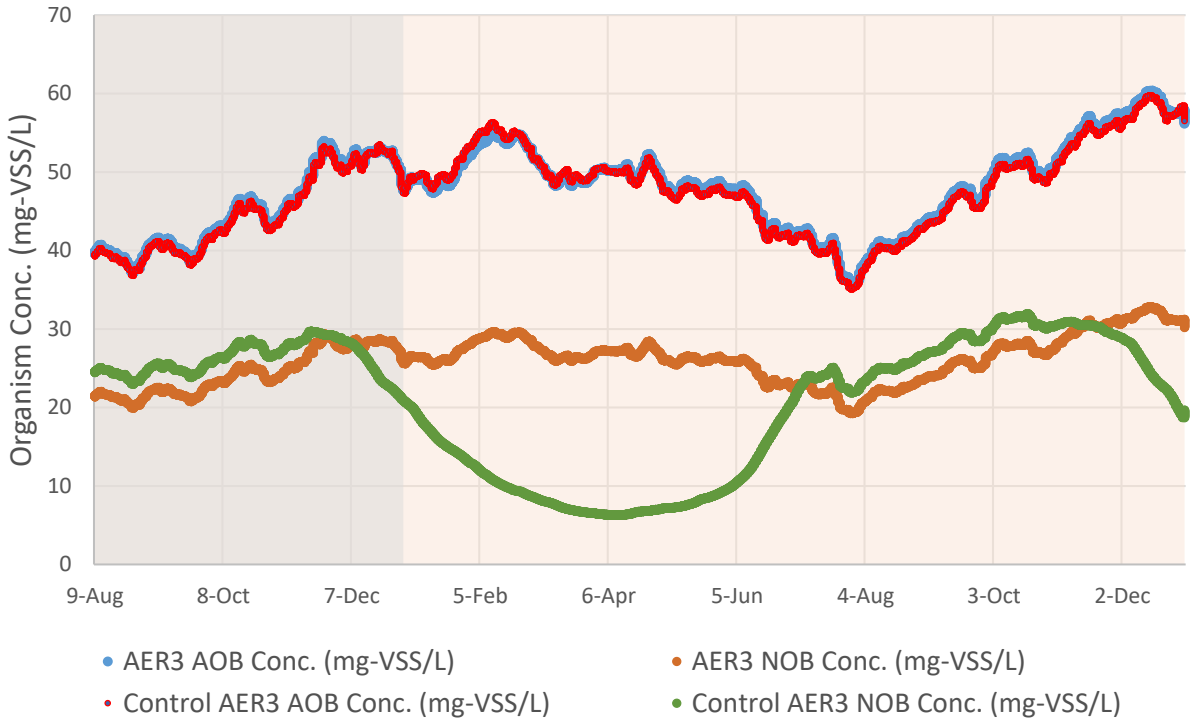

Figure 4.9 Kinetic model simulation compared to control simulation AOB and NOB population (08/09/2016 to 12/31/2017; shaded regions delineate year)

The AOB simulated with higher K_{DO} led to degradation of ammonia removal performance during colder water temperatures (Figure 4.10). The AOB population was stable at an SRT of 12.93 days, though the ammonia removal rates slowed down and predictions of poor ammonia removal were obtained. However, this degradation in performance is not as pronounced as experimentally observed during the winter and does not continue into to the end of June 2017 (Figure 2.15).

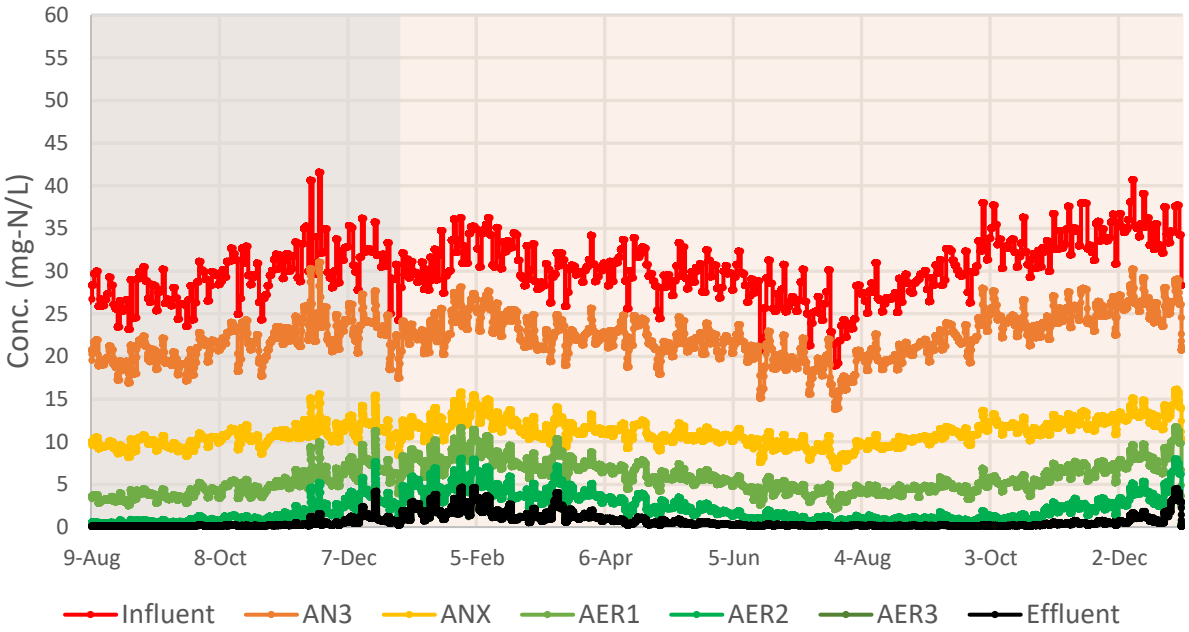

Figure 4.10 Kinetic model simulation ammonia (mg-N/L) concentrations (08/09/2016 to 12/31/2017; shaded regions delineate year)

With stable NOB population simulated throughout the winter, nitrite does not accumulate by the end of the aerobic zone (Figure 4.11). This better simulates the performance of the pilot (Figure 2.16).

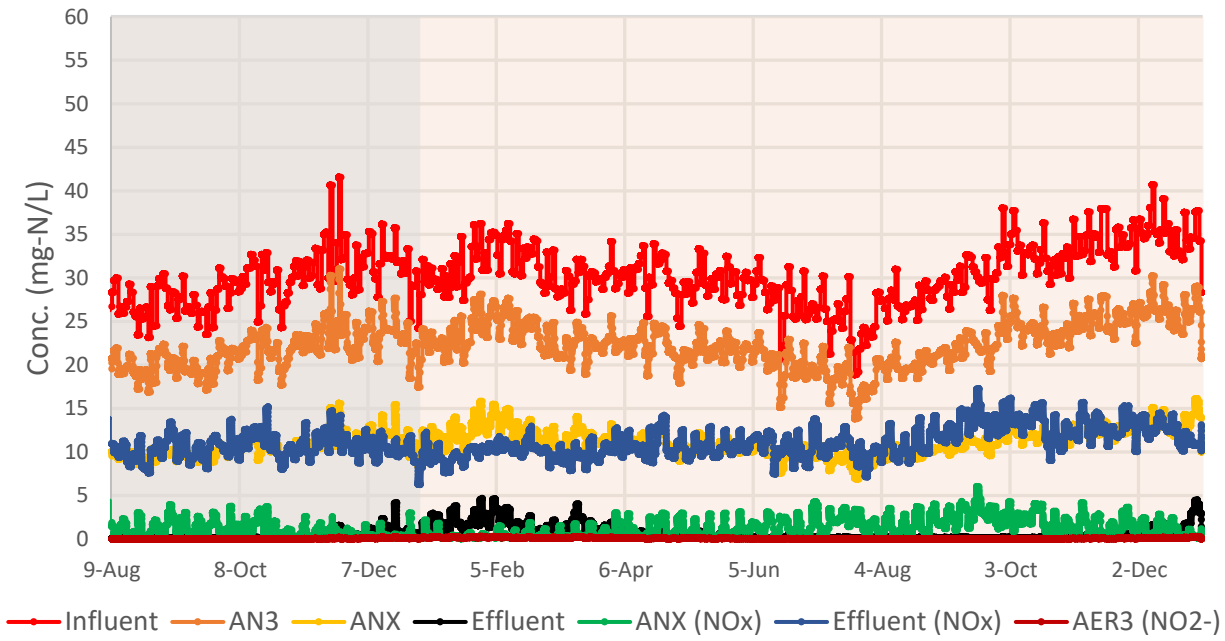

Figure 4.11 Kinetic model simulation ammonia (Influent, AN3, ANX, Effluent), anoxic and effluent NO_x = NO_2^- + NO_3^- (mg-N/L), and AER3 nitrite (mg-NO_2^--N/L) concentrations (08/09/2016 to 12/31/2017; shaded regions delineate year)

The simulation shows that NO_x accumulated in the anoxic (ANX) tank, which was not experimentally observed. There are several hypotheses that need further investigation, as discussed below.

The simulated denitrification may have been due to a mischaracterization of the tCOD influent. That is, there was more tCOD than the 2.1-times BOD_5 assumption used or there was a different COD fractionation for the settled wastewater that would better reflect the complete anoxic zone denitrification that was experimentally observed. The model could have overestimated the carbon consumption of PAOs in the anaerobic zone. The default model parameters for the simulated denitrification rate may not have been fast enough for anoxic zone denitrification or were not optimized for SND through the aerobic zone. The increased denitrification experienced by the pilot might have been due to DPAO activity. The low DO

conditions in the pilot or the on/off nature of the aeration control system may have contributed to SND in the aerobic zone.

The plot of the simulated carbonaceous and nitrification oxygen uptake rate (OUR) demonstrates the sensitivity of nitrification to cold water temperatures (Figure 4.12). The nitrification OUR in aerobic tank 1 (AER1) varied significantly with water temperature whereas the carbonaceous OUR in AER1 did not; partly due to the higher BOD loadings in the winter. The nitrification OUR in AER2 did not vary to the same extent because higher ammonia concentrations from AER1 offset temperature effects. The seasonal trends for nitrification OUR in AER3 further illustrate this idea. During warmer water temperatures there were lower ammonia oxidation rates in AER3 but as the water temperatures declined and ammonia seeped through the aeration train, the nitrification OUR in AER3 increased.

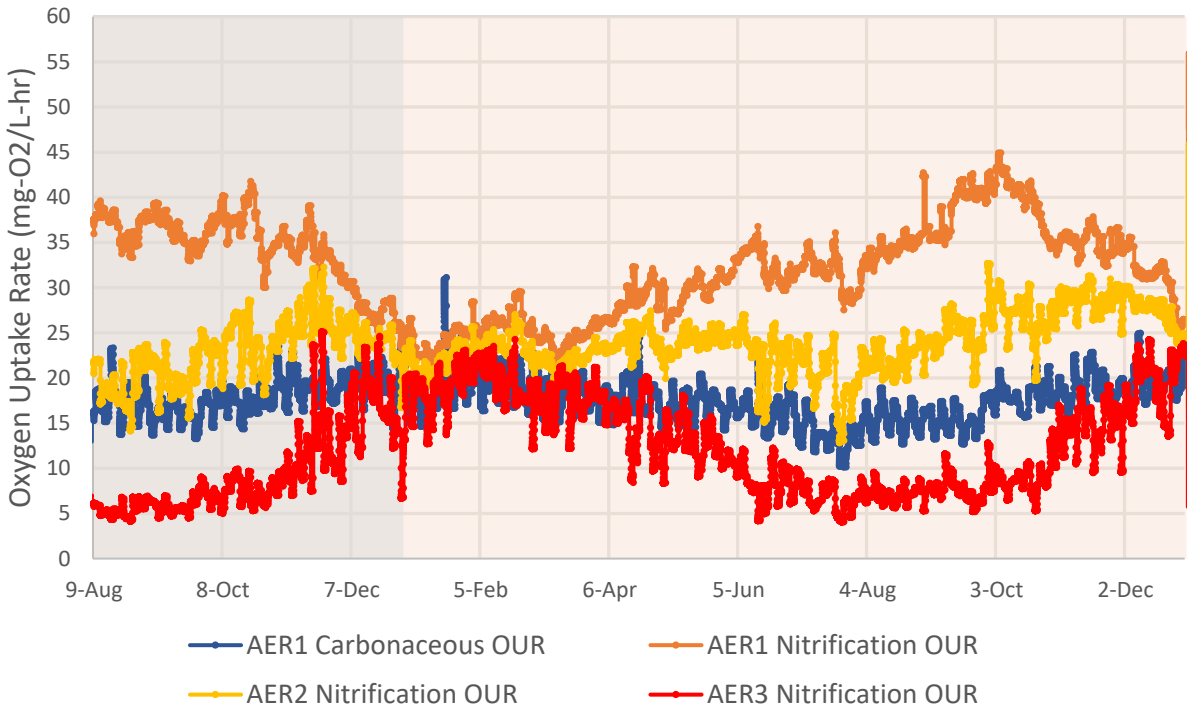

Figure 4.12 Kinetic model simulation carbonaceous and nitrification oxygen uptake rates (mg-O_2/L-hr) across aeration train (08/09/2016 to 12/31/2017; shaded regions delineate year)

Similar trends are seen with ammonia removal and nitrate production rates, which represent the AOB and NOB activities, respectively, within the specified tanks (Figure 4.13).

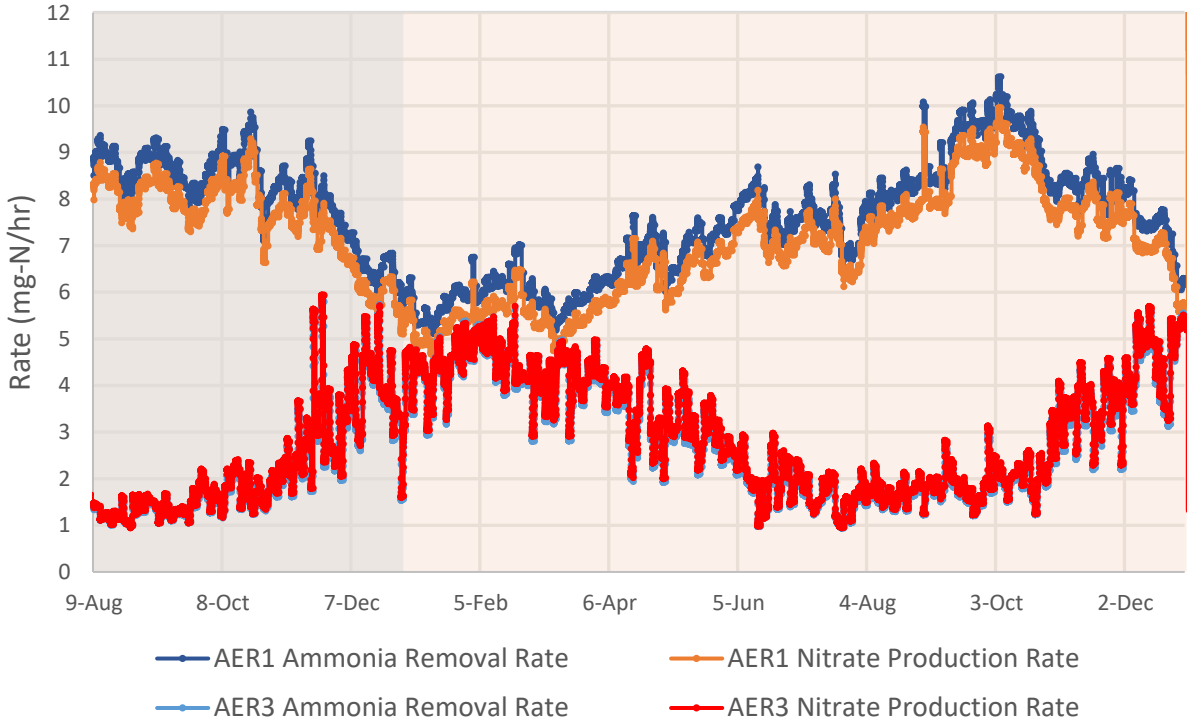

Figure 4.13 Kinetic model simulation nitrogen removal and nitrate production rates (mg-N/L-hr) across aeration train (08/09/2016 to 12/31/2017; shaded regions delineate year)

With the custom wastewater characterization, there was more phosphorus release in the anaerobic zone and subsequently greater phosphorus uptake by PAOs in the aerobic zone (Figure 4.14). This simulation better represents the experimentally observed performance of the pilot plant than the control simulation (Figure 4.8). The higher rbCOD and acetate fractionation, Fbs and Fac, allowed for consistent phosphorus removal performance. This simulation gives evidence to the hypothesis that the high VFA content of Nine Springs' wastewater leads to stable EBPR performance in the full-scale plant.

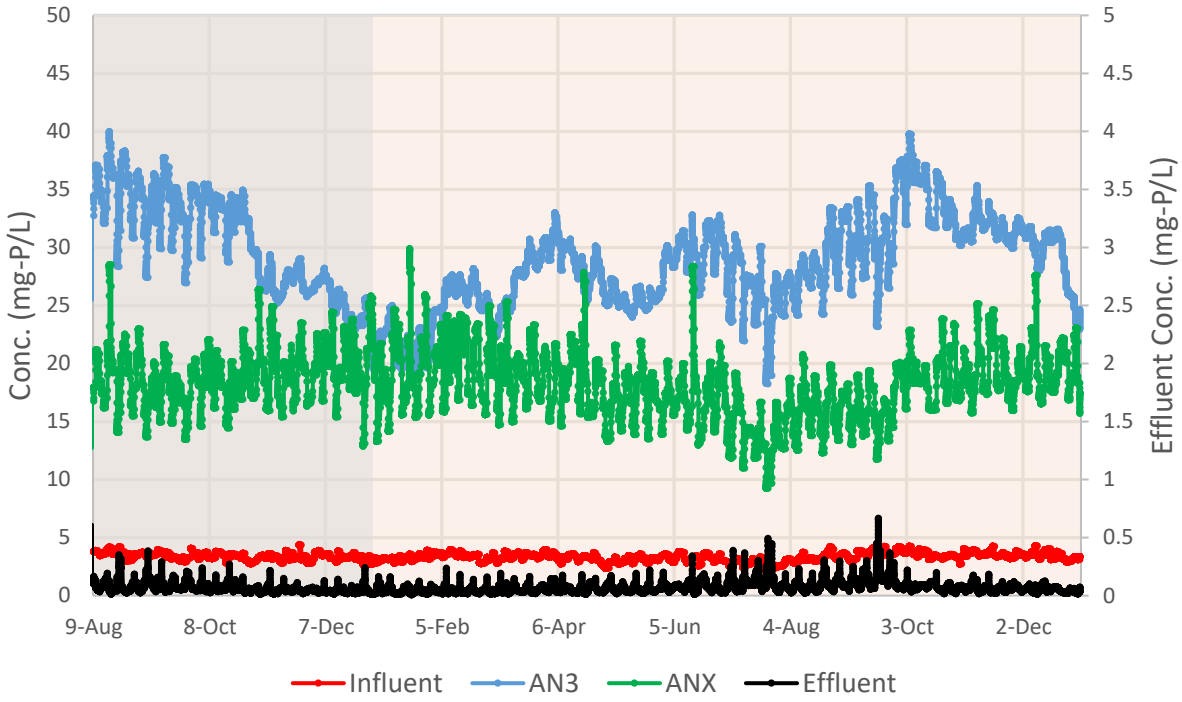

Figure 4.14 Kinetic model simulation phosphorus (mg-PO_4^{3-}-P/L) concentrations (08/09/2016 to 12/31/2017; shaded regions delineate year)

The simulated phosphorus performance was compared to the observed profile sampling TP concentration data (Figure 4.15). The simulated concentrations follow similar trends as the observed data. Note that the sampling procedure captures one time point of pilot plant performance.

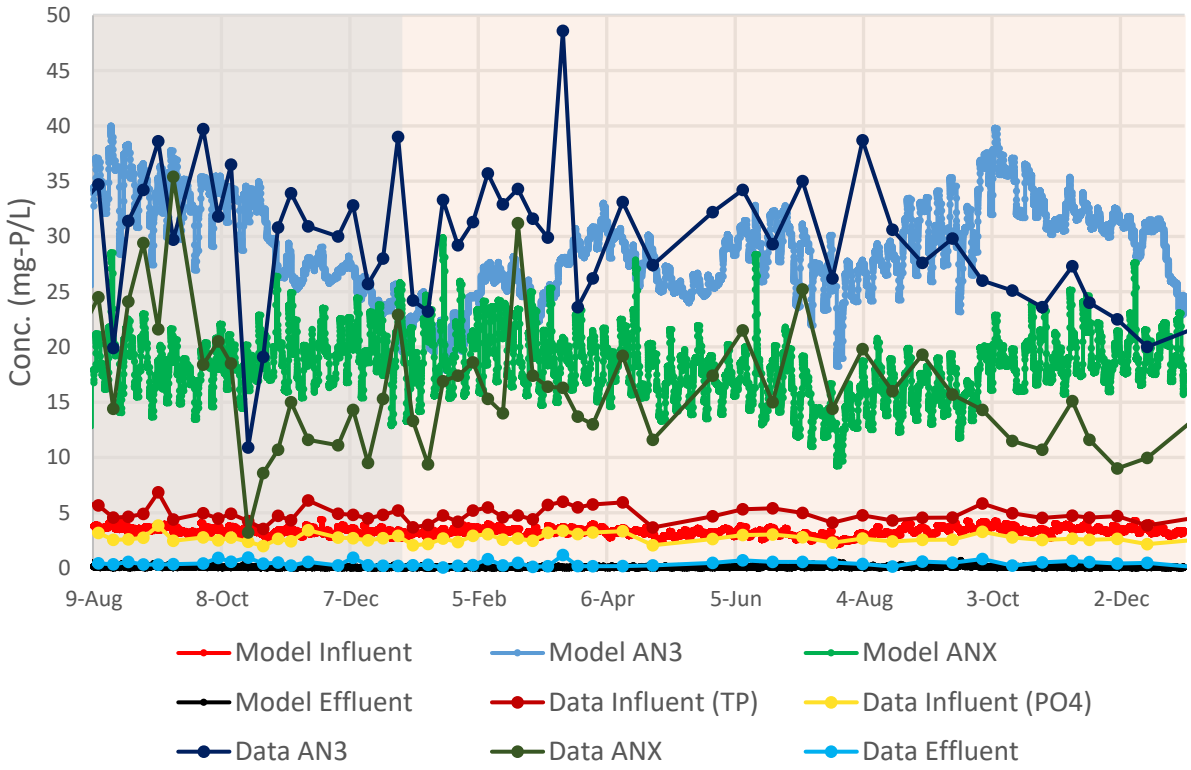

Figure 4.15 Kinetic model simulation compared to observed pilot plant profile "Data" phosphorus (mg-P/L) concentrations (08/09/2016 to 12/31/2017; shaded regions delineate year)

The influent nitrogen concentrations to the pilot were a driving factor for the seasonal nitrogen removal performance. The control simulation demonstrated that these higher nitrogen concentrations were consistently removed while this simulation demonstrated that, considering experimentally determined low-DO kinetic parameters, nitrogen concentration removal was not consistent during colder water temperatures. It was observed that the DO concentrations in the aerobic tanks of the pilot plant were not constant. The DO concentrations need to be considered as this is a critical factor in determining pilot plant performance.

4.4 Variable DO Simulation

The DO concentrations are an important factor for nutrient removal performance. The observed DO concentrations in the aerobic tanks were incorporated into the model to improve resolution of the simulations. A representative simulation of the experimentally observed pilot plant performance was achieved.

The model DO concentrations (Figure 4.16) were varied weekly according to the weekly averages measured in the aerobic tanks (Figures 2.11-2.13).

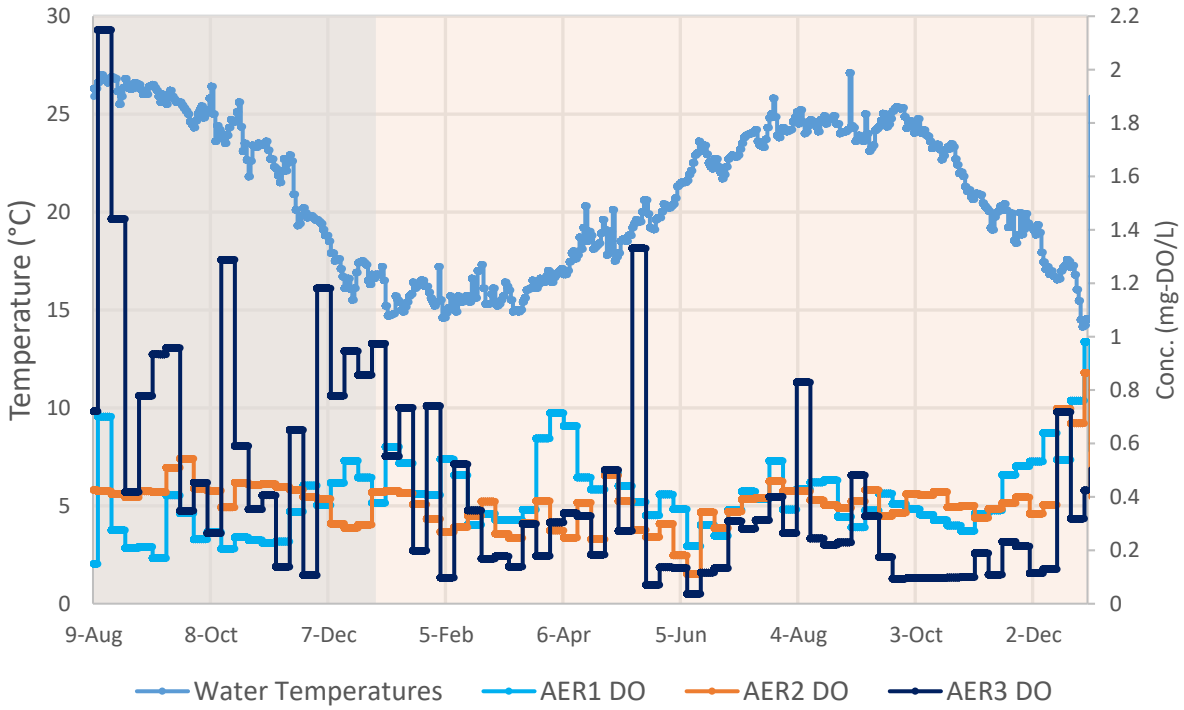

Figure 4.16 Variable DO model simulation water temperatures and varying DOs (08/09/2016 to 12/31/2017; shaded regions delineate year)

The compounding effects of temperature, low DO kinetic parameters, and varying DO concentrations led to a more variable AOB and NOB population simulation (Figure 4.17) than for the constant DO simulation (Figure 4.9). The anaerobic (AN3) AOB concentration was diluted by ½ from the aerobic population.

Similar AOB population trends were seen in the variable DO simulation as for the constant DO simulations until colder water temperatures were reached. The AOB populations in the winter were generally lower for the variable DO simulation, but there were two washout events that were significant to the simulated performance. With the suppressed DO concentrations in March 2017, the simulated AOB growth rates were slowed to where the population was diminished at the 12.93 day SRT. This same phenomena occurred in June 2017. During both events, the variable DO simulated AOB populations were reduced to less than the constant DO simulation.

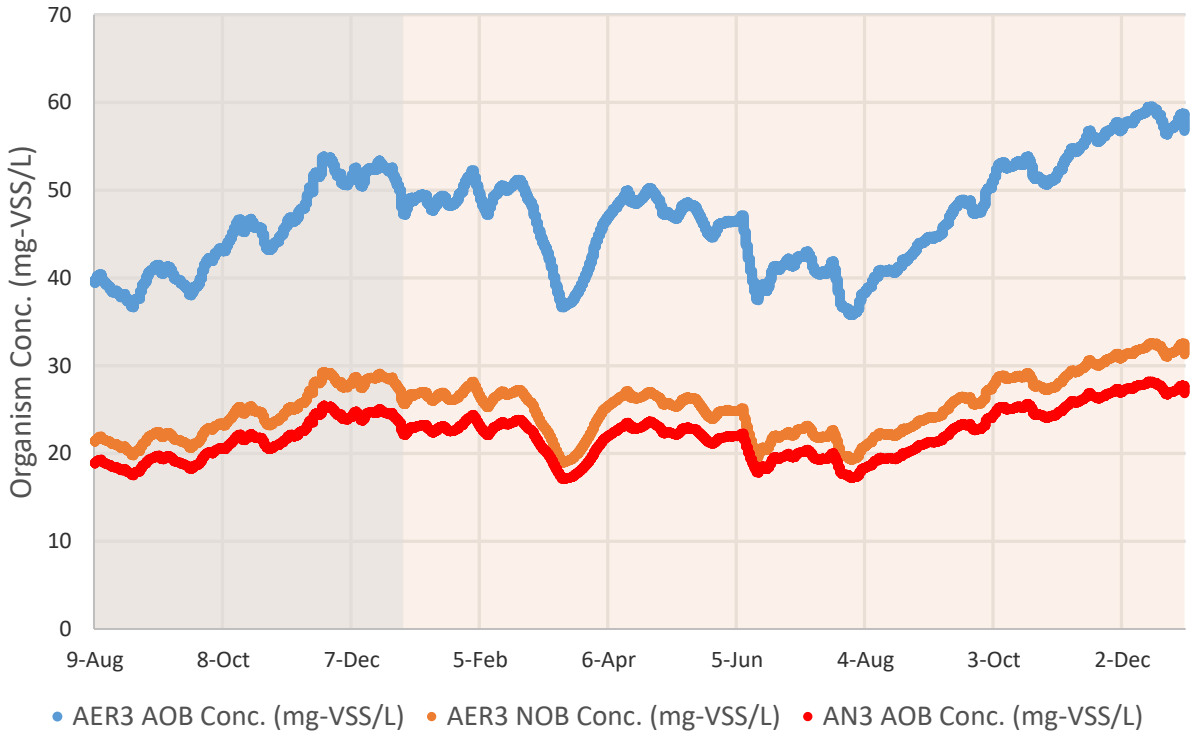

Figure 4.17 Variable DO model simulation AOB and NOB population (08/09/2016 to 12/31/2017; shaded regions delineate year)

The question of AOB proportion of biomass was addressed by comparing the AOB concentration (mg-VSS/L) to the total VSS concentration (Figure 4.18). The AOB biomass fraction (%) trends were buffered to a certain extent by the total biomass trends (Figure 4.4), though the washout events were still apparent. The simulated AOB fraction of the total biomass was about 1.5 %.

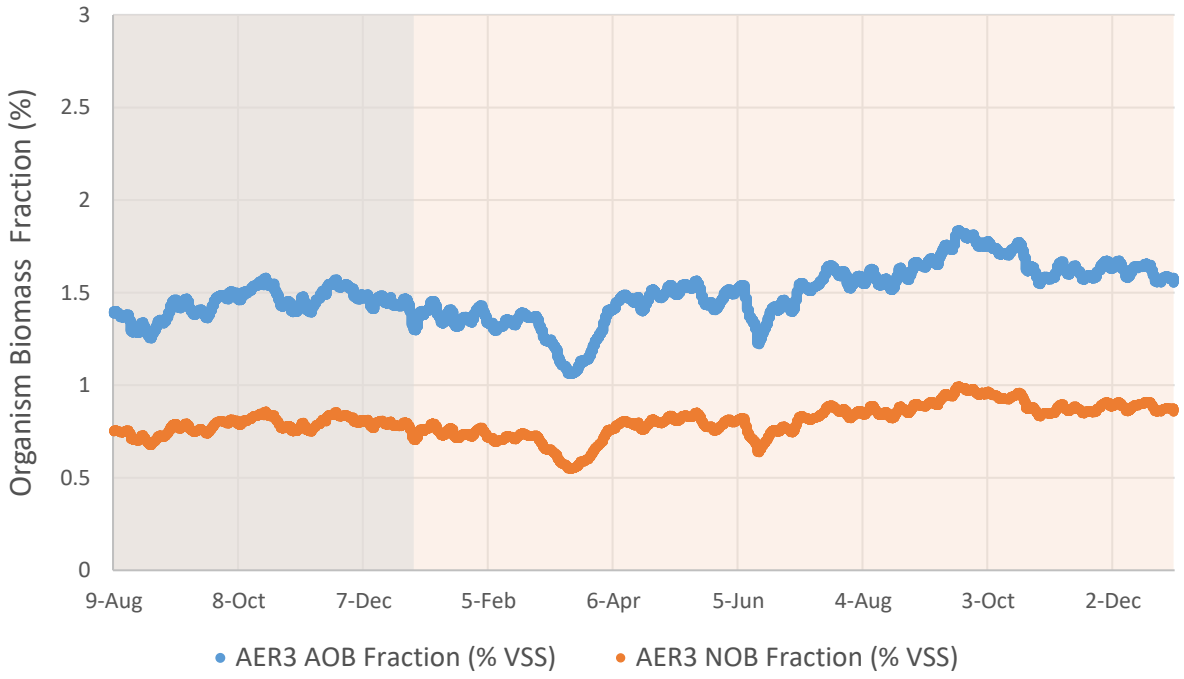

Figure 4.18 Variable DO model simulation AOB and NOB population fraction of biomass (% VSS) (08/09/2016 to 12/31/2017; shaded regions delineate year)

The PAO fraction of the biomass was significant (Figure 4.19). For EBPR systems, the PAOs have a distinct advantage by being able to consume carbon during anaerobic conditions. The simulated PAO fraction of the biomass was about 20%.

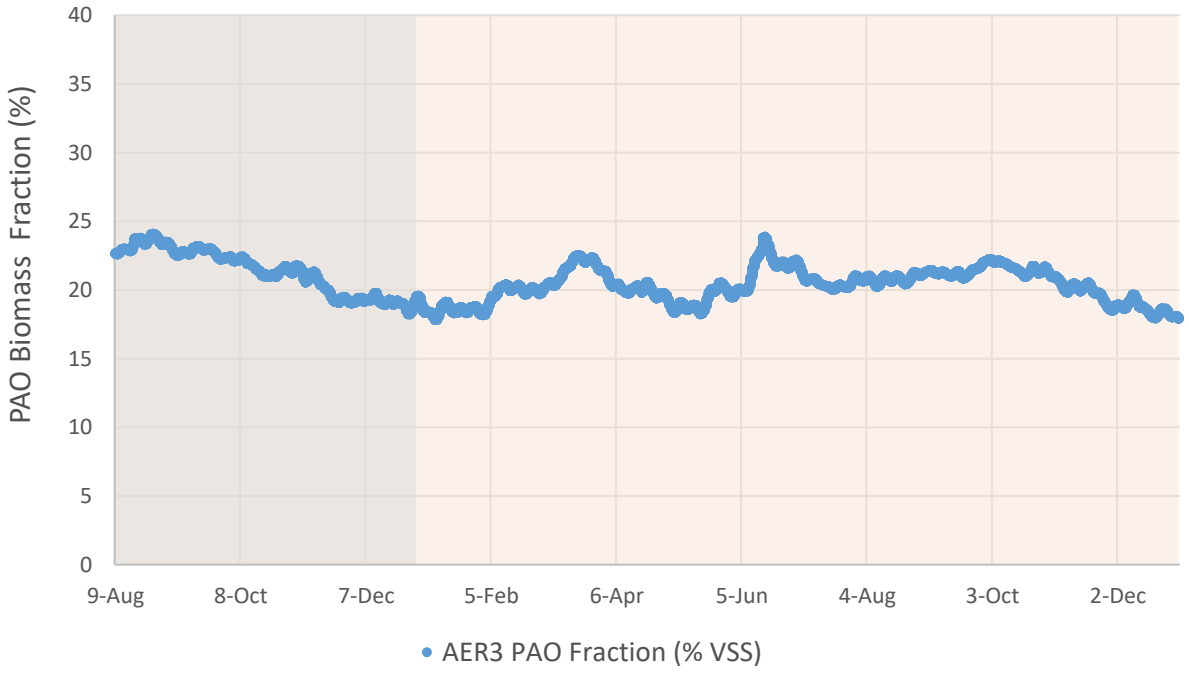

Figure 4.19 Variable DO model simulation PAO population fraction of biomass (% VSS) (08/09/2016 to 12/31/2017; shaded regions delineate year)

The diminished AOB populations through the winter and the washout events led to simulated ammonia concentrations that better represent the experimentally observed nitrogen removal performance (Figure 4.20). The March 2017 and June 2017 washout events were apparent in the ammonia concentration response.

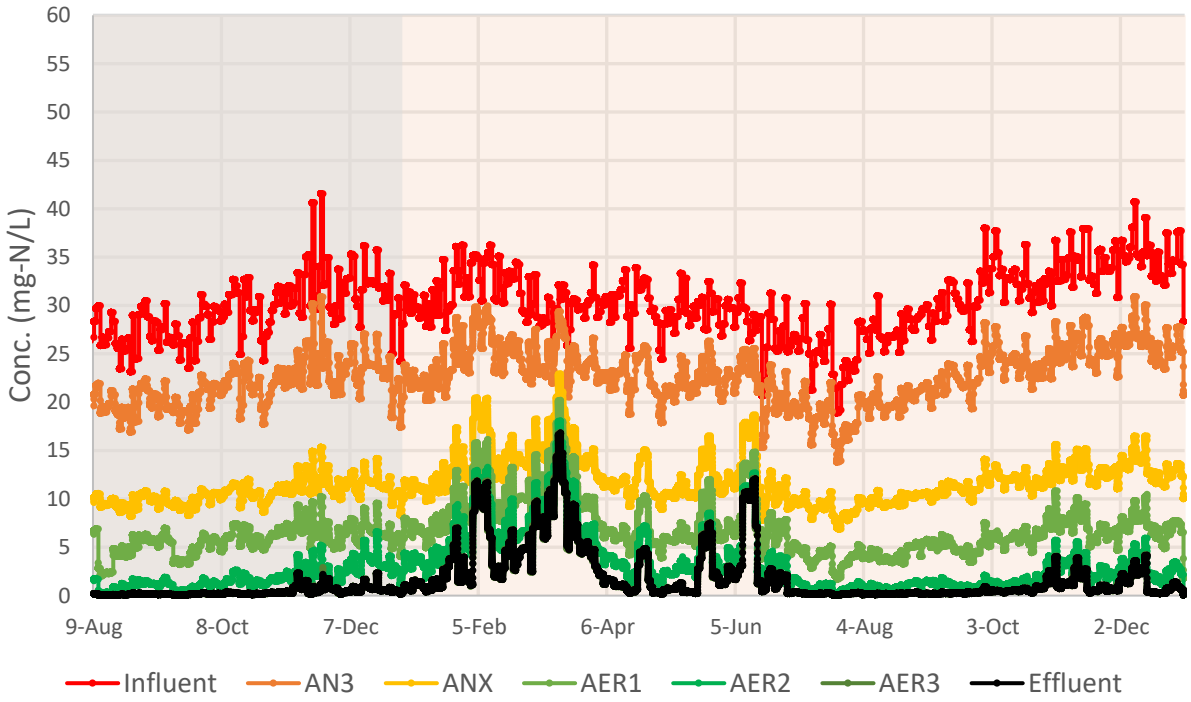

Figure 4.20 Variable DO model simulation ammonia (mg-N/L) concentrations (08/09/2016 to 12/31/2017; shaded regions delineate year)

The simulated ammonia concentrations were compared to the biweekly TKN data from the profile sampling (Figure 4.21). The simulated nitrogen removal degraded into the winter and continued to the end of June. The model did not consider diurnal loading variations or operational upsets.

The influent ammonia concentrations at the time of sampling followed the trends of the 24-hr time composite data (model influent). The time composite data averaged the daily variation in loading to the full-scale plant, the sampling procedure did not.

For the sampling event on March 16th, 2017, the effluent grab sample concentration was significantly lower than the model simulation. However, the ANX and AER1 grab samples were in agreement with the model. Previous to this sampling event, the pilot experienced an influent pump failure. Considering the pilot treatment train HRT of 9.5 hours, the effluent sample may

have been taken at a point where steady state conditions had not been reached throughout the system.

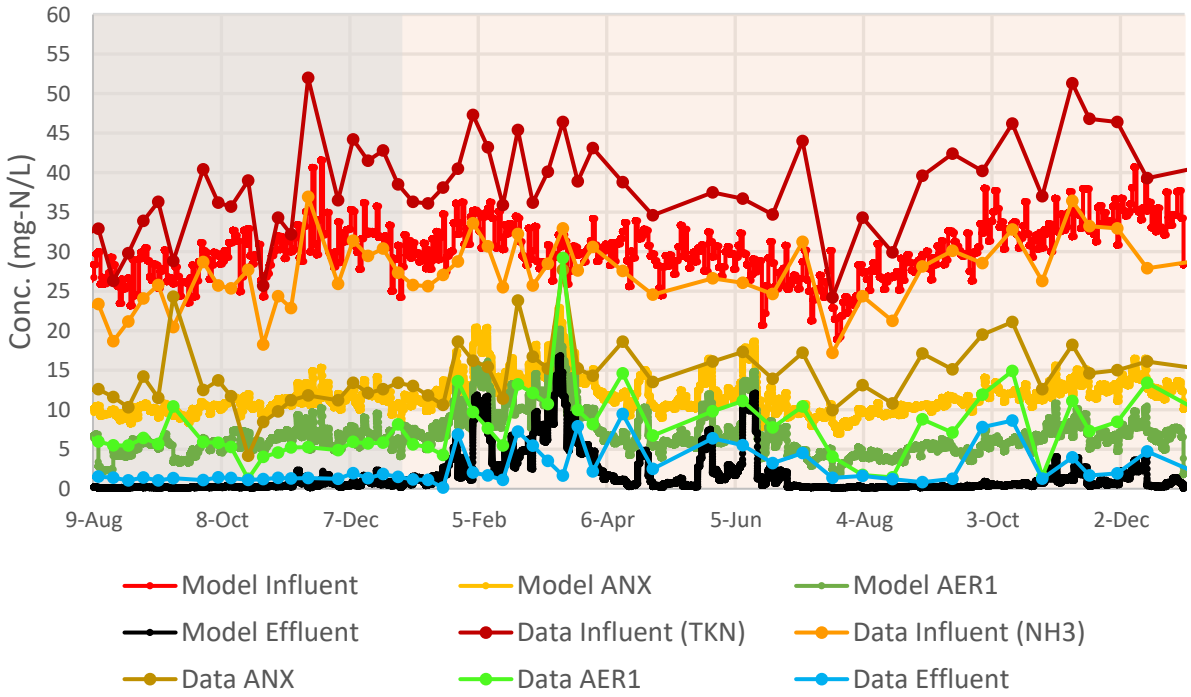

Figure 4.21 Variable DO model simulation ammonia compared to observed pilot plant profile TKN "Data" (mg-N/L) concentrations (08/09/2016 to 12/31/2017; shaded regions delineate year)

The grab sample effluent ammonia concentration data, taken every three days, were plotted with the model simulation (Figure 4.22). The initial ammonia removal upsets in January and February 2017 were in agreement between the data and the model, though the extent to which the simulated ammonia concentrations increased was not reflected in the grab sample data. The grab sample data exhibit sporadic return of ammonia removal performance. This may have been due to the time of day these samples were collected, where the loading may have been as much as 75% of the average loadings (Figure 2.18).

The upsets observed in April and May 2017 were predicted by the model. The ammonia concentrations for the washout event that occurred in June 2017 was reflected in both the simulation and the grab sample data. The operational upset in October, 2017 was not simulated, but the ammonia removal upset occurring in November was predicted by the model.

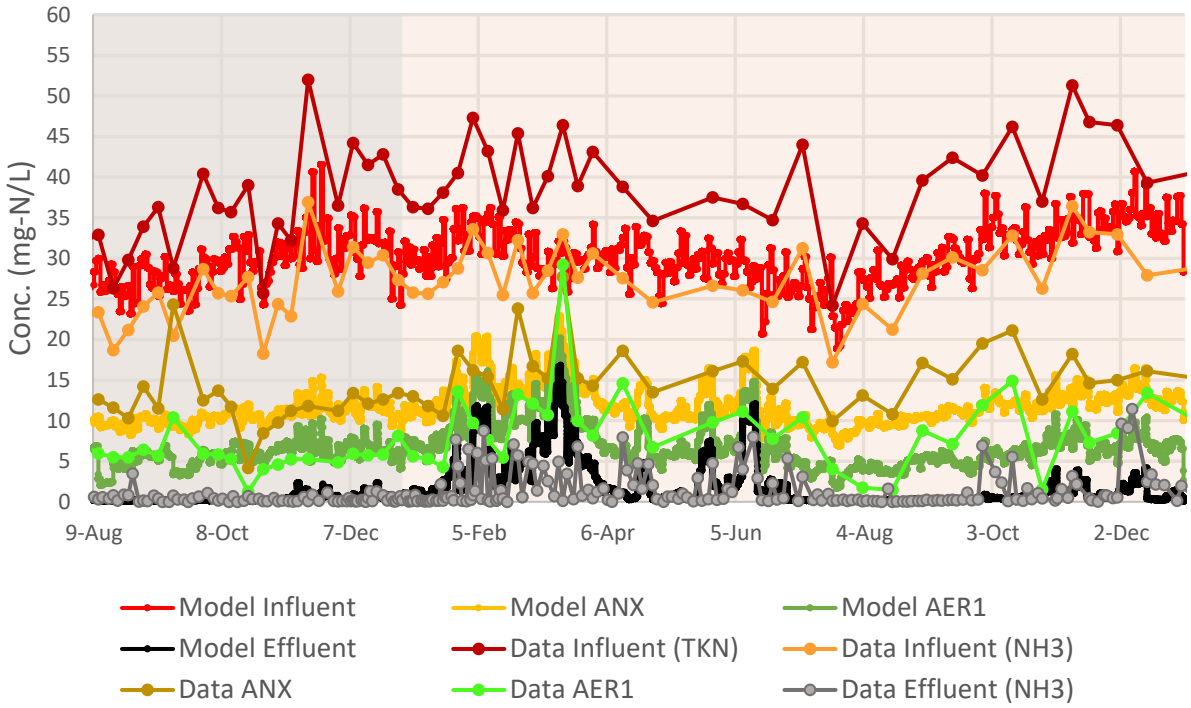

Figure 4.22 Variable DO model simulation ammonia compared to observed pilot plant profile TKN and effluent grab sample ammonia "Data" (mg-N/L) concentrations (08/09/2016 to 12/31/2017; shaded regions delineate year)

4.5 Simulating Nitrification in a Batch Reactor

The batch experiments showed experimentally observed differences in maximum ammonia removal rates (Section 3.3.2). These differences in observed rates at different times during the operational period could be explained by AOB population dynamics. To verify the AOB population dynamics predicted by the model, the batch experiments were simulated and the maximum ammonia removal rate for the simulated AOB populations were compared to those of the batch experiments.

The batch experiments were simulated at the times they were conducted during the operational period by artificially adding a batch reactor to the simulated UCT configuration (Figure 4.23). The batch reactor simulation replicates the conditions of the batch experiments conducted in the laboratory while not affecting the overall performance of the pilot plant.

The aerated batch reactor was continuously fed pilot sludge from the end of the anaerobic zone at a flow rate that achieved concentrations equal to that of the pilot plant while not diminishing the pilot concentrations. The batch reactor was continuously fed ammonia to prevent substrate limitations of removal rates. The DO concentration within the batch reactor was set at 5 mg-DO/L to achieve maximum removal rates and the batch temperatures were set to those of the AOB batch experiments.

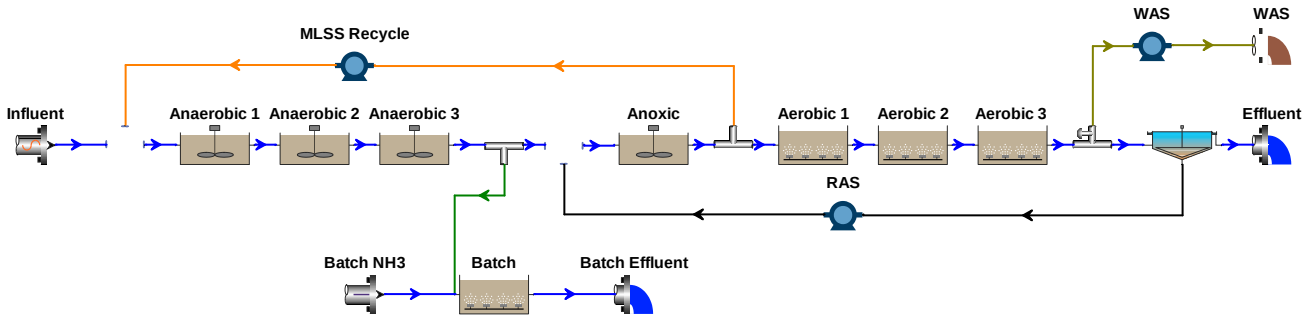

Figure 4.23 Model configuration for batch experiment simulation

The AOB population concentrations for the batch simulation were slightly higher than those for the variable DO simulation (DO Run) because of the ammonia fed to the batch reactor (Figure 4.24.)

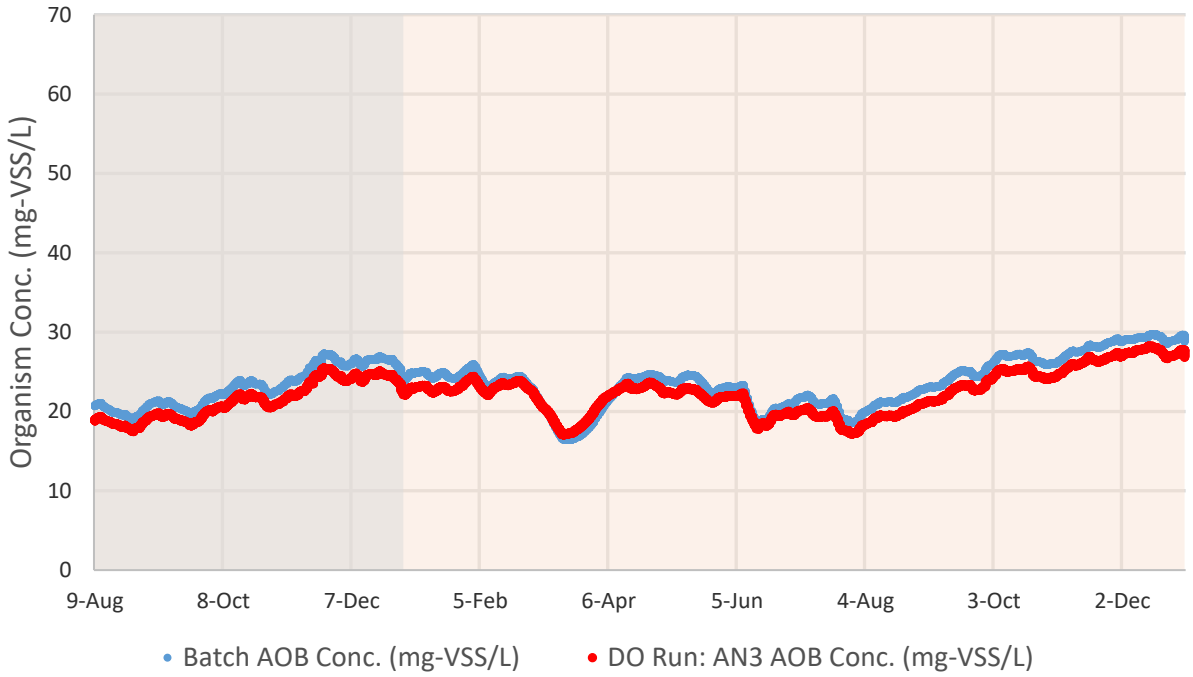

Figure 4.24 Batch test model simulation AOB population at end of anaerobic zone and within batch test (08/09/2016 to 12/31/2017; shaded regions delineate year)

The ammonia removal rates and batch temperatures are plotted (Figure 4.25). The simulated batch experiment temperatures were 22.5 and 24.3°C (Table 3.3). The inset values were the simulated ammonia removal rates within the batch reactor. Comparing these values to the maximum ammonia removal rates measured for the AOB batch experiments (03/20/2017: 6.40, 09/02/2017: 9.04 mg-N/L-hr), the simulated rates were within 10%. Therefore, the simulated, dynamic AOB populations explain the differences in maximum ammonia removal rates observed in the AOB batch experiments, performed at different times during operation.

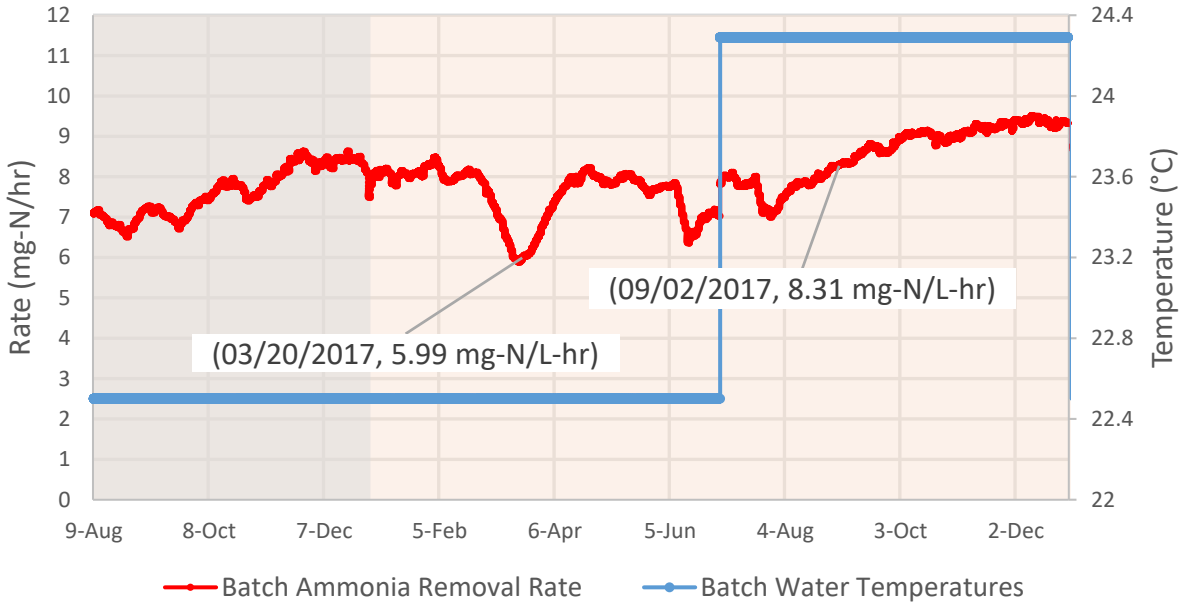

Figure 4.25 Batch test model simulation max ammonia removal rates (08/09/2016 to 12/31/2017; shaded regions delineate year)

The model adequately simulates pilot plant nutrient removal performance for UCT operation. Thus, these results suggest that the variable nutrient loading, water temperature, and observed variation in DO concentrations can explain seasonal pilot performance. The simulated, dynamic AOB populations explain the differences in maximum ammonia removal rates observed in the AOB batch experiments, performed at different times during operation.

CHAPTER 5 : SIMULATED CORRECTIONS

The model was used to investigate strategies for optimizing performance and overcoming nitrogen removal upsets seen in winter. These simulations utilize the variable DO model, replicating the UCT operation phase with operational and configuration adjustments to optimize performance. Operational and configuration adjustments added a biological safety factor to the nitrification process.

5.1 Increase RAS

To investigate the limits of TN removal for this pilot plant, the RAS flow rate was doubled from UCT operation (Figure 5.1). The effluent NO_x did not decrease compared to the earlier analysis, suggesting carbon limitations of the system. This simulations shows that further return of NOx without carbon addition does not improve the extent of nitrogen removal in the pilot plant. To investigate operational energy optimization, the RAS flow rate was reduced to 0.75x UCT operation; the effluent NO_x concentration increased in response.

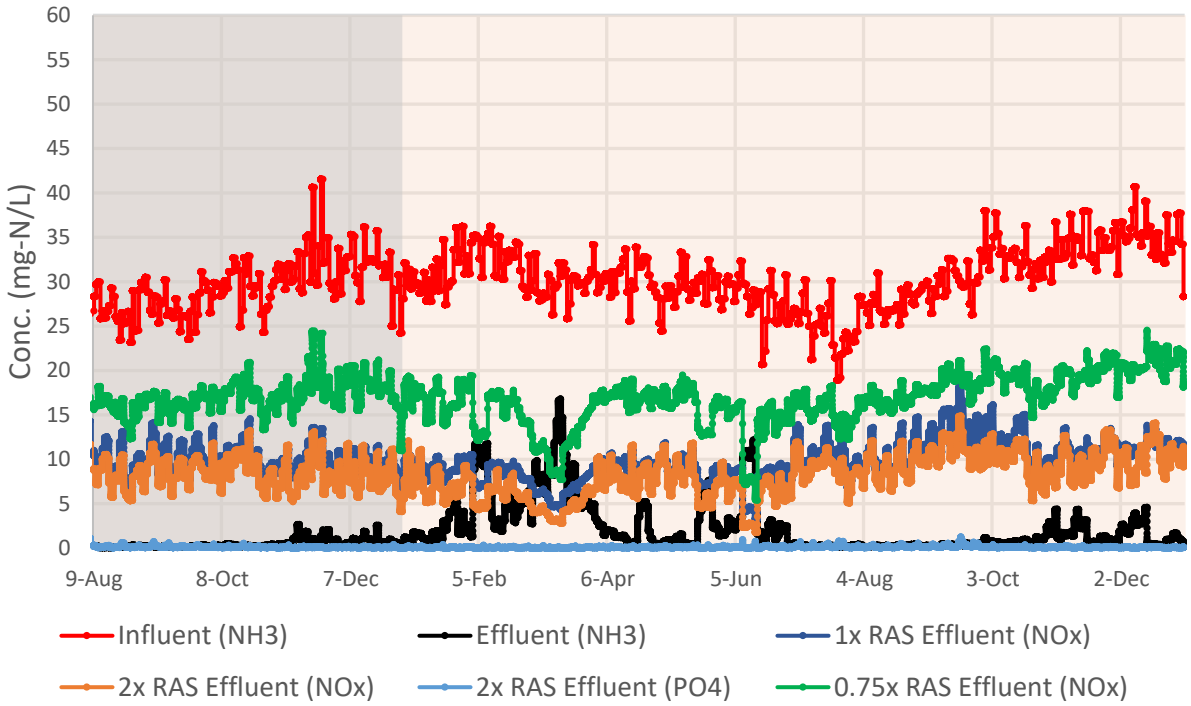

Figure 5.1 Effluent NOx and phosphorus concentrations for 2x RAS compared to 1x RAS flow rate (08/09/2016 to 12/31/2017; shaded regions delineate year)

5.2 Increase SRT

Reducing the rate of biomass wasting increases the MLSS concentration within the system (Equation 1.8) and could alleviate poor nitrification performance by retaining AOB and NOB in the winter period. By increasing the SRT, AOB populations did not experience the extent of washout during the winter (Figure 5.2). The simulated AOB populations with longer SRTs are greater than for the 12.93 day SRT.

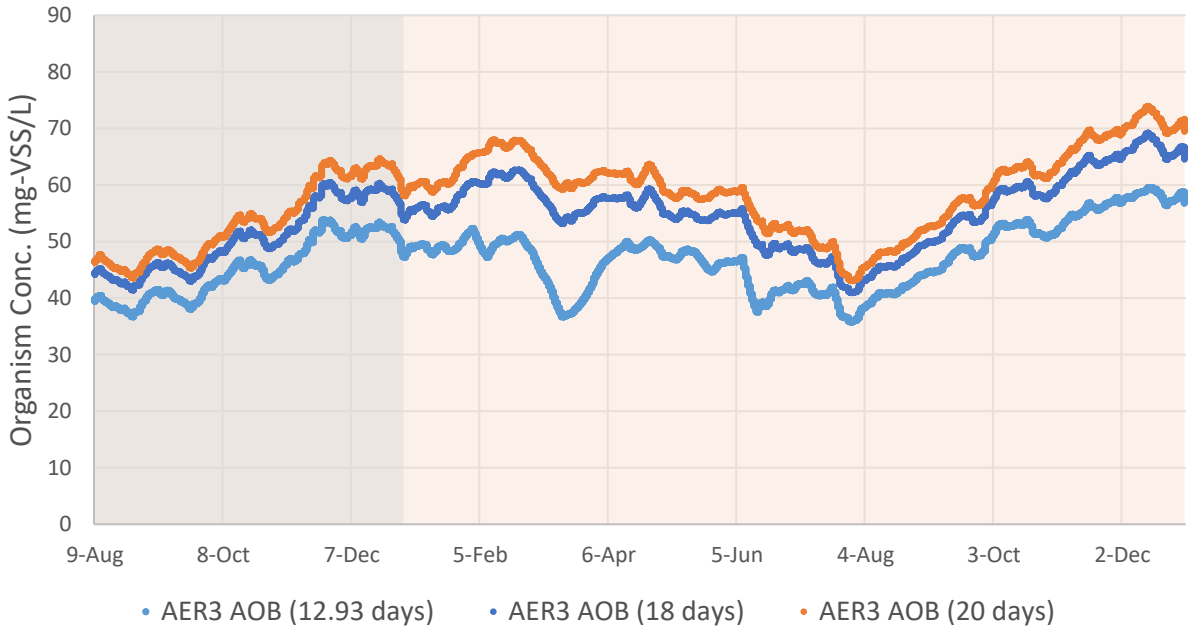

Figure 5.2 AOB concentration for SRT increase to 18 and 20 days (08/09/2016 to 12/31/2017; shaded regions delineate year)

This increase in AOB populations was not great enough to prevent ammonia removal upsets at an SRT of 20 days (Figure 5.3).

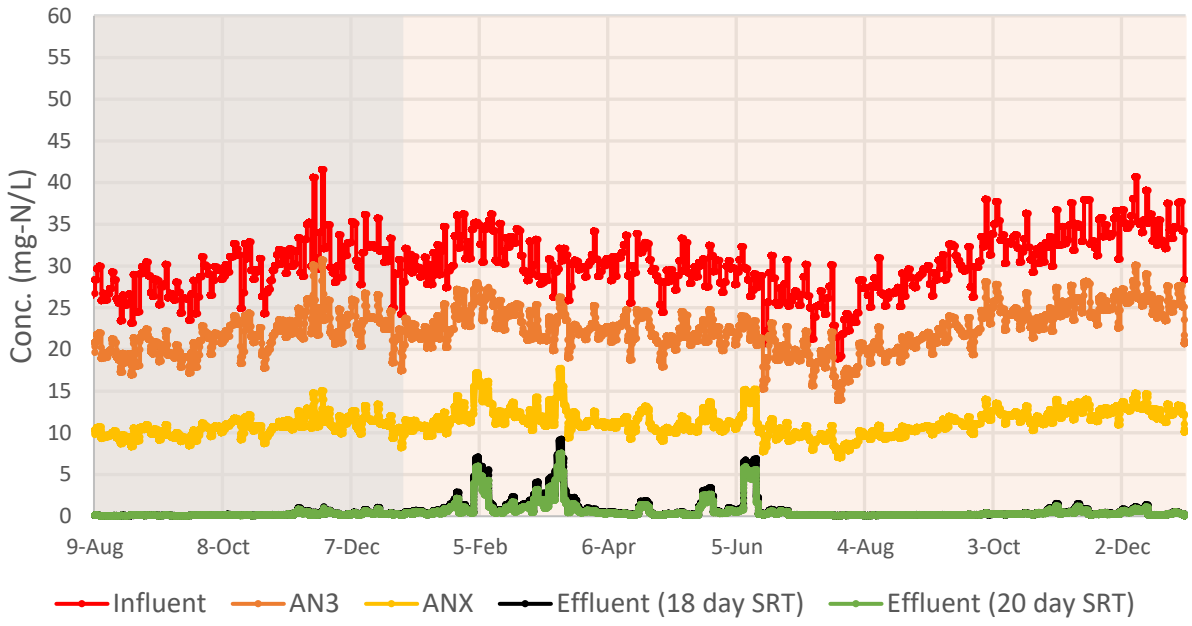

Figure 5.3 Ammonia removal for SRT increase to 18 and 20 days (08/09/2016 to 12/31/2017; shaded regions delineate year)

The simulations demonstrate that an operational adjustment of increasing the SRT alone will not prevent ammonia removal upsets. Additional measures need to be employed to provide consistent performance. The greater stability in performance with increased SRT needs to be weighed against the impacts of greater MLSS concentrations.

The simulated MLSS concentrations for an SRT increase to 16 and 18 days as compared to UCT operation are plotted (Figure 5.4). For the carbon loading over UCT operation the simulated MLSS concentration increased by about 30 and 40% for SRTs of 16 and 18 days.

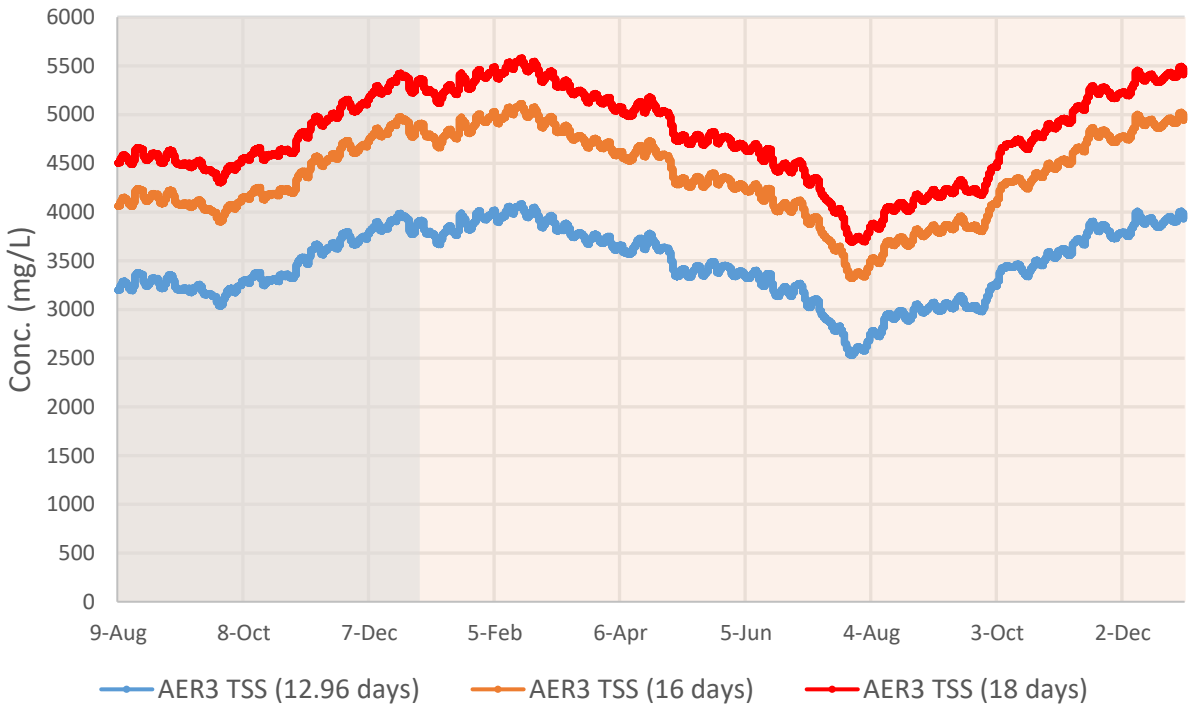

Figure 5.4 MLSS for SRT increase to 18 days (08/09/2016 to 12/31/2017; shaded regions delineate year)

The pilot plant clarifier performance was limited, and increasing the MLSS in the system would exacerbate these issues by increasing solids loading. Additionally, the low-DO pilot sludge demonstrated poor settling characteristics. Sludge settleability was characterized for the low DO pilot by performing 30-min settling tests during daily maintenance. While a sludge volume index

(SVI) of 100-150 mL/g is indicative of good settling sludge, for UCT operation the SVI was 189 ± 37 mL/g. The SVI followed seasonal trends; increasing in the winter with higher MLSS concentrations to greater than 200 mL/g and decreasing in the summer. Limited filamentous bulking can occur, reducing sludge settleability, with low-DO activated sludge exhibiting SVIs of 150-250 mL/g while more severe filamentous bulking sludge exhibits SVIs over 250 mL/g [Guo, 2010].

Increased sludge age, long anaerobic/anoxic HRTs, and cold water temperatures have been suggested to cause filamentous growth leading to poor settleability. Increasing the SRT could further impact the settling characteristics of the low DO pilot sludge. The long anaerobic/anoxic contact time, with low F/M ratio conditions, may have promoted filamentous growth within the bulk liquid [Eikelboom, 2000]. The pilot sludge floc formation may have been impacted by the paddle mixing of the reactors. A continuous aeration control regime would provide continuous mixing in the aerobic tanks where floc breakup by mechanical mixing can be avoided.

5.3 Increase DO

Normal operation of the Nine Springs full-scale plant maintains the aeration zone with DO set points between 1.2 and 1.5 mg-DO/L where the DO typically far exceeds these values by the end of the last pass [Reusser, 2002]. Unlike what is observed in the pilot plant, this operation allows for stable nitrification process performance where nitrification upsets do not occur in the winter. To evaluate if raising the DO in the pilot plant can maintain nitrification through the

winter the model was run with greater DO concentrations during the colder water temperature periods.

By counteracting the higher oxygen demand loadings to the pilot plant during times of colder water temperatures, the DO concentrations would not be suppressed to the extent observed. These simulations consider continuous DO concentrations varying on a weekly basis. They do not represent the on/off nature of the aeration control system of the pilot.

To simulate an increase in aeration, a factor was applied to the DO concentration patterns (Figure 4.16) from December 1st, 2016 to July 1st, 2017 and from November 1st, 2017 to December 31st, 2017. The average DO concentrations across the aerobic tanks for the UCT operation and the increased DO pattern simulations are plotted (Figure 5.5).

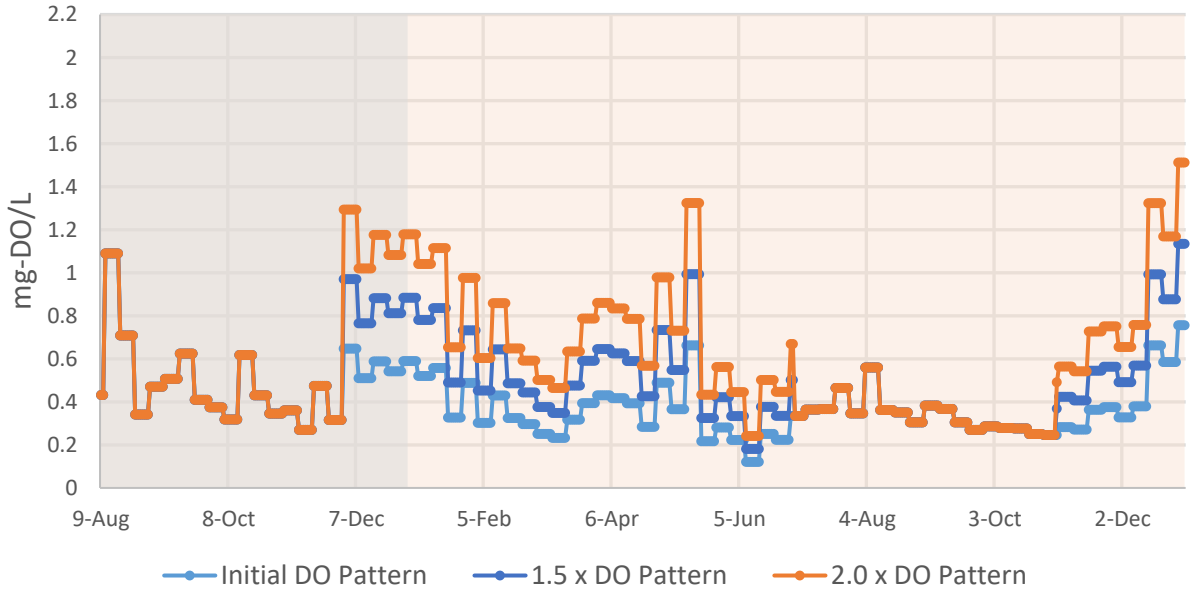

Figure 5.5 Aeration train average DO concentration pattern for DO increase simulations (08/09/2016 to 12/31/2017; shaded regions delineate year)

Increasing the DO in the aerobic tanks provided stable AOB populations. The increased DO prevented the washout of AOBs through the winter (Figure 5.6).

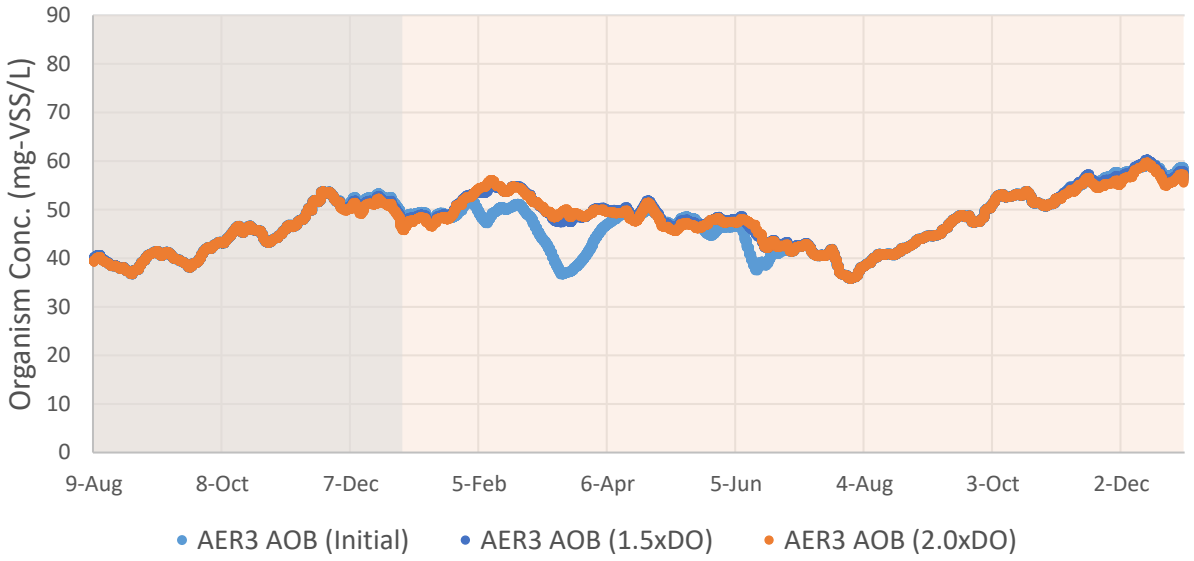

Figure 5.6 AOB concentration for DO increase simulations (08/09/2016 to 12/31/2017; shaded regions delineate year)

Increasing the DO provides greater ammonia removal rates. However, the simulation for increasing the DOs to 1.5-times the UCT operation still demonstrated ammonia removal upsets greater than 5 mg-N/L (Figure 5.7). Increasing the DOs to 2-times demonstrated better ammonia removal performance.

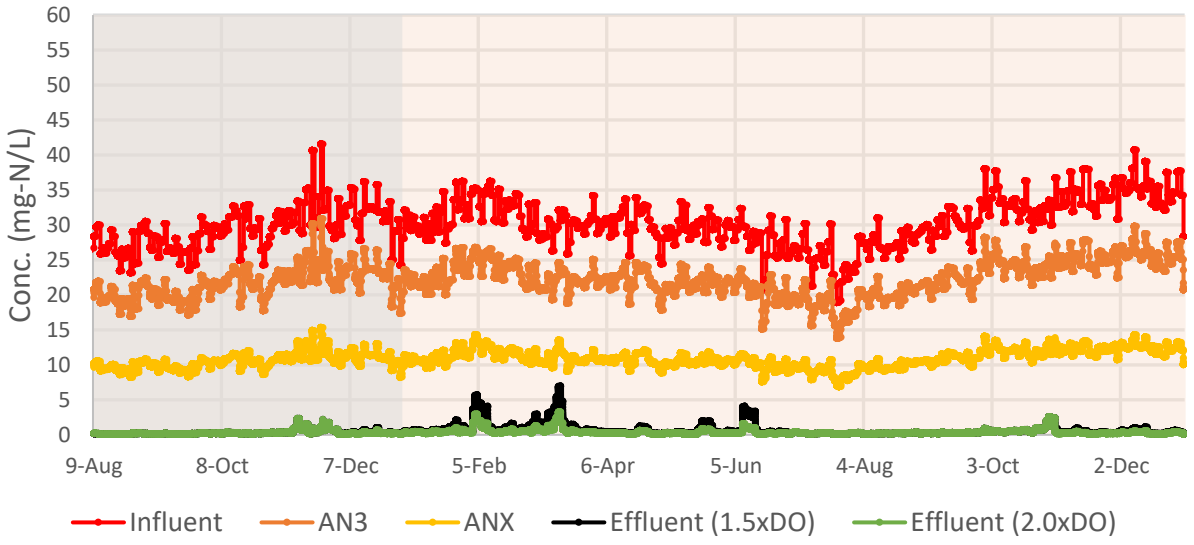

Figure 5.7 Ammonia removal for DO increase simulations (08/09/2016 to 12/31/2017; shaded regions delineate year)

The simulations demonstrate that doubling the DO concentrations in the aerobic tanks could provide consistent ammonia removal. The benefits in ammonia removal stability should be weighed against the increase in energy demand by increasing aeration. As the DO concentrations increase, greater aeration energies are required to raise the DO against the gradient from water saturation [Tchobanoglous, 2003]. There may be biological factors that these simulations do not consider.

This research has demonstrated that the kinetic parameters of the bacterial communities shift in response to sustained low DO conditions. It is unclear if these DO increases would cause an opposing shift to occur, therefore compromising process stability as the bacterial communities transition in response to changing conditions. A more stable transition could be achieved by successively raising and lowering the DO [Keene, 2016].

5.4 Increase SRT and DO

The simulations demonstrate that increasing the DO concentrations by 1.5-times UCT operation and increasing the SRT to 16 days consistently removes ammonia to below 5 mg-N/L (Figure 5.8). The 30% increase in MLSS concentration and the reduction in energy efficiency should be considered with this operational strategy.

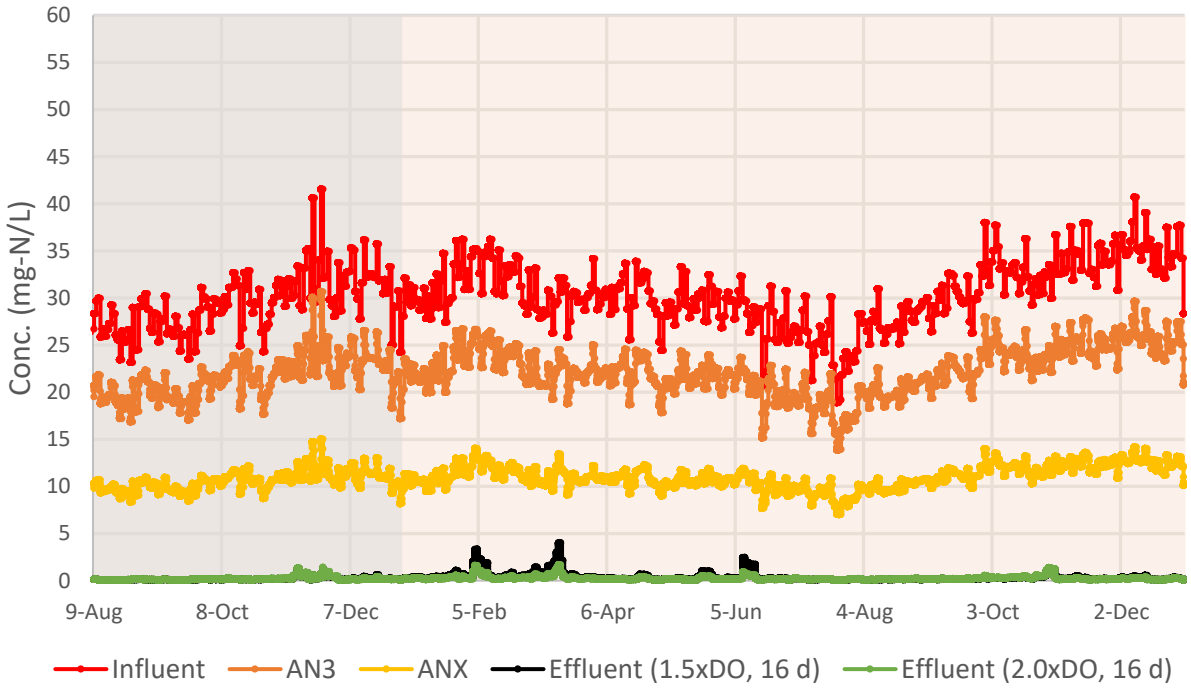

Figure 5.8 Ammonia removal for DO and SRT increase simulations (08/09/2016 to 12/31/2017; shaded regions delineate year)

5.5 Increase Aerobic HRT

The pilot plant configuration did not representatively reproduce the process of the full-scale plant (Section 2.1, Table 2.3). Simulations were run with adding aerobic tankage (Figure 5.9). Aerobic tank 2, with the DO concentration pattern experienced for UCT operation, was replicated to simulate the larger aeration zone.

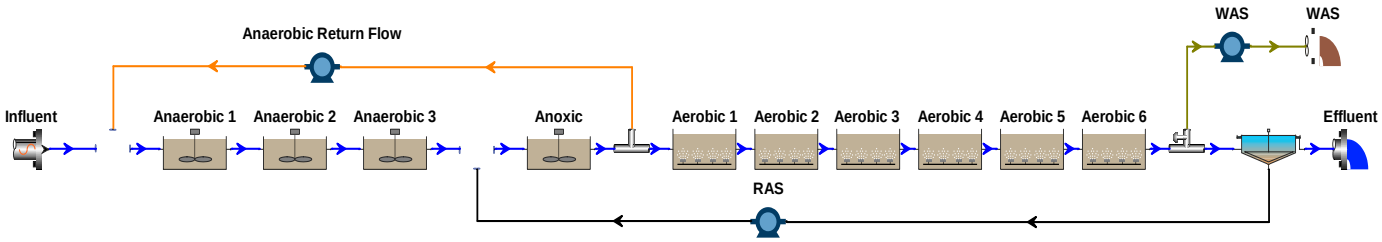

Figure 5.9 Model configuration for additional aerobic tanks

The total treatment train HRTs and volume fractions are listed in Table 5.1 for the pilot with additional aerobic tanks (from 3 for UCT operation) and the full-scale plant. The HRT for the full-scale plant was calculated considering an influent flow to one West plant treatment train of 4.38 MGD [Brown and Caldwell, 2017].

Table 5.1 Pilot and full-scale tank volume distribution

# Pilot Aerobic Tanks	3	4	5	6	Full-Scale
Anaerobic %	16	13	11	10	16
Anoxic %	21	17	15	13	6
Aerobic %	63	70	74	77	78
Treatment Train HRT (hr)	9.8	11.9	14.0	16.0	16.5

With three aerobic tanks added to the pilot, the aerobic volume fraction and the treatment train HRT are similar to that of the full-scale plant. The pilot plant had a greater anoxic zone than the full-scale plant, which contributed to the TN removal capacity. Though operational energy efficiency would be reduced by the additional aeration requirements, low DO conditions would be maintained throughout operation. Process stability and better representation of the full-scale operation would be achieved by adding tankage to the aeration zone.

By adding one aerobic tank and keeping the SRT at 12.93 days, the simulated ammonia concentrations rose to greater than 10 mg-N/L in the winter (Figure 5.10). Increasing the SRT to 16 days reduced ammonia concentrations further. Adding two aerobic tanks at an SRT of 16 days reduced ammonia concentrations, though they increased to over 5 mg-N/L in the winter.

The simulated addition of three aerobic tanks at an SRT of 16 days demonstrated that ammonia was consistently removed with effluent ammonia concentrations remaining below 5 mg-N/L throughout the winter. The effluent NOx concentration was not affected by the addition of aerobic tanks. The phosphorus removal was stable for these simulations.

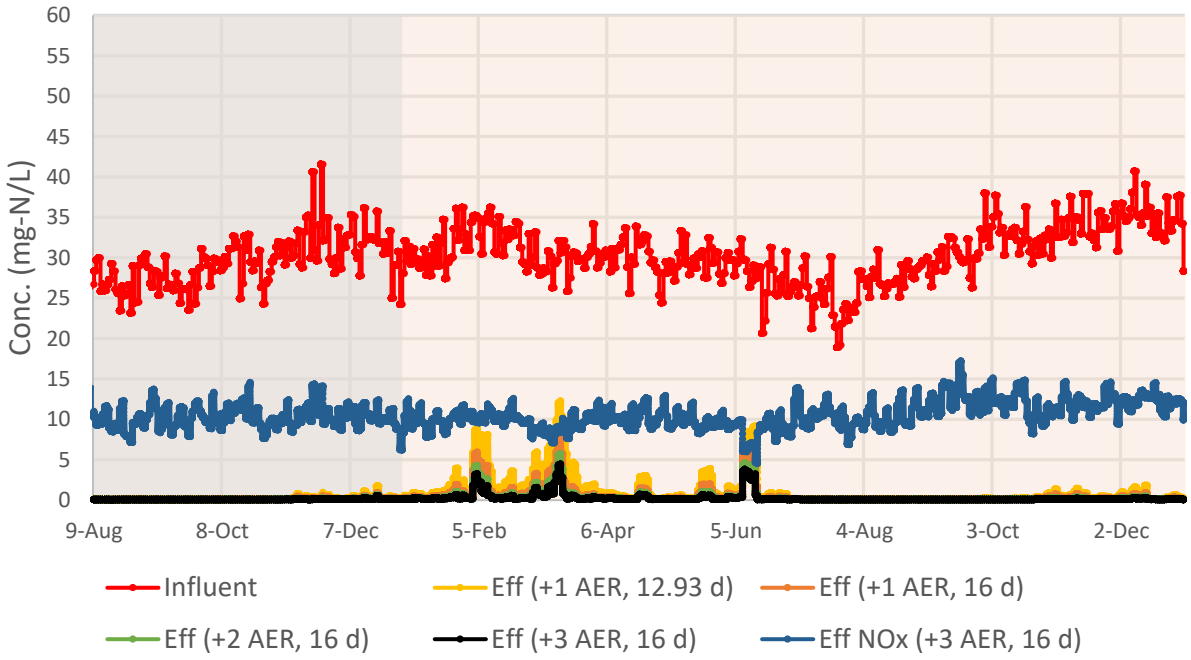

Figure 5.10 Ammonia and NOx removal for added aerobic tank simulations (08/09/2016 to 12/31/2017; shaded regions delineate year)

The Wisconsin Pollutant Discharge Elimination System (WPDES) permit for Nine Springs WWTP for the months of October to April stipulates a maximum monthly and weekly average ammonia discharge limit of 4.1 and 10 mg-NH_3-N/L, respectively. For the simulated addition of three aerobic tanks, the maximum effluent ammonia concentration occurred on March 15th, 2017 at 4.45 mg-N/L. However, the average for that month was 0.84 mg-N/L. The ammonia discharge limit for the May to September months are a maximum monthly and weekly average of 1.8 and 4.4 mg-N/L, respectively. The weekly average for the simulated upset occurring on June 8th, 2017 and continuing to June 15th, 2017 was 2.48 mg-N/L. These simulations demonstrate that the addition of three aerobic tanks at an SRT of 16 days would provide stable process performance that meets effluent water quality standards, while maintaining the energy-efficient low-DO operation.

Increasing the HRT reduces the steady state biomass concentration, Equation 1.8. The simulated MLSS concentrations are reduced by adding aerobic tankage (Figure 5.11). The addition of three aerobic tanks reduced the MLSS concentration by 25% from UCT operation. This would alleviate the solids loading to the clarifier and would provide greater process stability.

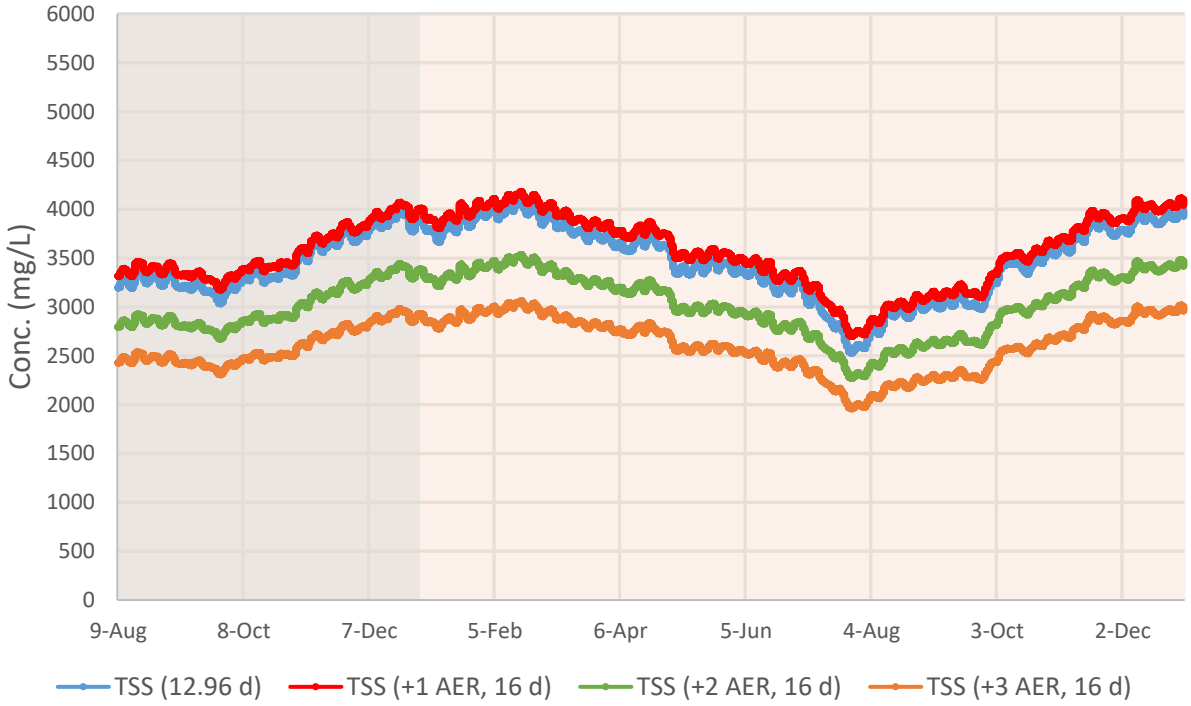

Figure 5.11 Aerobic tank 3 MLSS concentrations for added aerobic tank simulations (08/09/2016 to 12/31/2017; shaded regions delineate year)

CHAPTER 6 : RECOMMENDATIONS

6.1 Pilot-Plant Operation

The simulations demonstrate that increasing the SRT alone would have prevented washout of AOBs for UCT operation, but would not have corrected for rising ammonia concentrations in the winter. An effective strategy may be to increase DO concentrations in tangent with SRT increases during the winter, but this strategy would increase MLSS concentrations at the time of greatest carbon loading to the pilot, would increase energy demand, and would introduce unknown variables to the main objective of the research; low DO treatment.

Increasing the RAS flow rate does not provide beneficial TN removal because of carbon limitations. Decreasing the RAS flow rate would provide greater operational energy efficiency, but would increase effluent TN concentrations.

The on/off nature of the aeration control system may have been beneficial to SND through the aerobic zone but is not indicative of full-scale operation. A continuous aeration regime would better represent full-scale operation and would provide continuous mixing to the aerobic zone eliminating the need for paddle mixers.

6.2 Pilot-Plant Configuration

The proposed corrective action is the addition of three aerobic tanks with an increase in SRT to 16 days. This strategy provides a safety factor for preventing AOB washout and achieves stable ammonia removal performance. This configuration would reduce solids loading to the

nonideal pilot clarifier, providing greater process stability. Low DO concentrations are maintained throughout the year, though additional aeration reduces operational energy efficiency. The operation of the full-scale plant is better emulated with this pilot configuration and it accomplishes the research goal of proving stable, sustainable low DO wastewater treatment.

6.3 Future Research Objectives

For the next iteration of this research, further characterization of the low-DO organisms is suggested. The decay and growth rates of the low-DO organisms can be investigated through respirometry experiments. The performance of the low-DO denitrifiers are important for TN removal considerations and denitrification rate tests, both for nitrite and nitrate, may give insight into the SND experienced by the pilot. The temperature sensitivity of the low-DO nitrifiers is critical to process stability by causing washout during times of slow growth rates. Batch experiments to determine the Arrhenius temperature coefficient for the low-DO nitrifiers as compared to those in the full-scale plant would be useful.

This research did not consider the substrate half saturation constants of the low-DO AOB and NOB. To determine the ammonia and nitrite substrate half saturation constants for AOBs and NOBs an experiment utilizing a continuously fed batch reactor is proposed. By aerating the batch reactor to a high DO concentration, maximum removal rates would be achieved. The reactors would be continuously fed either ammonia or nitrite at different rates to maintain certain concentrations within the reactor. The products of nitrification and nitritation, NOx and NO_3^-, could then be measured to determine removal rates for those certain concentrations and calculate half saturation constants.

For future iterations of the pilot, the knowledge gained through this research should be used to design the process configuration and operation to afford process stability. The constant flow nature of the pilot is not indicative of real wastewater treatment conditions. Shock loading events to the pilot plant would be useful for assessing process stability of low DO operation.

The sampling procedure did not conclusively capture pilot performance. Time dependent studies by continuously sampling during high loading conditions could be performed to assess reactor response.

The on/off nature of the aeration control system is not indicative of real wastewater treatment aeration. The full-scale plant blowers operate by maintaining an outlet pressure with inlet guide vanes and increasing aeration to the aerobic zone by opening airflow control valves in response to DO concentration monitoring [Brown and Caldwell, 2017]. A similar control could be implemented to the pilot with a reducing valve. This aeration strategy would prevent the suppressed DO concentrations experienced during high loadings.

CHAPTER 7 : GENERAL CONCLUSIONS

This research demonstrated that kinetic parameters, process operation, and process configuration are important factors when treating wastewater using low DO concentrations. It should be recognized that pilot-scale operation experiences unique challenges that are not seen with real wastewater treatment. The knowledge gained through UCT operation should be used to more effectively prove stable low DO wastewater treatment. The general conclusions from this research are presented below:

- The low-DO enriched NOB and AOB communities have higher affinity for oxygen than high-DO enriched communities.
- Constant flow feed does not emulate full-scale operation.
- Sampling procedure did not conclusively capture pilot performance.
- Seasonal nutrient loadings affect biomass concentrations and effluent ammonia concentrations.
- Consistent EBPR performance can be explained by acetate and rbCOD fraction of Nine Springs' wastewater.
- Experimentally determined high affinity for oxygen of low-DO NOBs is important for explaining nitrification performance of low DO pilot plant for UCT operation.
- AOB population dynamics partly explains seasonal ammonia removal performance.
- The simulated low-DO AOB population is about 1.5% of the total biomass.
- The simulated low-DO AOB population dynamics can explain the differences in ammonia removal rates observed at different points throughout UCT operation.

- AOB washout events occur during times of suppressed DO concentrations, which are caused by high oxygen demand loadings, and cold water temperatures at a simulated SRT of 12.93 days.
- SRT increases can prevent these simulated washout events.
- With constant DO concentrations, an increase in aeration could correct against poor ammonia removal.
- UCT operation HRT did not emulate full-scale operation.
- Greater treatment train HRTs would reduce solids loadings to the nonideal pilot clarifier.
- Adding aerobic tanks and increasing SRT to 16 days would provide stable ammonia removal performance while maintaining low DO operation.

REFERENCES

American Society of Civil Engineers (ASCE). 2011. Failure to Act: The Economic Impact Of Current Investment Trends in Water and Wastewater Treatment Infrastructure. Reston, VA: ASCE.

American Public Health Association, A.W.W.A., Water Environment Federation, Standard Methods for the Examination of Water and Wastewater: 21st Edition. 2005, American Public Health Association.

Andrade, J.M., Estévez-Pérez, M.G., Statistical comparison of the slopes of two regression lines: A tutorial, Analytica Chimica Acta, Volume 838, 2014, p. 1-12.

Bauer, D, M Philbrick, and B Vallario. 2014. The Water-Energy Nexus: Challenges and Opportunities. DOE/EPSA-0002

Bellucci, M., et al., Low-Dissolved-Oxygen Nitrifying Systems Exploit Ammonia-Oxidizing Bacteria with Unusually High Yields. Appl Environ Microbiol, 2011. 77(21): p. 7787-96.

Brown and Caldwell in association with Strand Associates, Energy Baseline and Optimization Roadmap Study. 2014. p. 1-195.

Brown and Caldwell in association with Strand Associates, Technical Memorandum 5, Version 4. Biological Nutrient Removal Alternatives Evaluation. June 9, 2017. p. 1-192.

Camejo, Pamela Y., et al., Candidatus Accumulibacter phosphatis clades enriched under cyclic anaerobic and microaerobic conditions simultaneously use different electron acceptors, Water Research, Volume 102, 2016, Pages 125-137.

Denecke, M., and Liebig, T. (2003) Effect of carbon dioxide on nitrification rates. Bioprocess Biosystems Eng 25: 249–253.

Eikelboom, D.H., Process Control of Activated Sludge Plants by Microscopic Investigation. IWA Publishing, London, UK (2000).

Gillot, S., and J-M Choubert. "Biodegradable Organic Matter in Domestic Wastewaters: Comparison of Selected Fractionation Techniques." Water Science and Technology 62.3 (2010): p. 630-9.

Grande, Joseph, Annual Report on Water Quality Monitoring – 2014. Madison Water Utility, 2015.

Guo, Jian-Hua , et al., Energy saving achieved by limited filamentous bulking sludge under low dissolved oxygen, Bioresource Technology, Volume 101, Issue 4, 2010, Pages 1120-1126.

Harms, G., et al., Real-Time Pcr Quantification of Nitrifying Bacteria in a Municipal Wastewater Treatment Plant. Environmental Science & Technology, 2003. 37(2): p. 343-351.

Henze, M., Gujer, W., Mino, T., Matsuo, T., Wentzel, M.C., Marais, G.V.R., van Loosdrecht, M.C.M., 1999. Activated Sludge Model No. 2d, ASM2D. Water Sci. Technol. 39 (1), 165–182.

Keene, Natalie A., Reusser, Steve R., Scarborough, Matthew J., Grooms, Alan L., Seib, Matt Santo Domingo, Jorge, Noguera, Daniel R., Pilot plant demonstration of stable and efficient high rate biological nutrient removal with low dissolved oxygen conditions, Water Research, Volume 121, 2017, Pages 72-85.

Liu, G. and J. Wang, Long-Term Low Do Enriches and Shifts Nitrifier Community in Activated Sludge. Environmental Science & Technology, 2013. 47(10): p. 5109-5117.

Metcalf & Eddy, Inc. Wastewater Engineering : Treatment and Reuse. Boston :McGraw-Hill, 2003.

Mielczarek, Artur Tomasz, Nguyen, Hien Thi Thu, Nielsen, Jeppe Lund, Nielsen, Per Halkjær, Population dynamics of bacteria involved in enhanced biological phosphorus removal in Danish wastewater treatment plants, Water Research, Volume 47, Issue 4, 2013, Pages 1529-1544.

Monod, J., The Growth of Bacterial Cultures. Annual Review of Microbiology, 1949. 3: p. 371-394.

Nielsen, P.H., McMahon, K.D., Microbiology and microbial ecology of the activated sludge process. D. Jenkins, J. Wanner (Eds.), Activated Sludge – 100 Years and Counting, IWA Publishing, London (2014), pp. 53-75

Park, H.D. and D.R. Noguera, Characterization of Two Ammonia-Oxidizing Bacteria Isolated from Reactors Operated with Low Dissolved Oxygen Concentrations. Journal of Applied Microbiology, 2007. 102(5): p. 1401-1417.

Park, H.D. and D.R. Noguera, Evaluating the Effect of Dissolved Oxygen on Ammonia-Oxidizing Bacterial Communities in Activated Sludge. Water Res, 2004. 38(14-15): p. 3275-86.

Park, H.D., et al., Taking Advantage of Aerated-Anoxic Operation in a Full-Scale University of Cape Town Process. Water Environment Research, 2006. 78(6): p. 637-642.

Reusser, S.R., Effects of Biological Phosphorus Removal on Plant Operations and Capacity at the Nine Springs WWTP. 2002, Madison Metropolitan Sewerage District.

Rittmann, B.E. McCarty, P.L. Environmental Biotechnology: Principles and Applications. McGraw-Hill, New York (2001)

Ritz, C., Baty, F., Streibig, J. C., Gerhard, D. (2015) Dose-Response Analysis Using R. PLOS ONE, 10(12), e0146021.

Tchobanoglous, G.B., Franklin L.; Stensel, H. David, Wastewater Engineering: Treatment and Reuse. 4 ed, ed. Metcalf & Eddy Inc. 2003, New York, NY: McGraw-Hill.

US-EPA (1993) Manual: Nitrogen Control. Cincinnati, OH: US-Environmental Protection Agency (EPA).

Water Environment Research Foundation (WERF). 2011. Energy Production and Efficiency Research—The Roadmap to Net-Zero Energy. Alexandria, VA: WERF.

APPENDIX

Similar to the pilot experiments, AOB batch experiments were conducted with full-scale sludge samples collected from the end of the UCT configured West plant anaerobic zone. The best-fit kinetic parameters for AOB are listed in Table A.1. The estimated K_{DO} are significantly higher than for pilot experiments, Table 3.1, confirming a prior observation of higher affinity for oxygen of the low-DO enriched AOB communities [Keene, 2016].

The q_{max} for these experiments, conducted with sludge samples collected at different times throughout the year, do not show as great a seasonal variation as the pilot experiments, Table 3.1. This could indicate higher temperature sensitivity of the low-DO enriched AOB communities or could be explained by population dynamics. The AOB populations in the full-scale plant may be more stable than in the pilot plant due to greater process stability.

Table A.1 Full-scale individual model fit AOB Monod parameters

Experiment	Jun-15		Feb-17		Sep-17	
Parameter	$q_{max}\left(\frac{mg-N}{mg-VSS-d}\right)$	$K_{DO}\left(\frac{mg-DO}{L}\right)$	$q_{max}\left(\frac{mg-N}{mg-VSS-d}\right)$	$K_{DO}\left(\frac{mg-DO}{L}\right)$	$q_{max}\left(\frac{mg-N}{mg-VSS-d}\right)$	$K_{DO}\left(\frac{mg-DO}{L}\right)$
SSE Model Fit	0.15	1.33	0.14	0.80	0.17	0.87

The best-fit kinetic parameters for the combined data from the three full-scale AOB batch experiments are listed in Table A.2.

Table A.2 Full-scale combined model fit AOB Monod parameters

Parameter	$q_{max}\left(\frac{mg-N}{mg-VSS-d}\right)$	$K_{DO}\left(\frac{mg-DO}{L}\right)$
Model Fit ± SE	0.15 ± 0.011	1.00 ± 0.19
p-value*	<0.00001	0.000029

*p-value of significance from dose response model statistical analysis in R

The Monod model fit for the combined data from the three full-scale AOB batch experiments demonstrates a more gradual trend than the pilot experiments, illustrating the lower affinity for oxygen of the high-DO enriched AOB communities (Figure A.1 and Figure 3.1).

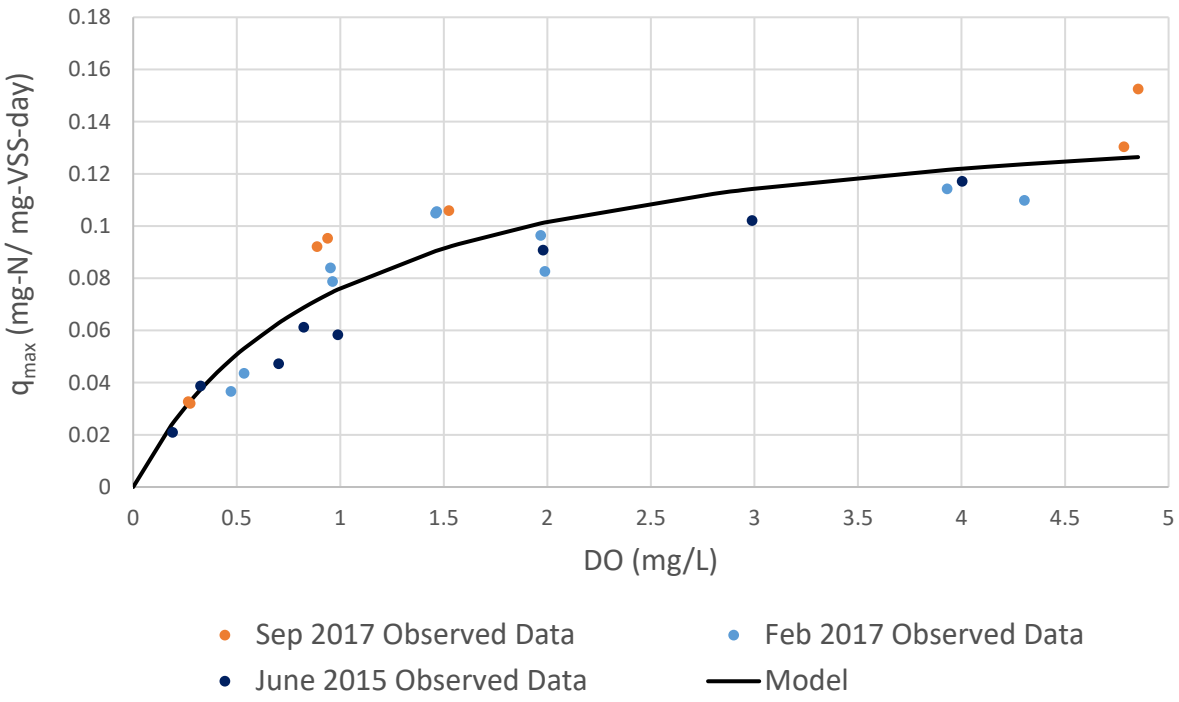

Figure A.1 Full-scale sludge AOB batch test data and Monod curves

Similar to the pilot experiments, NOB batch experiments were conducted with full-scale sludge samples collected from the end of the UCT configured West plant aerobic zone. The best-fit kinetic parameters for NOB are listed in Table A.3. The estimated K_{DO} are significantly higher than for pilot experiments, Table 3.3, demonstrating the higher affinity for oxygen of the low-DO enriched NOB communities.

The q_{max} for these experiments, conducted with sludge samples collected at different times throughout the year, do not show as great a seasonal variation as the pilot experiments, Table 3.3.

Table A.3 Full-scale individual model fit NOB Monod parameters

Experiment	Dec-16		Feb-17		Sep-17	
Parameter	$q_{max}\left(\frac{\text{mg-N}}{\text{mg-VSS-d}}\right)$	$K_{DO}\left(\frac{\text{mg-DO}}{L}\right)$	$q_{max}\left(\frac{\text{mg-N}}{\text{mg-VSS-d}}\right)$	$K_{DO}\left(\frac{\text{mg-DO}}{L}\right)$	$q_{max}\left(\frac{\text{mg-N}}{\text{mg-VSS-d}}\right)$	$K_{DO}\left(\frac{\text{mg-DO}}{L}\right)$
SSE Model Fit	0.10	0.54	0.09	0.78	0.12	0.57

The best-fit kinetic parameters for the combined data from the three full-scale NOB batch experiments are listed in Table A.4.

Table A.4 Full-scale combined model fit NOB Monod parameters

Parameter	$q_{max}\left(\frac{\text{mg-N}}{\text{mg-VSS-d}}\right)$	$K_{DO}\left(\frac{\text{mg-DO}}{L}\right)$
Model Fit ± SE	0.10 ± 0.0087	0.67 ± 0.16
p-value*	<0.00001	0.00030

*p-value of significance from dose response model statistical analysis in R

The Monod model fit for the combined data from the three full-scale NOB batch experiments demonstrates a more gradual trend than the pilot experiments, illustrating the lower affinity for oxygen of the high-DO enriched NOB communities (Figure A.2 and Figure 3.3).

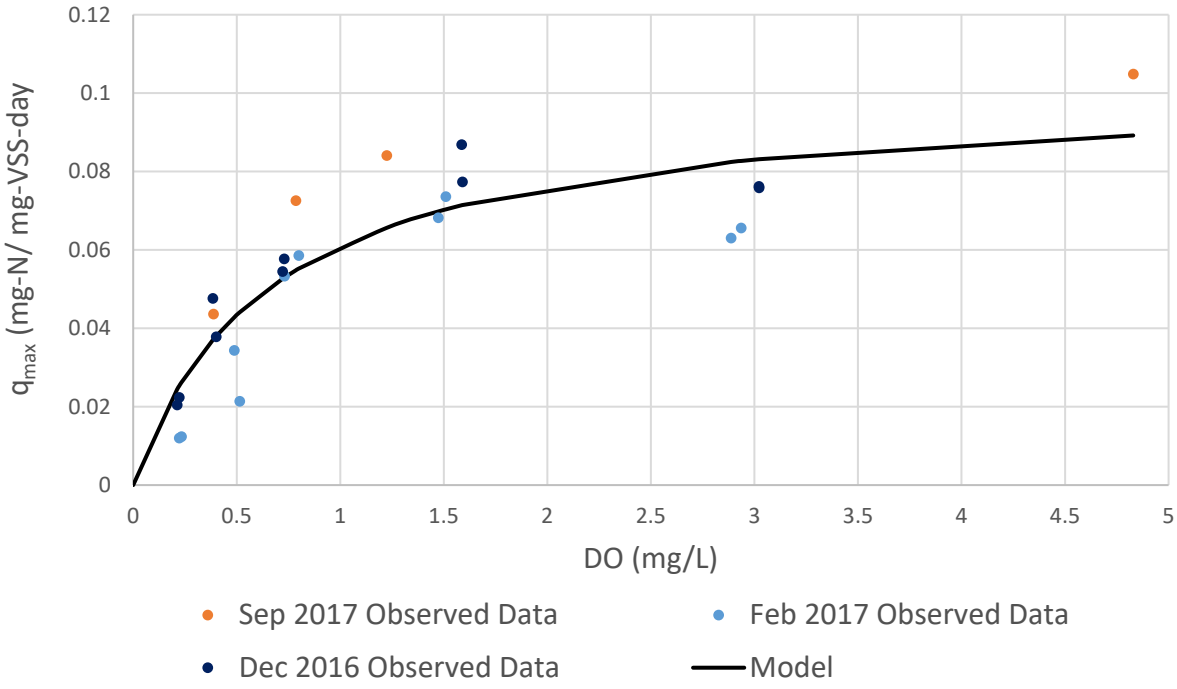

Figure A.2 Full-scale sludge NOB batch test data and Monod curves

Scum was removed from the top of the clarifier during daily pilot maintenance. From November 4th, 2017, approximately 10 mL of scum sample were collected from the removed scum along with pilot MLSS sampling. This solids measurement was incorporated into Equation 2.1. The calculated SRTs without considering and with considering scum wasting are listed in Table A.5 and plotted (Figure A.3).

Table A.5 Solids retention time with and without considering scum wasting

SRT no SCUM (days)	*SRT considering SCUM (days)*	*SCUM wasting (gpd)*
12.0 ± 2.1	10.8 ± 2.2	2.0 ± 1.4

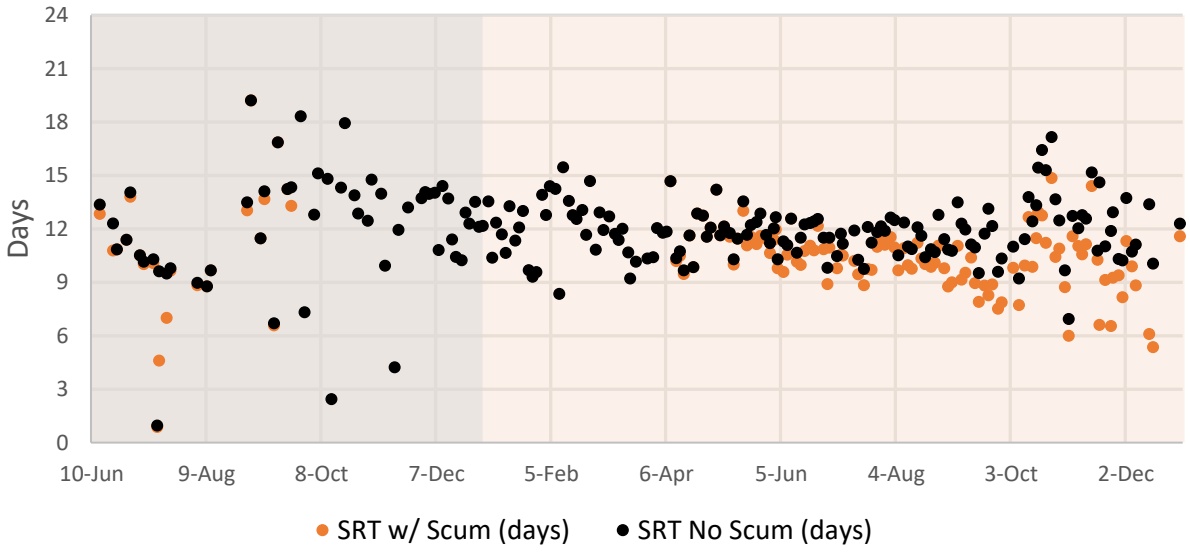

Figure A.3 Pilot plant SRT with and without scum wasting consideration (06/10/2016 to 12/31/2017; shaded regions delineate year)

The PE orthophosphate and TP concentration data used to calculate the Nine Springs' primary settled wastewater PO_4^{3-}/TP ratio are plotted (Figure A.4).

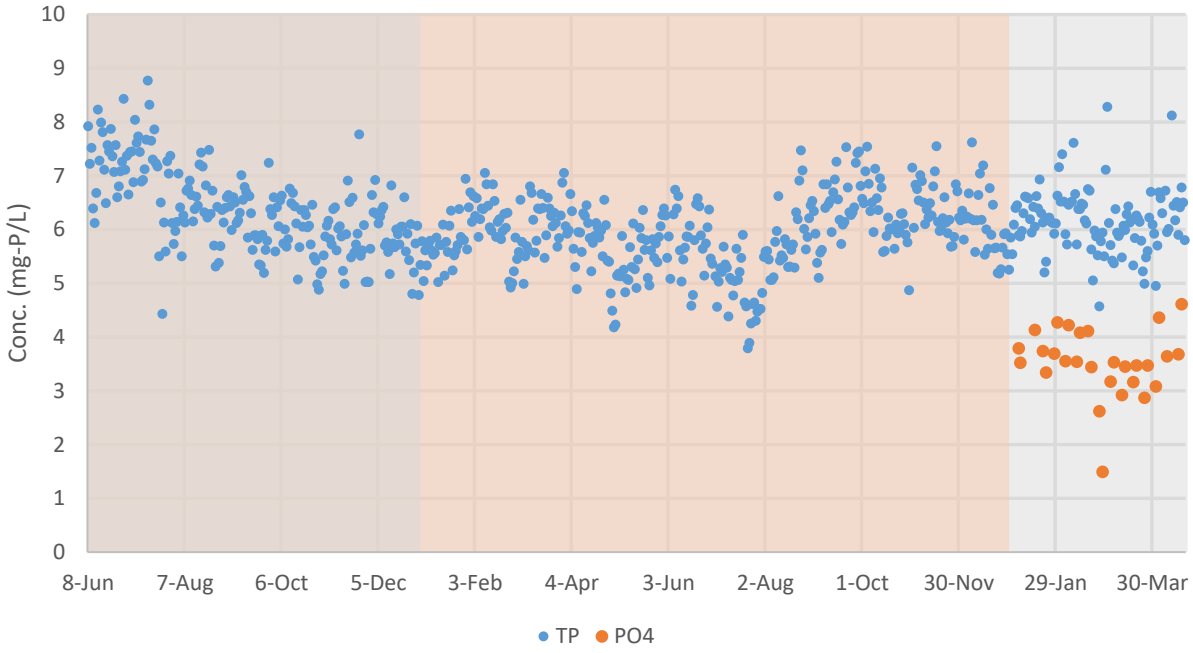

Figure A.4 Full-scale primary effluent seasonal TP and PO_4^{3-} concentrations (06/10/2016 to 4/19/2018; shaded regions delineate year)